1 OF 2

AD A118017

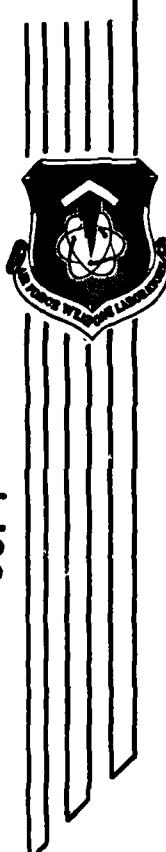# CHEMICAL PRODUCTION OF EXCITED NF

R. D. Coombe, et al.

Rockwell International Science Center
1049 Camino Dos Rios
Thousand Oaks, CA 91360

July 1982

Final Report

Approved for public release; distribution unlimited.

DTIC FILE COPY

SELECTED
AUG 1 0 1982

A

AIR FORCE WEAPONS LABORATORY
Air Force Systems Command
Kirtland Air Force Base, NM 87117

82 08 10 027

This final report was prepared by the Rockwell International Science Center, Thousand Oaks, California, under Contract F29601-79-C-0016, Job Order ILIR8117 with the Air Force Weapons Laboratory, Kirtland Air Force Base, New Mexico. Captain Ernest Kunstadt (ARAP) was the Laboratory Project Officer-in-Charge.
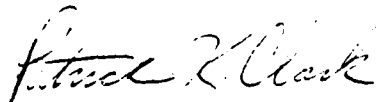
This report has been reviewed by the Public Affairs Office and is releasable to the National Technical Information Service (NTIS). At NTIS, it will be available to the general public, including foreign nations.

If your address has changed, if you wish to be removed from our mailing list, or if your organization no longer employs the addressee, please notify AFWL/ARAP, Kirtland AFB, NM 87117 to help us maintain a current mailing list.

This technical report has been reviewed and is approved for publication.
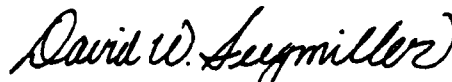

PATRICK K. CLARK
1st Lt, USAF
Project Officer

FOR THE COMMANDER

WILLIAM E. MCDERMOTT
Lt Colonel, USAF
Chief, New Laser Concepts Branch

DAVID W. SEEGMILLER
Colonel, USAF
Chief, Advanced Laser Tech Division

REPORT DOCUMENTATION PAGE		READ INSTRUCTIONS BEFORE COMPLETING FORM
1. REPORT NUMBER AFWL-TR-81-211	2. GOVT ACCESSION NO. AD A118017	3. RECIPIENT'S CATALOG NUMBER
4. TITLE (and Subtitle) CHEMICAL PRODUCTION OF EXCITED NF		5. TYPE OF REPORT & PERIOD COVERED Final Report
		6. PERFORMING ORG. REPORT NUMBER
7. AUTHOR(s) R. D. Coombe A. T. Pritt, Jr. D. Patel F. J. Wodarczyk		8. CONTRACT OR GRANT NUMBER(s) F29601-79-C-0016
9. PERFORMING ORGANIZATION NAME AND ADDRESS Rockwell International Science Center 1049 Camino Dos Rios Thousand Oaks, CA 91360		10. PROGRAM ELEMENT, PROJECT, TASK AREA & WORK UNIT NUMBERS 61101F/ILIR8117
11. CONTROLLING OFFICE NAME AND ADDRESS Air Force Weapons Laboratory (ARAP) Kirtland Air Force Base, NM 87117		12. REPORT DATE July 1982
		13. NUMBER OF PAGES 122
14. MONITORING AGENCY NAME & ADDRESS(if different from Controlling Office)		15. SECURITY CLASS. (of this report) Unclassified
		15a. DECLASSIFICATION/DOWNGRADING SCHEDULE

16. DISTRIBUTION STATEMENT (of this Report)

Approved for public release; distribution unlimited.

17. DISTRIBUTION STATEMENT (of the abstract entered in Block 20, if different from Report)

18. SUPPLEMENTARY NOTES

19. KEY WORDS (Continue on reverse side if necessary and identify by block number)

Azides   Lasers
Free Radicals   Gas Phase Kinetics
Electronic Excitation
Nitrogen Halides

20. ABSTRACT (Continue on reverse side if necessary and identify by block number)

The $a^1\Delta$ and $b^1\Sigma^+$ states of NF, NCl and NBr can be efficiently generated by reactions of $F+HN_3$ followed by halogen atom reactions with the azide radical, N_3. Scalability of these systems is sensitive to the buildup of N_3 concentrations since N_3+N_3 reactions undermine the overall efficiency. Large concentrations of N_3 are encountered when the halogen atom reaction with N_3 is significantly slower than its formation step, $F+HN_3$. Hence scaling of $NF(a^1\Delta)$ is not feasible, but that of $NCl(b^1\Sigma^+)$ and $NBr(b^1\Sigma^+)$ shows promise. A diagnostic tool sensitive
(over)

20. ABSTRACT (continued)

to optical gains or absorptions of $<2 \times 10^{-6} cm^{-1}$ was developed. In the NCl flame, the medium was transparent everywhere to the diagnostic probe, indicating fast removal of $NCl(b^1\Sigma^+)$ by reactions with Cl and/or F atoms which are present in large excess. Strong absorptions were observed in the NBr flame in accord with an expected short radiative lifetime of the $b^1\Sigma^+$ state. Energy transfer from $NF(a^1\Delta)$ to atomic Bi generating the $6^2D_{3/2}$ metastable state proceeds at gas kinetic rates. Using a single frequency CW dye laser, the first high resolution spectrum Bi $6^4S_{3/2}-6^2D_{3/2}$ was measured, and the radiative lifetime of the $6^2D_{3/2}$ state determined. Although an NF-Bi gain experiment was not performed, the appropriate diagnostic system was demonstrated.

TABLE OF CONTENTS

1

LIST OF FIGURES

LIST OF FIGURES

I. INTRODUCTION

Since the initial demonstration by Clyne and White[1] that elec-
tronically excited NF could be produced by a fast bimolecular reaction,
nitrogen halide diatomics have drawn considerable interest as candidates for
chemically pumped lasers. This interest stems in part from the electronic
structure of these molecules, shown in Fig. 1, in the form of a potential
energy diagram for NF. The nitrogen halides are isoelectronic to the group
VIA diatomics, and hence have low lying $a^1\Delta$ and $b^1\Sigma^+$ excited electronic
states. Transitions from these states to the $X^3\Sigma^-$ ground state are nominally
forbidden, and the radiative lifetimes of the excited states may be quite
long, particularly for the lighter members of the group. Malins and Setser[2]
have reported the lifetime of $NF(a^1\Delta)$ to be τ_{rad} = 5.6 s. Hence, excited
nitrogen halides may be considered as energy storage agents capable of
transferring their energy to a desired lasing species, or, for the shorter
lived states, as lasing molecules themselves. The $a^1\Delta$ and $b^1\Sigma^+$ states exhibit
little or no Franck-Condon shift with respect to the ground state, and
consequently their emission spectra, in the near IR and visible regions,
respectively, are dominated by strong Δv = 0 sequences with very narrow
bandwidths.[3,4]

Figure 1 also serves to demonstrate the major drawbacks to be
overcome by any potential nitrogen-halide-based laser. Since there is no
Franck-Condon shift and the major transitions terminate on levels which are
thermally populated at room temperature, the pumping reaction must be

5
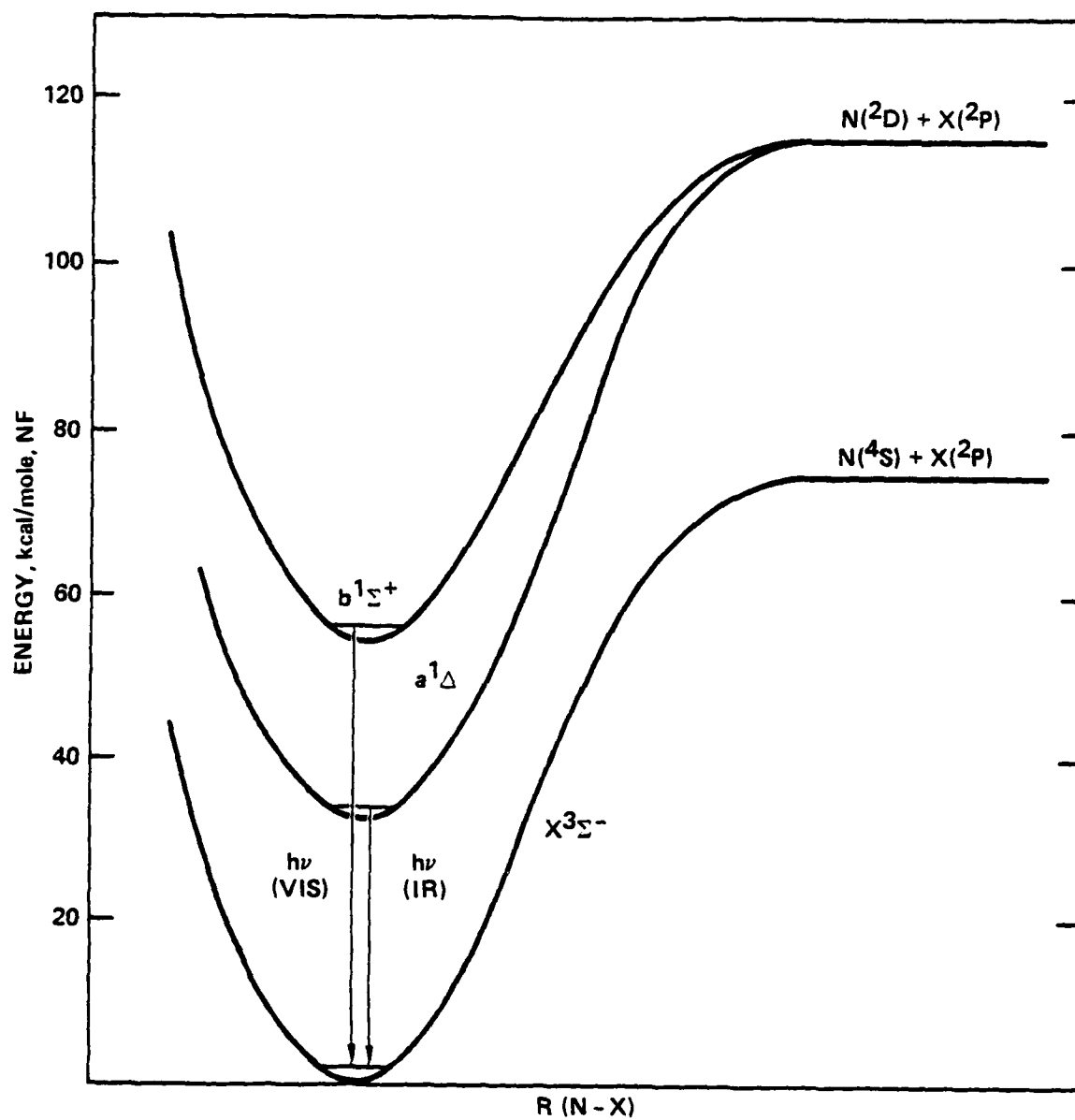
Figure 1. Potential energy diagram for the $X^3\Sigma^-$, $a^1\Delta$, and $b^1\Sigma^+$ states of NF molecule.

dynamically constrained to produce the excited states in order to generate a population inversion. Also, the $b^1\Sigma^+$ and $a^1\Delta$ excited states lie only ~ 20 and ~ 40 kcal/mole below the dissociation limit of the ground state (for NF), respectively, and therefore nitrogen halide molecules in these states are susceptible to reactive quenching processes in which the N-X (X = halogen) bond is broken. Any effective nitrogen halide laser system must overcome these two problems: it must be dynamically constrained to produce the excited states, and the gas mixture must not contain appreciable concentrations of reactive quenchers.

Herbelin and co-workers at the Aerospace Corporation[5] have shown the chemical system studied by Clyne and White accommodated at least the first of these requirements. These authors have reported that the reaction of hydrogen on deuterium atoms with NF_2 radicals produces $NF(a^1\Delta)$ in very large proportion:

$$H + NF_2 \rightarrow HF + NF(a^1\Delta) \tag{1}$$

Herbelin's work has suggested that the branching ratio for formulation of $NF(a^1\Delta)$ in this process is essentially unity, and this conclusion has been recently corroborated by the experiments of Cheah and Clyne.[6] The dynamic constraint operative in the system is thought to be spin conservation.[7] It has been argued that the hydrogen atom attacks the nitrogen in NF_2 to form an excited singlet difluoramine intermediate, which must decompose to singlet HF and singlet NF. The Aerospace group has also shown that the $b^1\Sigma^+$ state of NF

7

can be produced by near-resonant energy pooling between $NF(a^1\Delta)$ and a variety of metastable energy transfer agents.[5,7] These metastables include vibrationally excited HF, $O_2(a^1\Delta)$, and $I*(5^2P_{1/2})$. Sloan and co-workers[8] have presented data which suggest that energy pooling with excited HF, a process involving $\Delta v = 2$ transitions in the HF, occurs at a rate comparable to rotational relaxation in this molecule (i.e., with nearly gas kinetic efficiency).

The principal drawback to the NF_2 system is that hydrogen atoms, necessary reagents for the production of $NF(a^1\Delta)$, are also efficient reactive quenchers of both the $a^1\Delta$ and $b^1\Sigma^+$ states:

$$H + NF(a^1\Delta, b^1\Sigma^+) \rightarrow HF + N \qquad (2)$$
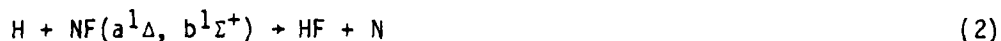
Reaction (2) is believed to produce electronically excited $N(^2D)$ atoms.[5,6] Since reaction (2) is quite rapid ($k_2 \approx 10^{-12}$ cm^3 molecule^{-1} s^{-1}),[6] it could severely limit the performance of any laser based on the NF_2 system.

To date, reactions analogous to process (1) have not been demonstrated for the production of excited NCl or NBr. Several years ago, however, Clark and Clyne[9] reported the generation of $NCl(^1\Sigma^+)$ and $NBr(^1\Sigma^+)$ by the reactions of chlorine or bromine atoms with ClN_3. Emissions were observed from only the $^1\Sigma^+$ states of the excited molecules. These authors postulated that the excited species were produced by reactions of Cl or Br atoms with gas phase N_3 radicals, themselves generated by abstraction of the chlorine atom from ClN_3.

8

Clyne's work formed the basis of the preliminary experiments performed at the Rockwell Science Center in 1978, in which the reaction of fluorine atoms with gas phase HN_3 was studied.[10] These experiments were performed using a discharge-flow apparatus in which the reagents were mixed in a linear flow tube. Fluorine atoms were produced by microwave discharge of F_2/Ar or CF_4/Ar mixtures. Gas phase HN_3 was produced by metering a 75% aqueous solution of H_2SO_4 onto a bed of NaN_3; the gaseous HN_3 product was swept from the reactor by a stream of argon. A small portion of the HN_3/Ar stream was bled into the vacuum system and admitted to the fluorine atom flow through a movable injector. The spectrum of the reaction flame was dominated by emissions from $NF(b^1\Sigma^+)$ near 529 nm and $NF(a^1\Delta)$ near 874 nm (the $\Delta v = 0$ sequences of transitions to the ground state), and included weak HF vibrational overtone emission (from levels up to $v = 5$) and nitrogen first positive $(B^3\pi_g-A^3\Sigma_u^+)$ emission. The $NF(b^1\Sigma^+)$ emission was observed to scale quadratically with the $NF(a^1\Delta)$ intensity, which at low densities varied roughly linearly with the HN_3 flow rate. The experiments were performed with a large excess of fluorine atoms.

On the basis of these results, the following mechanism was postulated:

$$F + HN_3 \rightarrow HF\ddagger + N_3 \tag{3}$$

$$F + N_3 \rightarrow NF(a^1\Delta) + N_2 \tag{4}$$

$$NF(a^1\Delta) + HF\ddagger(v) \rightarrow NF(b^1\Sigma^+) + HF\ddagger(v - 2) \tag{5}$$
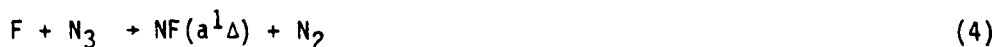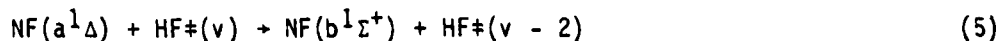
Addition of quenchers of vibrationally excited HF to the flow (e.g., CO_2), was found to dramatically reduce the $NF(b^1\Sigma^+)$ intensity, while increasing the $NF(a^1\Delta)$ intensity, as expected from the proposed mechanism. The limiting rate in the system was determined by monitoring the temporal profile of the $NF(a^1\Delta)$ emission. For kinetics pseudo-first order in fluorine atoms, this rate constant was found to be $k_{lim} = 2 \times 10^{-12}$ cm^3 molecule^{-1} s^{-1}. It was not known whether this rate constant applied to reaction (3) or reaction (4).

As noted above, reaction (4) must be strongly constrained to produce the $a^1\Delta$ state of NF for the F + HN_3 chemical system to be a viable laser candidate. In fact, strong constraints are expected on the basis of spin conservation. To illustrate this point, Fig. 2 shows a diagram indicating the relative energy of initial and final states for the analogous Cl + N_3 reaction. The reaction is assumed to proceed through a real or virtual ClN_3-like intermediate (the Cl + N_3 case was chosen for this illustration since the heat of formation of ClN_3 has been measured).[9] The Cl (^2P) and $N_3(^2\pi)$ reagents may combine on either singlet or triplet reaction coordinates. The singlet path lies lowest in energy; the energy of the intermediate has been shown in the figure as the ground state ($^1A'$) of the ClN_3 molecule. The singlet intermediate should correlate directly to $NCl(a^1\Delta)$ or $NCl(b^1\Sigma^+)$. Judging from the onset of the absorption spectrum of ClN_3,[11,12] corresponding to transitions to the lowest lying singlet state, the lowest triplet states of this molecule should lie at energies greater than that of the Cl + N_3 reagents. Hence, an

10
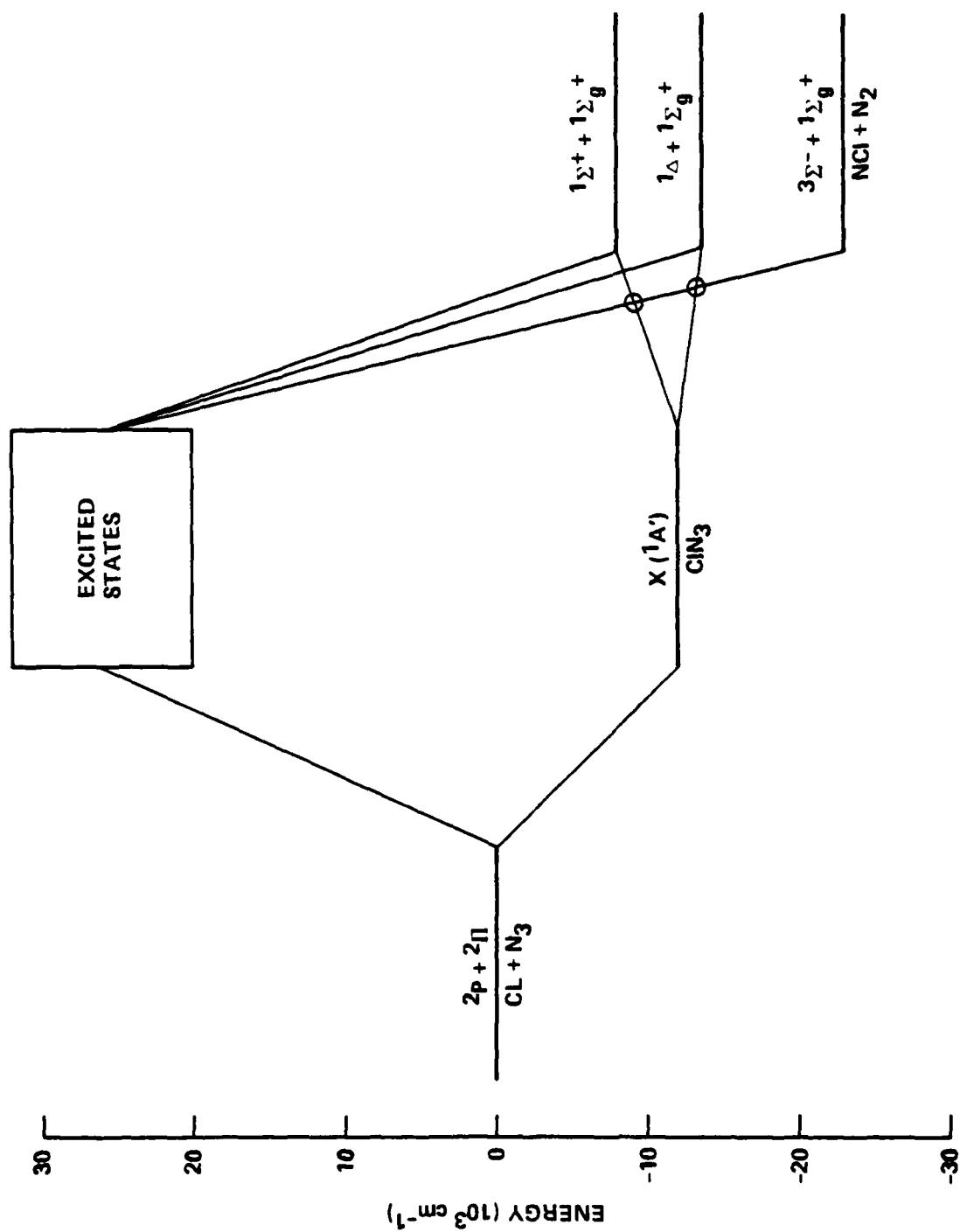
Figure 2. Energetics of the Cl + N₃ reaction. (The reaction should proceed via a ClN₃-like intermediate lying at an energy higher than that of the free ClN₃ molecule, which is shown in the figure).

11

energy barrier should exist in the adiabatic triplet coordinate, effectively preventing direct formation of ground state ($^3\Sigma^-$) NCl. Production of the ground state might still occur via crossing of the singlet and triplet coordinates in the product channel, however. It is expected that such processes will be improbable for the lighter NX molecules (smaller spin-orbit coupling), but might be significant for heavier species such as NBr or NI.

A preliminary test of this hypothesis was made by measuring the photon yield for emission from NF($a^1\Delta$). These experiments were performed by calibrating the absolute photon collection efficiency of the detection system of the apparatus, using the O + NO flame as a chemical actinometer.[13] An estimate of the peak density of NF($a^1\Delta$) was determined from $N = \alpha I/A$, where I is the measured intensity, A is the NF radiative lifetime, and α is the calibration factor. These experiments suggested that the yield, defined as the NF($a^1\Delta$) density relative to the initial HN_3 density, was in excess of 40%. Although these results were only semi-quantitative, they supported our hypothesis concerning the role of spin constraints in the system.

Subsequent to these preliminary experiments, a contract for further research on nitrogen halide systems was awarded to the Rockwell Science Center by the Air Force Weapons Laboratory. This report describes the work performed and results obtained in this effort, which spanned the period from December 1978 through July 1981. The overall objectives of the program were as follows:

12

1. To determine the behavior of the F + HN$_3$ system upon scaling to densities commensurate with a small scale gain demonstration.

2. To assess similar chemical systems producing electronically excited NCl and NBr.

3. To demonstrate optical gain on those nitrogen halide systems which could be scaled to the appropriate densities.

The first segment of the program addressed scaling of the NF system. In view of the radiative lifetimes of the $b^1\Sigma^+$ and $a^1\Delta$ states of this molecule, scaling to densities required for a gain of 10^{-4} cm^{-1} required the development of completely new systems for the generation of fluorine atoms and HN$_3$. The second phase of the program involved small-scale measurements on azide flames producing excited NCl and NBr, using techniques similar to those employed in the preliminary experiments described above.[10] The third phase of the program, gain experiments, involved the development of an apparatus with which gains or absorption as small as 10^{-4} per round trip transit through the medium could be measured. This system was based on measurement of the phase shift of a modulated probe beam transmitted through a resonant cavity surrounding the medium, and was similar to a system described by Herbelin and co-workers for the measurement of mirror reflectivities.[14] In the final phase of the program, this gain diagnostic was used in preliminary measurements on the NF($a^1\Delta$) - Bi($6^4S_{3/2}$) energy transfer system.

13

During the period of time spanned by this program, a related effort directed toward measurement of the fundamental properties of the nitrogen halide molecules and the kinetics and mechanisms of their formation was underway in our laboratory. Data obtained in the program were used extensively in interpreting the results described in this report.

II. CHEMICAL GENERATION OF EXCITED NF

As noted above, the primary objective of this first part of the
program was to assess the ability of the $F + HN_3$ chemical system to scale to
densities at which an optical gain of 10^{-4} cm^{-1} would be produced on the
$b^1\Sigma^+ \rightarrow X^3\Sigma^-$ transition of NF. The first issue to consider is the gain levels
to which our preliminary experiments[10] corresponded. The optical gain (or
absorption) coefficient at the center of a single rotational line in the 0,0
band of the $b^1\Sigma^+ - X^3\Sigma^-$ transition is given by the following expression:

$$G = \frac{2}{\Delta\nu} \ \frac{\ln 2}{\pi} \cdot \frac{\lambda^2}{8\pi} \cdot A_{ij} \left(N_i - \frac{g_i}{g_j} N_j \right) \tag{6}$$

where $\Delta\nu$ is the linewidth of the transition, λ is its wavelength, A_{ij} is the
rate of spontaneous emission from the upper (i) to the lower (j) state, g_i and
g_j are the degeneracies, and N_i and N_j are number densities, respectively.
For the conditions of our experiment, $\Delta\nu$ should be close to the Doppler
linewidth for NF near 529 nm, 1.1 GHz at 350 K. Since each rotational level
in the $b^1\Sigma^+$ state can radiate to five different levels in the grounbd $X^3\Sigma^-$
state (correponding to the ^SR, ^QR, ^QQ, ^QP, and ^OP branches of this
transition[3]), the measured spontaneous emission rate for the $b^1\Sigma^+$ state,[15] $A =$
44 s^{-1}, must be divided by five to obtain the radiative rate for an individual
transition. Since we presume the spin constraints favoring production of

15

excited state to be strong, we will assume the ground state density, N_j, to be zero. Finally, assuming an equilibrium distribution among the rotational levels of the $b^1\Sigma^+$ state corresponding to T = 350K, and furthermore that only the v' = 0 vibrational level is populated (nearly 90% of the emission found in the experiments was from v' = 0),[10] $N_i \approx 10^{11}$ cm^{-3}. These conditions result in a gain given by $G \approx 1 \times 10^{-7}$ cm^{-1}. Hence, a scale up of approximately three orders of magnitude is required for a gain of 10^{-4} cm^{-1}, corresponding to $N_i \approx 10^{14}$ cm^{-3}, or a total $NF(b^1\Sigma^+, v' = 0)$ density of $\sim 10^{15}$ cm^{-3}. In order to approach these densities in a flow system, it was necessary to consider completely different sources of fluorine atoms and HN_3 capable of producing torr-level partial pressures of these species in the flow.

1.   Generation of Gaseous HN_3

The principal constraint taken into account in the design of the HN_3 generator was that at no time was the vapor to condense, nor was the HN_3 partial pressure to exceed 100 torr. This constraint was applied strictly as a safety precaution, since condensed HN_3 is known to be unpredictably explosive. The 100-torr limit placed on the pressure was to insure that condensation could occur nowhere in the system at room temperature. The vapor pressure of liquid HN_3 is not well known; safe operation with gaseous HN_3 pressures as high as 200 torr have been reported, however.*

---

*A.P. Baranavski, private communication, Naval Research Laboratories, 1981.

Either of two basic concepts may be applied to the generation of large scale flows of HN_3. First, a large ballast tank might be filled with HN_3 to a pressure of ~ 100 torr; the tank would then be evacuated through the reactor during a run. Assuming that in the reactor the gases passed through a cross-sectional area of 5 cm^2 at a linear velocity of 5000 cm s^{-1}, a partial pressure of 1 torr of HN_3 would correspond to a flow rate of ~ 1 mole s^{-1}. At this flow rate, a ten-minute run would evacuate a tank with a volume of ~ 100 ℓ. Clearly, this approach is intractable from the standpoint of both safety and ease of operation. A more feasible idea is the use of a device which continuously generates HN_3 for consumption in the reactor. Such a generator would simply be a scaled-up version of the H_2SO_4/NaN_3 reactor used in the preliminary experiments.[10] A diagram of this smaller-scale generator is shown in Fig. 3. Solid NaN_3 is contained in a three-necked flask, as shown. A 75% aqueous solution of H_2SO_4 is added dropwise to the NaN_3 via a long section of 1-mm stainless steel tubing attached to a syringe. The tubing enters the flask through a rubber septum. The syringe is driven at a metered rate by a syringe pump (Sage Instruments). The HN_3 vapor produced by the reaction is swept from the reactor by a stream of argon. The reactor effluent is passed through a trap containing anhydrous $CaSO_4$ ("Drierite") to remove unwanted water vapor from the stream prior to being vented to a fume hood (the entire apparatus was positioned behind a blast shield inside the hood). For a typical chemiluminescence experiment, the H_2SO_4 flowed at ~ 10 drops per minute, resulting in an HN_3:Ar proportion in the effluent stream of ~ 1:10. Since the generator was operated at atmospheric pressure, the partial pressure

17
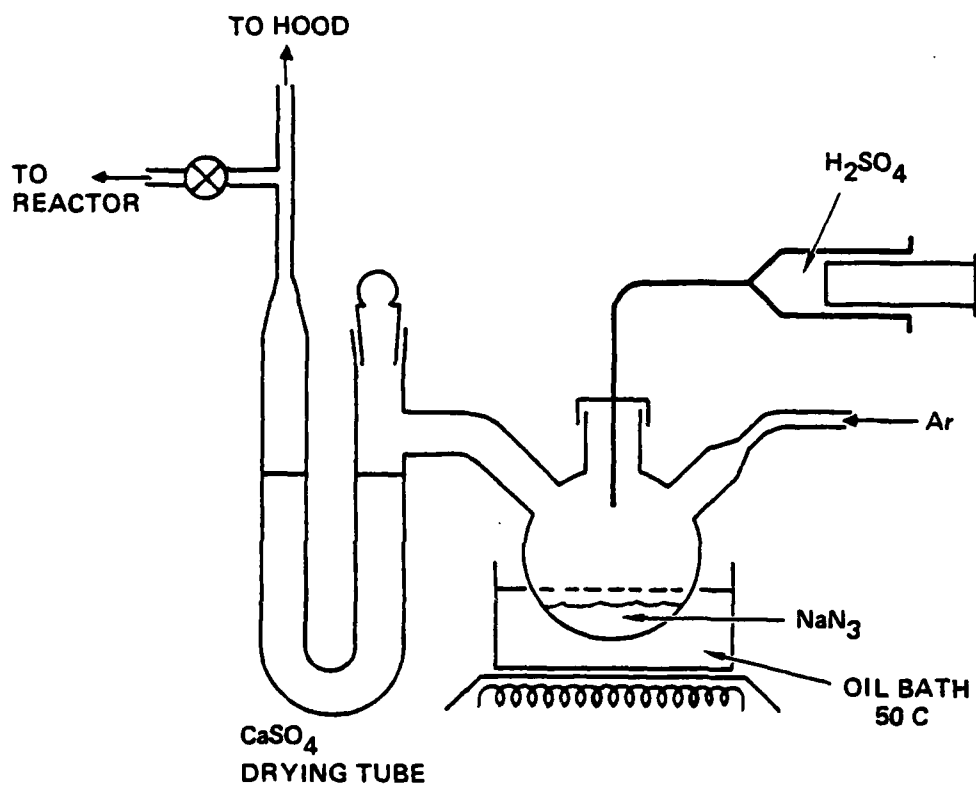
Figure 3. Small-scale HN₃ generation of gas phase HN₃.

18

of HN_3 in the vessel was ~ 80 torr. As an additional precaution against the formation of condensed HN_3, the reaction vessel was partially immersed in an oil bath heated to ~ 325K. The HN_3/Ar mixture was bled into the vacuum system through a metering valve for use in the chemiluminescence experiments.

This small-scale generator produced flows of HN_3 (in the reactor) on the order of 0.01 mmol s^{-1}. Given the extremely slow flow rates of H_2SO_4 and Ar used, it seems likely that it would be capable of generating perhaps four times this flow rate at its performance limit. Hence, an increase by a factor of ~ 25 was required for the scaling experiments. For stoichiometric reactions between H_2SO_4 and NaN_3, the consumption rates of these two species would be 1.6 cm^3 min^{-1} of concentrated H_2SO_4 (96%) and 3.9 g min^{-1} of NaN_3. Tests with the small scale generator showed that H_2O dilution of the H_2SO_4 was necessary to produce an appreciable reaction rate with the solid NaN_3; either the concentrated H_2SO_4 was too viscous to adequately wet the solid, or some dissolution of the azide salt is required. Hence, the total $H_2SO_4:H_2O$ = 3:1 flow rate in the scaled generator would be ~ 2.1 cm^3 min^{-1}.

In scaling the small reactor, several additional constraints must be accounted for. First, the rate may be limited by wetting of the NaN_3, i.e., diffusion of the acid solution through the solid. Also, it would be undesirable to use a carrier gas in an atmospheric pressure generator for the large system, since the small proportion of HN_3 in the carrier would require a substantial pressure (~ 10 torr for 1 torr of HN_3) in the flow reactor. The apparatus constructed to accommodate these constraints and produce the large HN_3 flow rates required is shown in Fig. 4. The reaction chamber consisted of

19
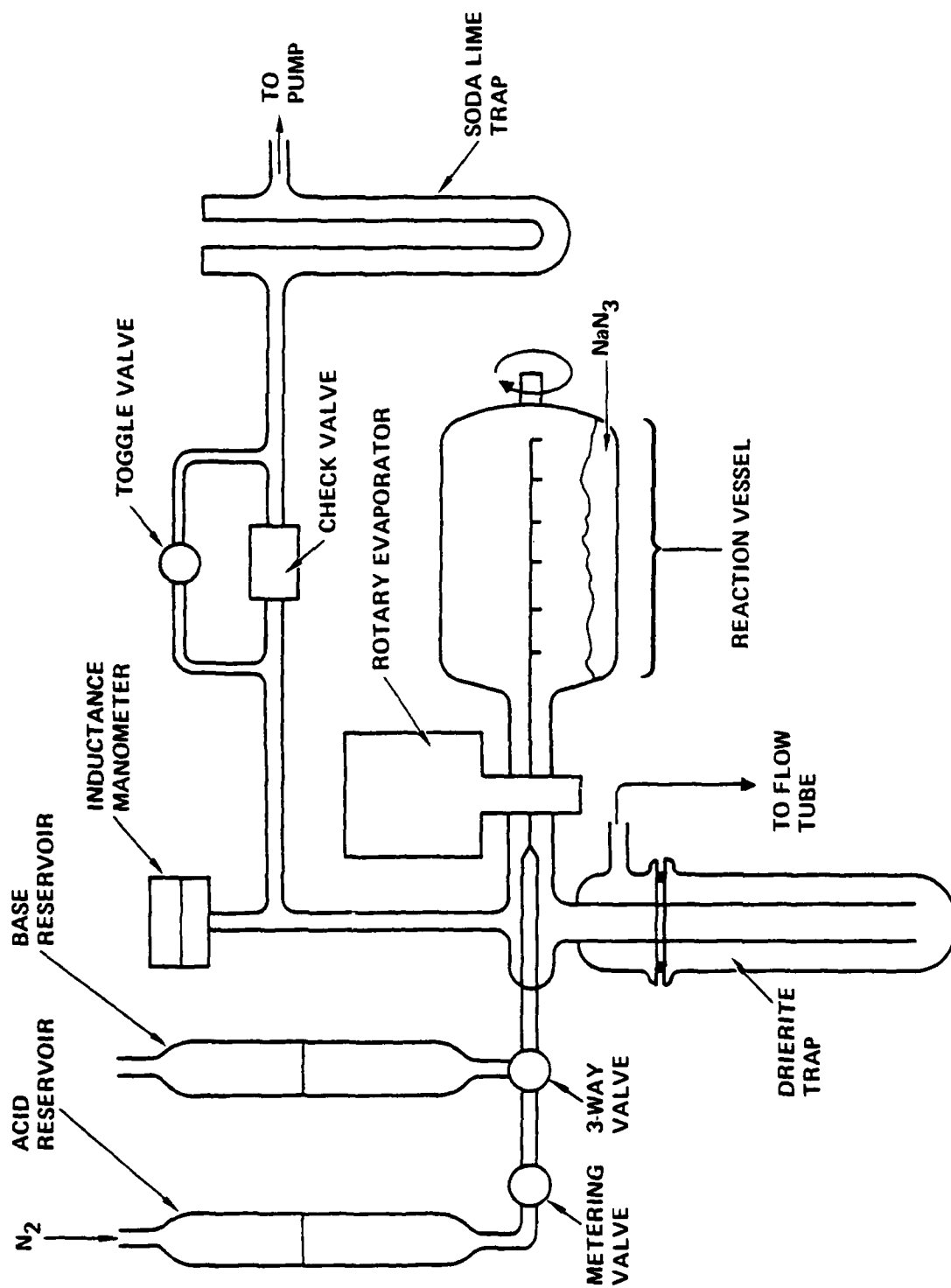
Figure 4. Apparatus for the generation of large flows of gaseous scale HN_3.

20

a large Pyrex flask ($\sim$ 2 ℓ) which was rotated by a common rotary evaporator (Buchler Instruments). Rotation served to tumble the NaN_3, in order to produce a more uniform wetting pattern. The aqueous acid solution was contained in a reservoir shown to the left of the figure, and was metered into the reaction vessel via a linear array of six droppers extending from a common feed line. The acid flow was regulated by a small metering valve. The tumbler-dropper design was the result of small-scale tests using water and NaCl. These tests showed the wetting pattern of the tumbled salt to be good, and indicated that for vacuum conditions, the dropper design with the liquid flow regulated by a valve was necessary for adequate flow control.

The reactor effluent passed through a large trap containing "Drierite" (anhydrous $CaSO_4$) prior to entering the flow system. The pressure in the reactor was continuously monitored with a Validyne inductance manometer, as shown in the figure. In addition to the normal path to the flow tube, a secondary vacuum system was attached to the generator for regulation of the reactor pressure and disposal of the HN_3 vapor in the reactor after a run. This system consisted of a large toggle valve (operated remotely by a simple chain), a trap containing soda lime (to reactively remove the HN_3 from the flow), and a small pump vented up the hood. Initially, a 100-torr check valve was installed in parallel with the toggle valve to insure that the pressure did not exceed this value; the check valve was eventually removed, however, since it continually malfunctioned. In practice, the pressure was very easily regulated with the toggle valve.

A second reagent reservoir (see Fig. 4) contained an aqueous basic solution, typically NaOH. Addition of this solution to the system was used to

21

rapidly quench the reaction. The basic solution was admitted upstream of the metering valve such that large amounts might be added rapidly. In practice, this system was used only to stop the reaction at the end of a run. Both the acid and base solutions could be drained from the reservoir via a system which consisted simply of a three-way valve (which acted as an exit port) and a filter flask connected to the house vacuum system. The entire HN_3 reactor was constructed in the fume hood, and a Lucite blast shield erected in front of it. A photograph of the apparatus is shown in Fig. 5.

This generator design was quite successful in that it was found to generate copious quantities of gaseous HN_3. A reactor pressure of 100 torr was readily achieved, and could be easily regulated by variation of the acid flow and use of the toggle valve described above. Two systems were installed to monitor the flow rate of HN_3 produced by the reactor. The reactor effluent (from the Drierite trap) was admitted to the flow system via a large regulating valve. The monitoring systems were installed between the generator and this valve. First, a UV absorption system was used to measure the purity of the HN_3. The absorption was measured through a 1.0-cm-long cell, using the 253.7 nm line of a mercury lamp as a light source. The HN_3 extinction coefficient is 17.9 ℓ mole^{-1} cm^{-1} at this wavelength,[16] yielding an absorption of ~ 20% for a pressure of 100 torr. Absorptions corresponding to essentially pure HN_3 were observed for experiments at higher HN_3 flow rates. Experiments at lower flow rates (at the beginning of each run) indicated smaller HN_3 percentages, suggesting that some air was still being purged just after start-up. The second monitoring system measured the flow rate of HN_3 admitted to the flow reactor. Standard mass flowmeters could not be used in this case,
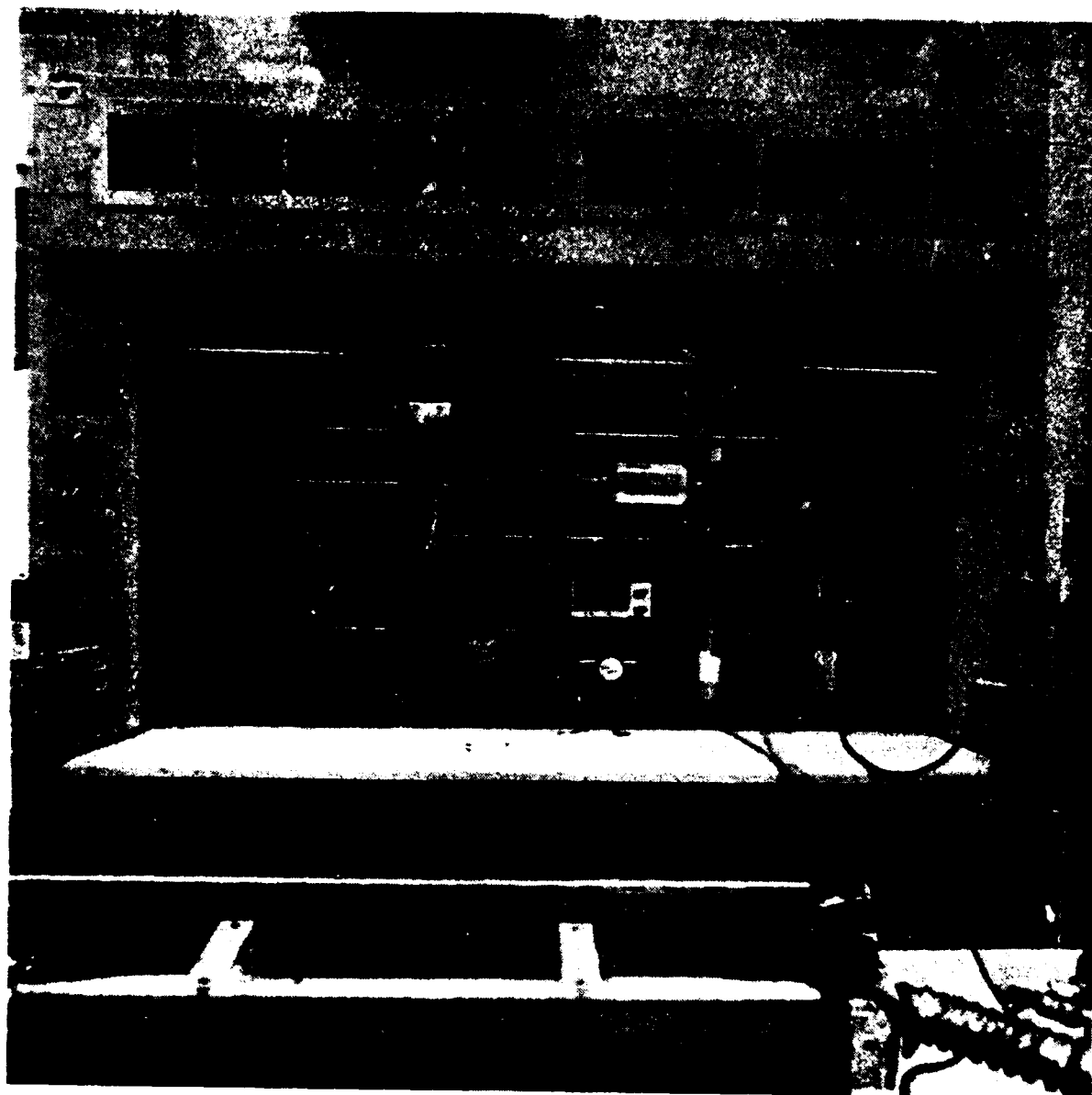
Figure 5. Photograph of the large-scale HN$_3$ generator.

since the back pressure was only 100 torr (close to the value of the limiting pressure drop across such a meter). Hence, HN_3 flow rates were monitored by measuring the pressure drop down a 5.0-cm length of 0.6-mm tubing using an MKS Baratron differential capacitance manometer. The pressure drop was calibrated against known flow rates of N_2 for a back pressure of 1.0 atm. The N_2 flow rates were calibrated against HN_3 (back pressure 100 torr) by measuring the time required to fill a fixed volume. Large-scale tests of the HN_3 generator showed that HN_3 flow rates well in excess of 0.3 mmol s^{-1} could be achieved, yielding partial pressures in the flow tube greater than 300 mtorr at ~ 5000 cm s^{-1}. The experiments indicated that substantially larger flow rates could be achieved by increasing the H_2SO_4 flow.

2.   Large-Scale Discharge-Flow Reactor

Fluorine atom flows of the magnitude required for the experiments might be generated by a precombustor, a kilowatt microwave discharge, or by a high current DC discharge through parent gases. Of these three, the DC discharge is the most readily applicable to a laboratory scale apparatus. The discharge unit used in the F + HN_3 experiments was originally part of a small CW HF laser based on a design by Hinchen[17] and subsequent refinements by Spencer.* The device consisted of a Pyrex discharge tube surrounded by a water-cooled jacket (Lucite). Eight nickel rods arranged in an annulus about the centerline of the tube formed the cathode of the discharge. The anode was simply the other stainless steel endplate of the tube. The power supply used

---

*D.J. Spencer, private communication, Aerospace Corp., 1975.

in the experiments was a Universal Voltronics 20-kV, 600-mA power unit. In
previous experiments with this system, fluorine atoms were produced by passing
the discharge through SF_6-He mixtures. The device produced an optimum concen-
tration of ⌄ 2 torr of atoms for flow rates of SF_6 = 4 mmol s^{-1} and He = 7.5
mmol s^{-1} at total pressure of 6.5 torr and a linear velocity of 6000 cm
s^{-1}.[19]

The DC discharge tube was connected to the flow reactor via a water
cooled section of copper tubing, 2.5 cm in diameter and 20 cm long. This
section acted as the anode of the discharge. It was positioned so as to
laterally offset the discharge tube from the flow reactor by ⌄ 9 cm. This
offset was necessary to isolate light generated in the discharge from the flow
tube. The entire discharge tube was mounted on an optical rail inside an
opaque Lucite box.

A simple linear design was adopted for the initial flow reactor; it
was a 22-mm-i.d. section of quartz tubing 1.0 m in length. The tube was
cooled by passing water through an outer jacket, also of quartz. The inner
surface was coated with halocarbon wax to protect against etching by the
fluorine atom stream. The tube was attached to both the discharge unit and
the vacuum system by Ultra-Torr "O"-ring fittings. Figure 6 shows a detail of
the connection to the anode of the discharge. For the initial experiments,
HN_3 was injected into the stream of fluorine atoms via a stainless steel ring
fabricated from 1.6-mm tubing. The ring was perforated with eight 0.5-mm
holes, positioned to inject the HN_3 upstream into the atom flow. The
regulating valve for control of the flow is shown just above the injector.
The injector assembly was electronically isolated from the discharge anode by

25
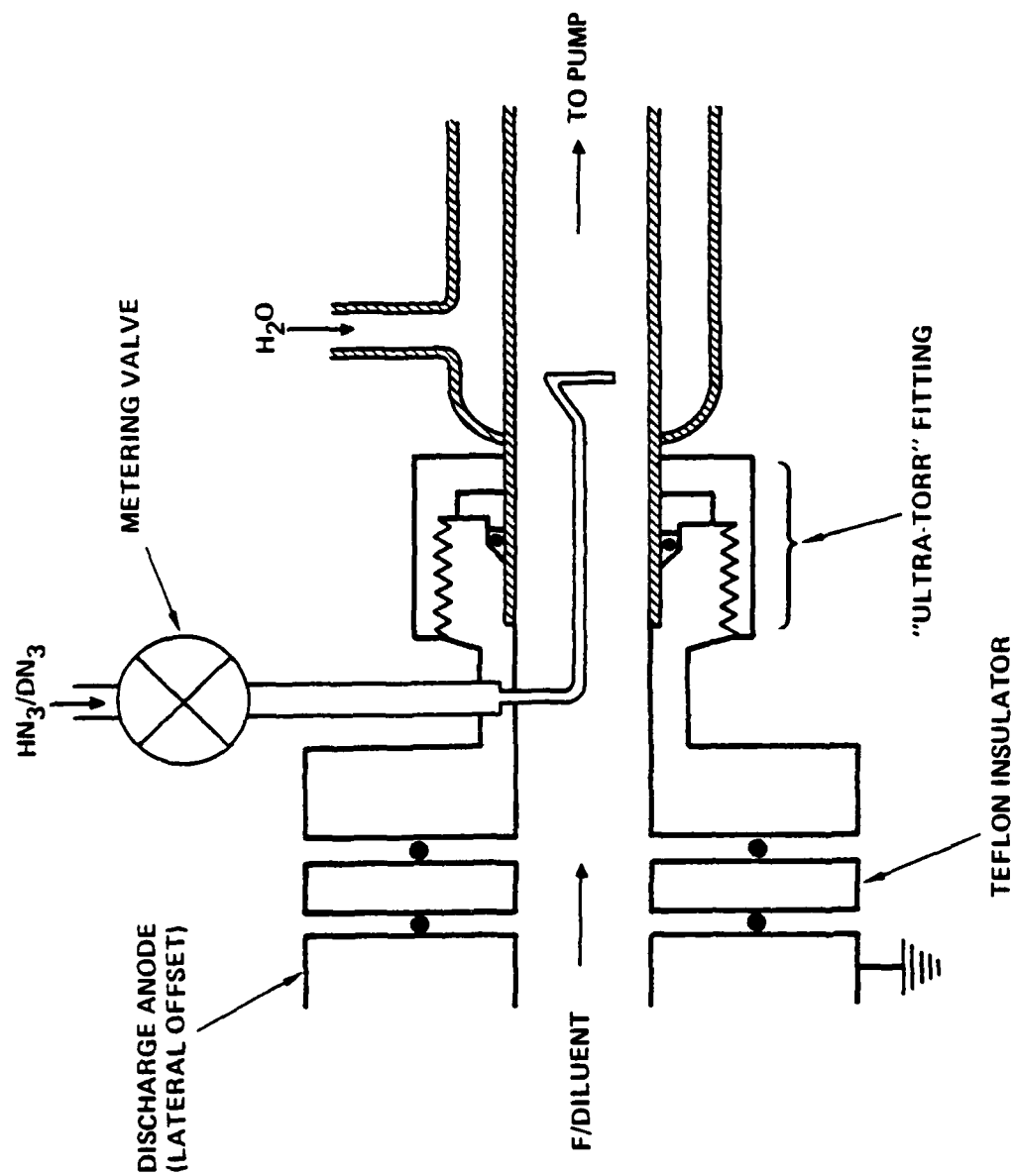
Figure 6. Detail of the linear flow tube showing the anode of the dc discharge, the ring injector for admission of HN₃ to the flow, and the water-cooled flow tube.

METERING VALVE

HN₃/DN₃

H₂O

TO PUMP

"ULTRA-TORR" FITTING

DISCHARGE ANODE
(LATERAL OFFSET)

F/DILUENT

TEFLON INSULATOR

a 6.0-mm-thick Teflon disc. This configuration effectively prevented arcing of the discharge to the injector.

The flow reactor was continuously evacuated by a Kinney 500-ft^3/min pump located under the laboratory building. A commercial scrubber capable of removing fluorine from the gas stream was installed on the exit port of the pump to prevent venting of the raw reactor effluent to the atmosphere. The gas pressure in the flow tube was measured with an MKS Baratron capacitance manometer. The flow rates of reagent gases other than HN_3 (SF_6 or F_2, Cl_2, He, N_2, and NO) were measured using a Tylan mass flowmeter. These flowmeters were calibrated for N_2 flows. Actual flow rates for the gases used were obtained using conversion factors supplied by the manufacturers. Measurements of the pressure rise caused by known flow rates of N_2 showed that the linear velocity in the 22-mm-i.d. flow tube was nearly 8000 cm s^{-1} for a pressure of 10 torr. Minor throttling of the pump reduced the velocity to 5000 cm s^{-1}. A photograph of the DC discharge and flow tube assembly is shown in Fig. 7.

Initial tests of the discharge unit were made using SF_6/He mixtures. The discharge was very unstable for these mixtures, and rather small concentrations of fluorine atoms were produced, as evidenced by the additon of Cl_2 to the stream via the injector. In this case, F atoms react rapidly with Cl_2 to produce Cl atoms, and recombination of the chlorine atoms results in a characteristic red emission:

$$F + Cl_2 \rightarrow ClF + Cl \tag{7}$$

27

Figure 7. Photograph of the discharge-flow apparatus.

$$Cl + Cl + M \rightarrow Cl_2^* + M \qquad\qquad (8)$$

$$Cl_2^* \rightarrow Cl_2 + h\nu \text{ (red)} \qquad\qquad (9)$$

Ganguli and Kaufman[18] have shown these reactions to be an effective chemiluminescent titration for fluorine atoms, and this method was used in our preliminary experiments on the F + HN_3 system.[10] Molecular fluorine was found to be far superior to SF_6 as a parent species for fluorine atoms. Addition of Cl_2 to a stream of discharged He/F_2 resulted in a very bright Cl_2 afterglow whose intensity could be easily monitored with a small monochromator (Oriel 0.16 m) and an uncooled RCA 1P28, photomultiplier tube. A typical titration curve (Cl_2 flow rate vs intensity) is shown in Fig. 8. The data shown yield an endpoint corresponding to a fluorine atom flow rate of 0.40 mmoles s^{-1}, or a partial pressure of about 450 mtorr for the conditions of the run. Comparison to the F_2 flow rate indicated that ~ 35% of the F_2 molecules were dissociated. Similar tests were performed for other F_2 flow rates and the results are shown in Fig. 9. The data indicated that the fractional dissociation remained approximately constant as the F_2 flow rate was increased. An F_2 flow rate of ~ 1 mmole s^{-1} produced nearly 1 torr of fluorine atoms. Further titrations were performed just after the apparatus had been changed to incorporate a larger injector (see Fig. 9). These resulted in a smaller fractional dissociation (~ 25%, curve B in the figure), presumably due to heterogeneous recombination of the atoms on the metal surface.
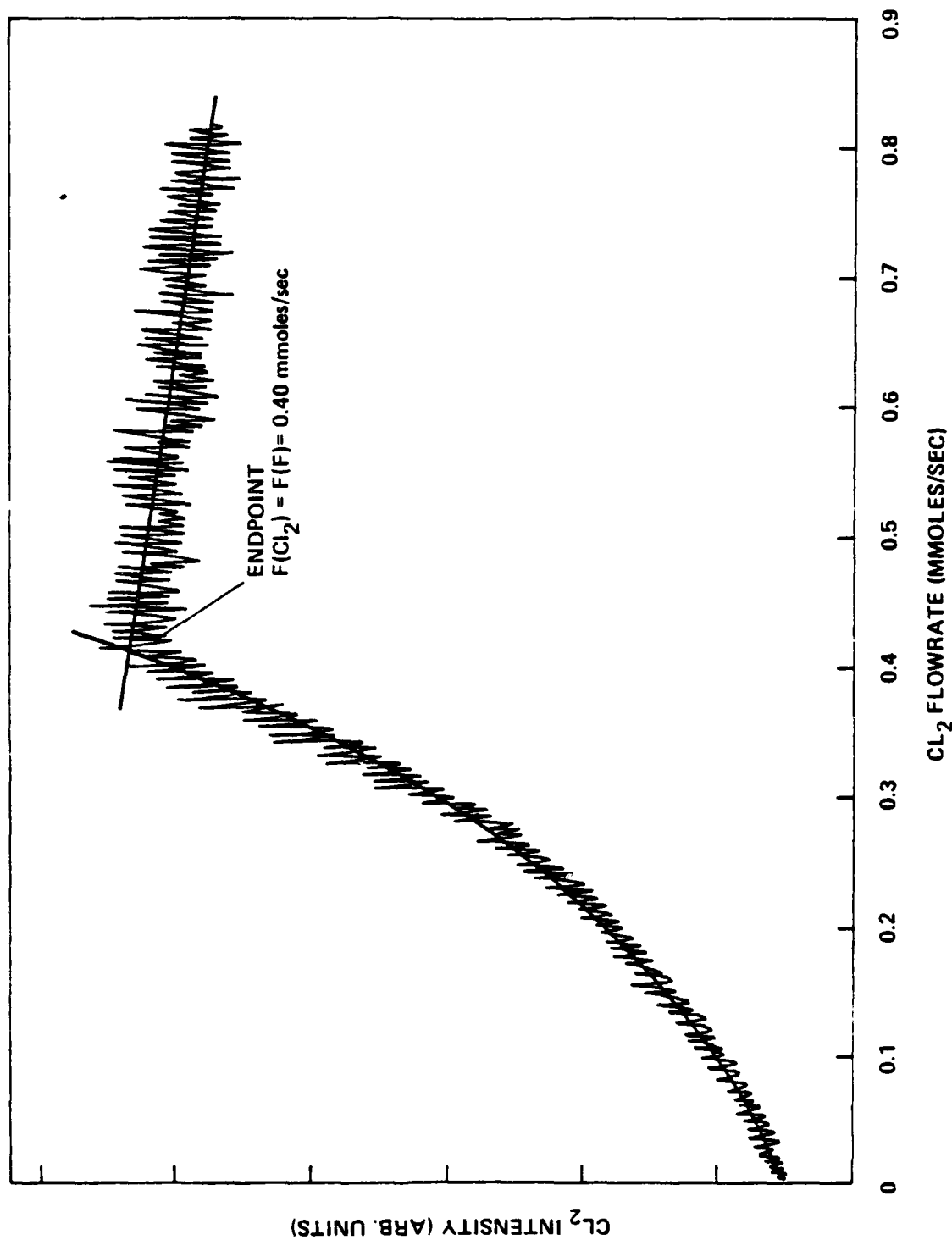
Figure 8. Results of a typical Cl_2 titration for the determination of the fluorine atom flow rate. (At the endpoint, the flow rate of Cl_2 is equal to the flow rate of fluorine atoms.)

30
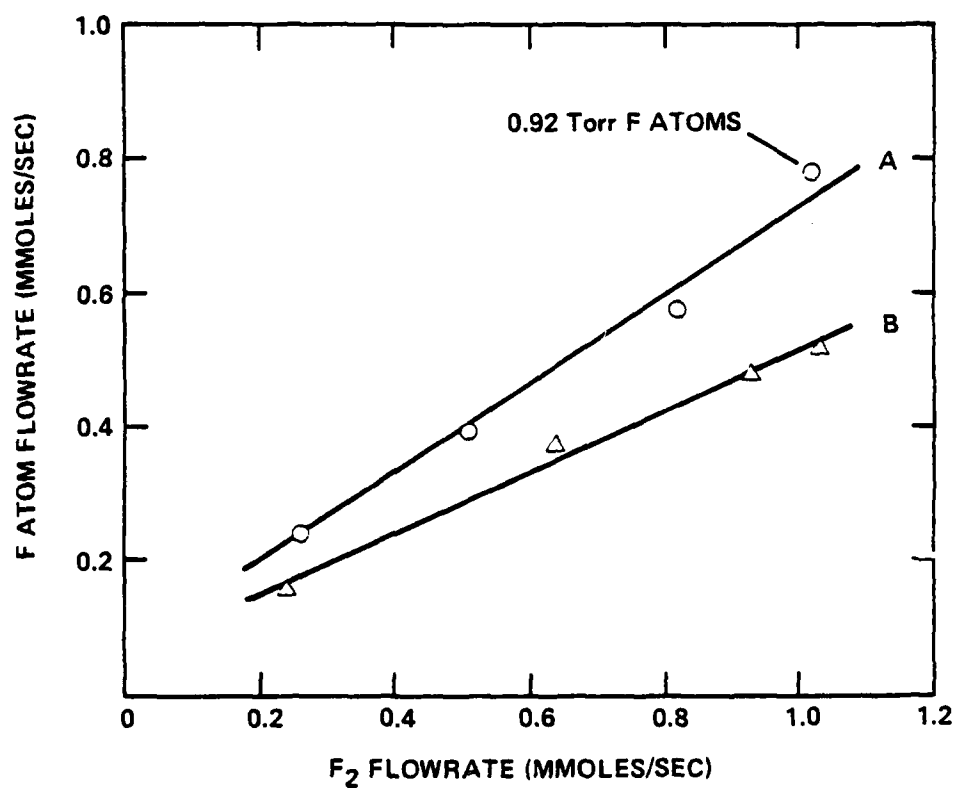
Figure 9. Variation of the fluorine atom flow rate with the F₂ flow rate in the discharge-flow apparatus. (Curve A represents data taken with the small ring injector in place; curve B shows data obtained with the larger tube injector in the apparatus.)

31

3.   Large-Scale Tests of the $F + HN_3$ and $F + DN_3$ Reactions

The first large scale tests were performed by adding HN_3 to the fluorine atom stream via the small ring injector described above. Additions of HN_3 to give a pressure rise of up to 250 mtorr above the ~ 5.0 torr pressure of the $F/F_2/He$ stream resulted in a brilliant yellow-green flame about 10 cm in length. About 10 seconds after the introduction of the HN_3, the emission rapidly collapsed to a short orange flame. We believe this behavior to be caused by thermal decomposition of the HN_3 inside the injector prior to reaction. The ring injector was itself engulfed in the flame and acted as the pricipal pressure drop in the system. It seems likely that the decomposition was caused by the relatively high pressure inside the injector, coupled with the temperature rise produced by the flame. This problem was completely eliminated by replacing the ring injector with an open-ended 5-mm-diameter tube pointed down the flow direction. Under these conditions, the regulating valve acted as the principal pressure drop and no decomposition flame was produced. Preliminary measurements of the $NF(b^1\Sigma^+)$ and $NF(a^1\Delta)$ emissions in the flame, near 529 nm and 874 nm, respectively, were made with uncooled RCA 1P28 and RCA 4832 (GaAs) photomultiplier tubes, respectively. Narrow band interference filters (bandwidth ~ 5 nm) were used to isolate the NF emissions in each case. For F atom partial pressures on the order of 0.5 torr, the data in the low HN_3 flow rate regime (< 0.1 mole s^{-1}) reproduced the small-scale flow tube results, i.e., the $b^1\Sigma^+$ emission rose to a faster than linear rate with increasing HN_3, and the $a^1\Delta$ emission rose roughly linearly, falling off at the higher flow rates. We note, however, that because of the

finite bandwidth of the interference filter, the near IR signal recorded may include emission from excited N_2 ($B^3\pi_g$) (the v', v" = 2,1 band of the first positive emission) in addition to $NF(a^1\Delta)$. Neither the visible nor near-IR signals appeared to peak and decay before all the F atoms were consumed (as indicated by titration with Cl_2 downstream).

Further experiments with the discharge-flow system were performed by using DN_3 instead of HN_3, so that quenching of $NF(a^1\Delta)$ by vibrationally excited HF (to produce $NF(b^1\Sigma^+)$) might be avoided. DN_3 was produced, using D_2SO_4/D_2O mixtures in the azide generator described above. Prior to the actual generation of DN_3, the generator and flow lines were passivated with D_2O for a period of ~ 24 hours. Infrared analysis of the generator effluent under operating conditions showed the azide product consisted of > 90% DN_3.

$NF(a^1\Delta)$ emission produced by the F + DN_3 reaction was monitored with the 9-pin GaAs photomultiplier tube noted above. A narrow band interference filter centered at 875.9 nm was positioned in front of the PMT, and an aperture of 2.5 mm limited the light collection. Spectra of the F + DN_3 emissions were recorded both with and without the filter, using a 0.5-m monochromator (McKee-Pederson) and a cooled GaAs PMT. The spectra showed that the filter in fact transmitted only the $NF(a^1\Delta)$ emission near 874.2 nm and effectively blocked the nearby N_2 first positive emission. The light collection efficiency of the detection apparatus (uncooled GaAs PMT) was calibrated by using the O + NO reaction as a chemical actinometer. In this tchnique, a known concentration of O atoms is produced by adding NO (through the injector used for HN_3) to a stream of N atoms (produced by passing N_2 through the

33

discharge) until an endpoint is reached at the extinction of the afterglow. At the endpoint, the O atom flow rate is equal to the NO flow rate. Further addition of NO to the system produced NO_2 emission from the O + NO reaction, for which the absolute photon yield has been measured.[13] Measurements using this technique yield a parameter α which, when multiplied by the measured intensity, gives the flow rate of photons produced by the reaction. Since the $NF(a^1\Delta)$ intensity was measured at a given point in the flow tube, the photon flow rate can be equated to NA, where N is the $NF(a^1\Delta)$ number density in the emitting volume and A is the spontaneous emission rate $(0.18\ s^{-1})$.[2] Hence,

$$[NF(a^1\Delta)] = \alpha I/A \tag{10}$$

The value of α determined in the calibrations was quite reproducible, in the sense that calibrations were made at several points down the length of the linear flow tube, and each measurement gave the same value of α within the accuracy of the input parameters.

The intensity of the $NF(a^1\Delta)$ emission produced by the reaction rose rapidly with the initial addition of DN_3 to the stream of fluorine atoms, gradually rolling off to a peak value for DN_3 flow rates in excess of the F atom flow rate. The time decay of the excited NF in the direction of the flow was not rapid, the signal falling an order of magnitude over a distance of ~ 15 cm $(\tau_d \sim 2\ ms)$. The yields (relative to the DN_3 flow rate) measured at maximum intensity were extremely small, on the order of 5%. A number of observations suggested that this result was caused by slow mixing in the flow

34

reactor. First, visual observation of the flame (i.e., the green $NF(b^1\Sigma^+)$ emission produced by trace HN_3) indicated a sheath of high intensity surrounded by a low intensity core, presumably containing unreacted DN_3. Increasing the DN_3 flow rate lengthened the flame, but did not affect the peak $NF(a^1\Delta)$ intensity. Also, observation of the N + NO titration reaction (k = 10^{-11} cm^3 $molecule^{-1}$ s^{-1}) at the high flow rates used for the F + DN_3 system yielded endpoints which were measurable only at distances greater than 25 cm downstream of the injector. Use of a perforated sphere mixing element on the DN_3 injector (the open-ended 5-mm tube noted above) did not improve the results, and eventually it became very hot, leading to DN_3 decomposition as noted with the ring injector.

Hence, *mixing of the reagents appeared to be a fundamental problem,* in that mechanical mixing (as by the perforated sphere) required a pressure drop across the mixing element, resulting in catastrophic DN_3 decomposition as the uncooled element was heated by the reaction. Since the pressure in the system was necessarily on the order of 5 torr (the production of large concentrations of F atoms by the discharge required a large diluent flow), some form of mechanical mixing was necessary. Hence, at this point it was decided to replace the linear flow tube by a Hinchen-Spencer type water-cooled mixing head.[17]* This head is basically a transverse flow device in which the fluorine atom/diluent flow from the discharge is passed through a cooled channel 10 m wide and 3 mm high. Reagents were injected into the stream by a

---

*D.J. Spencer, private communication, Aerospace Corp., 1975.

35

linear array of holes, 30 on each of the top and bottom surfaces of the channel. For our experiments, the ends of the channel were closed by CaF_2 windows 5.0 cm in length.

A diagram of the transverse flow arrangement is shown in Fig. 10. The apparatus is quite similar to that described previously, except that the flow tube was replaced by the mixing head. Titrations of the fluorine atom flow in the reaction zone were performed by addition of Cl_2 as in previous experiments. These tests indicated that the discharge through F_2/He mixtures produced a maximum of 250 mtorr of fluorine atoms; discharges through SF_6/He produced a maximum of 100 mtorr of atoms. One advantage of the transverse flow arrangement was that the concentration of DN_3 in the reaction zone could be determined directly by UV absorption measurements near 205 nm. The light source used was a D_2 lamp whose output was folded through the reactor (see Fig. 10) to given an absorption pathlength of 20.3 cm. DN_3 present at 100 mtorr yielded an absorption of ~ 10% for those conditions.[16] These measurements resulted in a much improved measure of the true DN_3 flow rate. The DN_3 absorption was observed to be completely removed by the stream of F atoms from the discharge, indicating good mixing in the region probed by the experiments.

$NF(a^1\Delta)$ emissions produced in the reactor were observed by using the uncooled GaAs PMT as before. The light collection efficiency of the system was again calibrated, using the $0 + NO$ reaction,[13] and the initial $N + NO$ titration yielded a good endpoint in the observation zone, a further indication of good mixing. The time decay of the $NF(a^1\Delta)$ produced in the reactor was monitored by movement of the detector down the 5.0-cm observation window in the direction of flow. The experiments again indicated a relatively

36
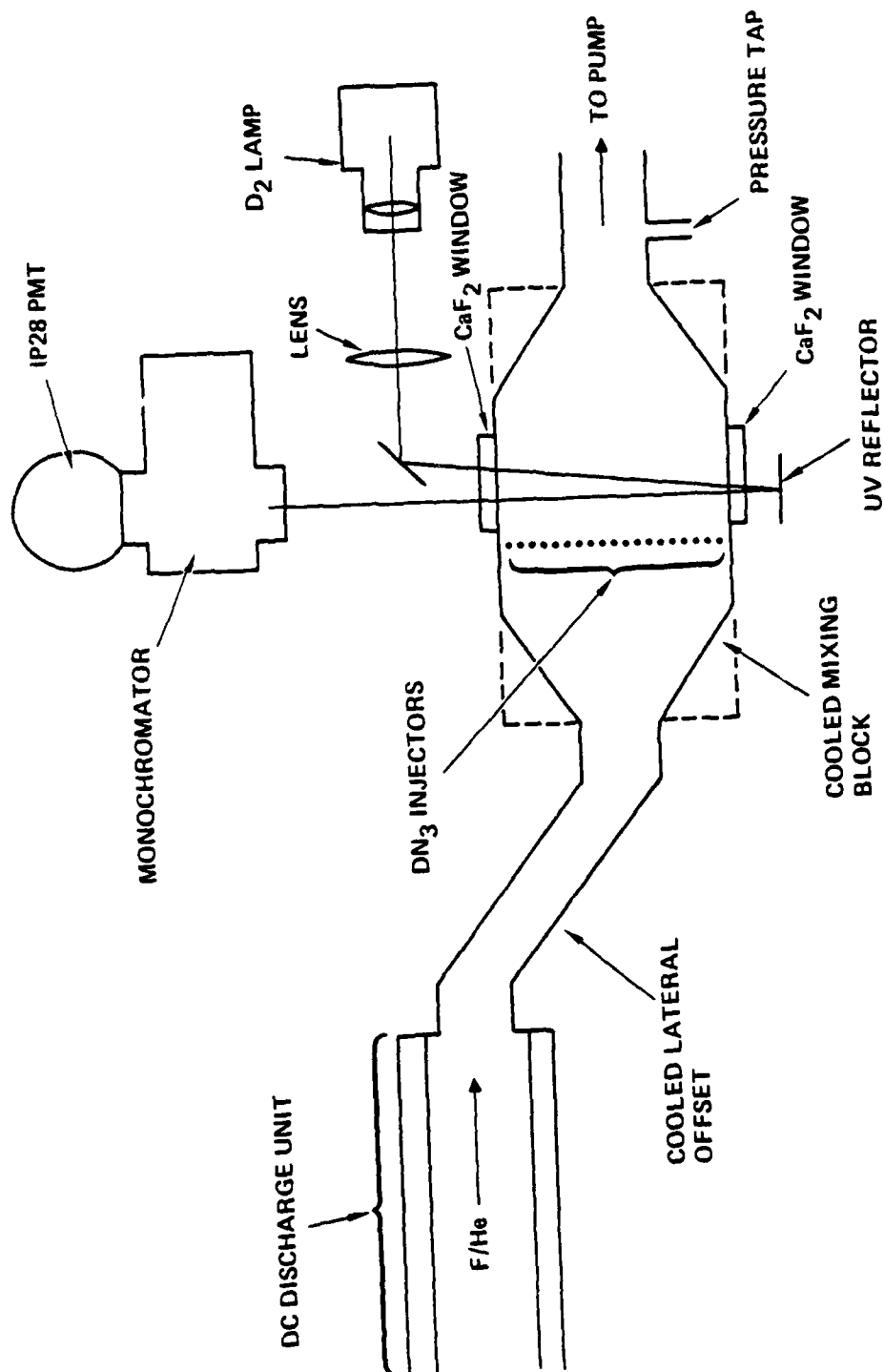
Figure 10. Schematic diagram of the 10-cm transverse flow apparatus, showing the optical train for direct detection of DN_3.

slow time decay, although faster than in the linear flow tube. For peak F and DN$_3$ concentrations, the excited NF(a$^1\Delta$) decayed in ~ 4 cm. Absolute concentrations of NF(a$^1\Delta$) were measured vs the DN$_3$ flow rate by recording the calibrated PMT response and the calibrated Baratron flowmeter reading with an x-y plotter. Typical results are shown in Fig. 11. The data shown were measured, using SF$_6$ as a source of fluorine atoms, such that the partial pressure of F atoms was ~ 100 mtorr. The temperature in the water cooled system was measured, using a Pt/10% Rh-Pt thermocouple, and found to be only a few degrees above ambient. The data show that the NF(a$^1\Delta$) concentration rises very rapidly with the addition of DN$_3$ to the system, reaching a flat peak at ~ 3.9 × 10^{14} cm^{-3} (~ 12 mtorr partial pressure) for a DN$_3$ concentration several times that of the fluorine atoms. Clearly, the NF(a$^1\Delta$) yield relative to the DN$_3$ flow rate declines rapidly with increasing DN$_3$ density. We note, however, that over most of the density regime indicated in the figure, fluorine atoms were the limiting reagent. Since, according to our postulated mechanism (reactions (3) and (4)), two F atoms are required to produce one NF(a$^1\Delta$) molecule, the limiting density in this and similar experiments was about 1.6 × 10^{15} cm^{-3} (~ 50 mtorr partial pressure). Relative to this value, the peak NF(a$^1\Delta$) yield indicated by Fig. 11 is ~ 24%. The fact that the yield at the F atom-DN$_3$ stoichiometry point was only one-third this value indicates that something was awry in the experiment, however, or that the simple model of Eqs. 3 and 4 does not hold at high reagent densities. If in fact the fluorine atoms were acting as a limiting reagent, the NF(a$^1\Delta$) density would level off or decline for DN$_3$ densities beyond the stoichiometry point.

38
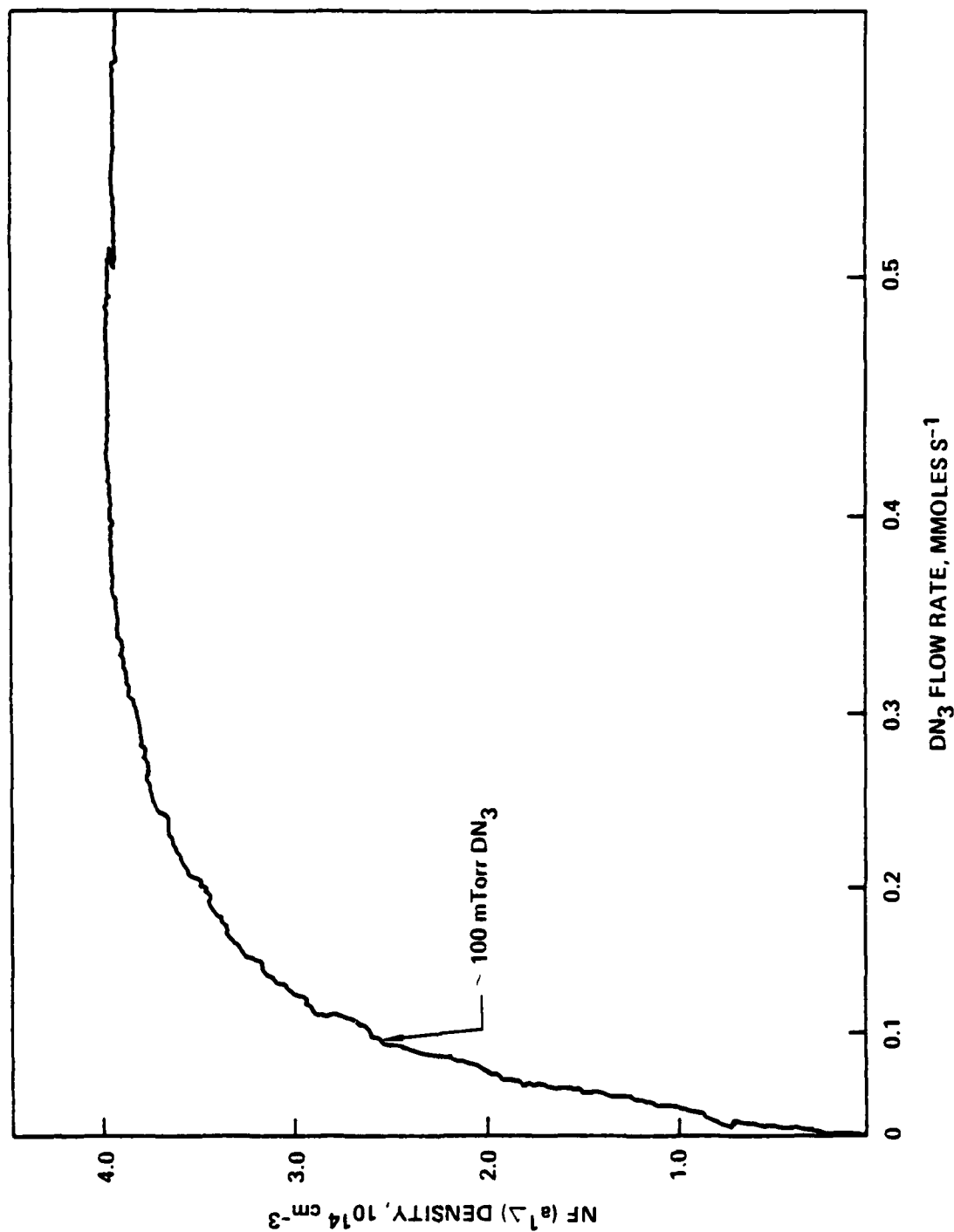
Figure 11. The absolute density of NF($a^1\Delta$) produced by the F+DN$_3$ reaction in the transverse flow apparatus vs the DN$_3$ flow rate. (The initial partial pressure of fluorine atoms was 100 mtorr.)

39

The spectrum of the emission produced in the transverse flow head in the vicinity of 874 nm was recorded with a 0.5-m monochromator and a cooled GaAs PMT. The PMT response was measured with a PAR photon counting apparatus, and the results are shown in Fig. 12. The $NF(a^1\Delta) \rightarrow X^3\Sigma^-$ transition is still the dominant feature, but N_2 first positive emissions have become quite strong. The spectrum exhibits no evidence of HF $v = 3 \rightarrow v = 0$ overtone emission in this region.

In order to more thoroughly investigate the discrepancy between the high density data and the simple model supported by our preliminary low density experiments, it was decided that experiments directed toward measuring the $NF(a^1\Delta)$ yield vs DN_3 flow rate would be performed for low reagent densities. For this purpose, our original flow tube apparatus[10] was reassembled.

4.   Low Density Yield Experiments

Low density yield experiments on the F + HN_3 reaction were performed with a cylindrical Teflon flow tube which has been thoroughly described in the literature.[10] In brief, the tube has an internal diameter of 3.1 cm. Atoms are created by passage of parent gas/diluent mixtures (in this case F_2/Ar) through a 100 W microwave discharge positioned ~ 50 cm upstream of the fixed observation port. HN_3 entered the system through a movable slide tube internal to the Teflon flow tube; the outer surface of this tube was Teflon coated to prevent excessive atom recombination. Movement of the slide allowed time resolution of the emissions observed at the view port.

40

865 nm   870 nm   875 nm

$NF \, a^1\Delta \rightarrow X^3\Sigma^-$

$N_2 \, B(^3\Pi_g) \rightarrow A(^3\Sigma_u^+)$
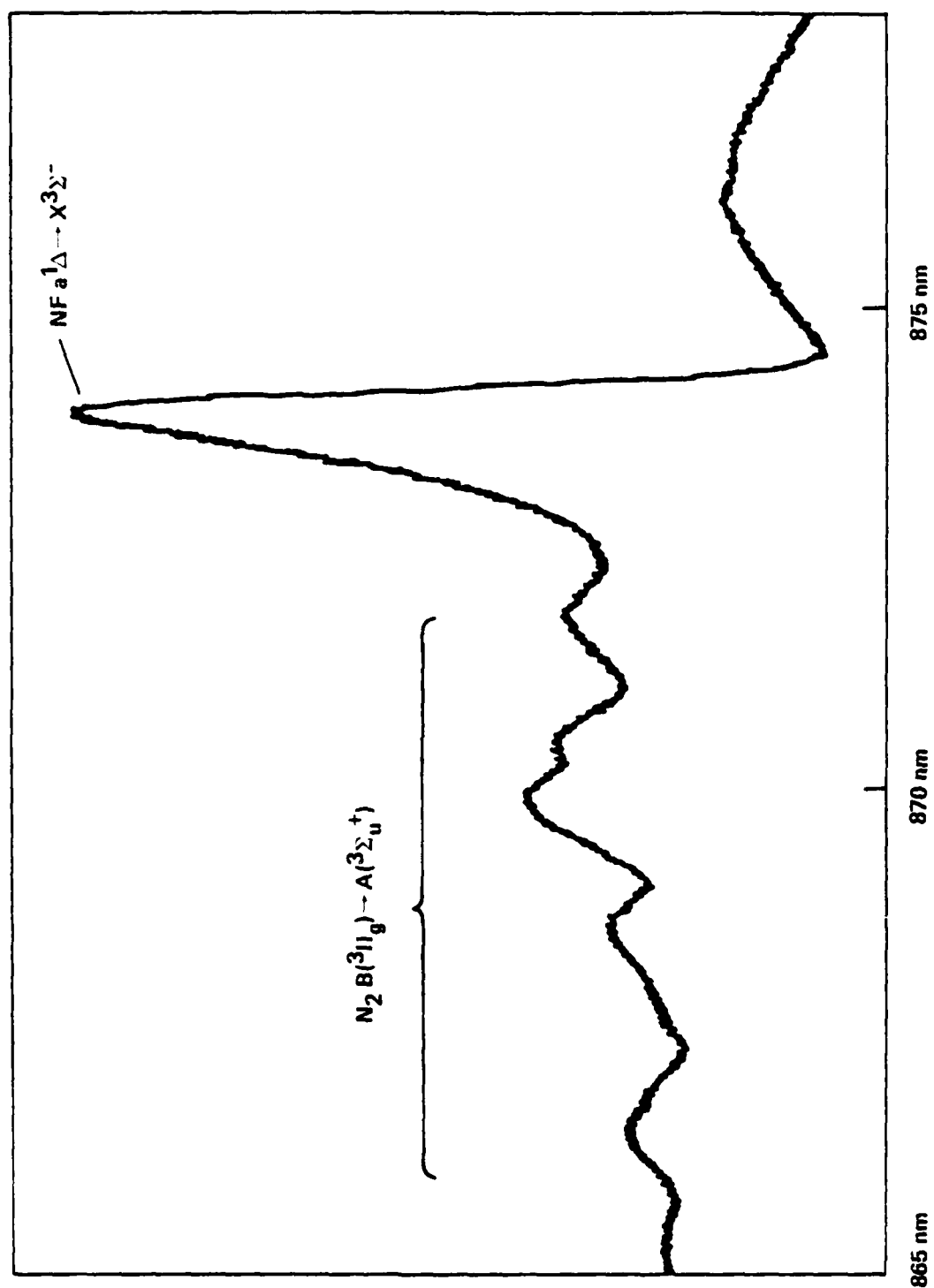
Figure 12. Spectrum of emission in the vicinity of 870 nm produced by the the F+DN$_3$ reaction in the transverse flow apparatus. (The spectrum shows contributions from both excited N$_2$(B$^2\pi_g$) and NF(a$^1\Delta$).)

41

The fluorine atom densities produced by the microwave discharge were again calibrated using the Cl_2 titration. These tests indicated that nearly 100 mtorr of F atoms could be produced for large F_2 flows. In the first experiment in which the apparatus was used, HN_3 was obtained from the large-scale generator, with the goal of probing the reaction at initial HN_3 pressures of 10 to 50 mtorr and total pressures on the order of 1.0 torr. After the very first such experiment, however, an explosion occurred in the laboratory during clean-up of the HN_3 generator. The explosion occurred approximately one hour after the run, and was apparently caused by condensed HN_3 in the reaction vessel. At this point, experiments on the F + HN_3 system ceased, pending a satisfactory re-design of the generator to insure complete removal of the HN_3. Several weeks were spent on designing and testing a removal system based on reaction of HN_3 with aqueous HNO_2. The products of this reaction are H_2O and the innocuous gases N_2 and N_2O. Although preliminary tests indicated that such a system was feasible, it was apparent that assembly of a generator incorporating this system would be a sizable engineering effort well outside the scope of the program. Hence, all further experiments were performed with the small-scale atmospheric pressure generator described above and shown in Fig. 3. This generator was capable of producing HN_3 pressures in the flow tube as large as 20 mtorr.

Emissions produced within the flow tube were observed through the fixed observation port, which was a 2.5-cm-diameter CaF_2 window sealed to the tube via a Viton "O" ring. The emission was dispersed by a 0.5-m monochromator and detected by the cooled GaAs PMT and photon counting system. The light

42

collection efficiency of the system was calibrated, using the O + NO reaction
as described above. The calibration procedure yielded a value of α (see Eq.
(10) above) in fair agreement with previous experiments using this
apparatus. Photon yields for the production of $NF(a^1\Delta)$ were measured as a
function of several experimental variables. A number of techniques were used
in these experiments which should make the data more reliable than that
obtained in our preliminary measurements. First, a mass flowmeter was used to
measure the Ar/HN_3 flow rate, resulting in more precise knowledge of the HN_3
concentration in the system. Perhaps a more significant change was the
measurement of initial $NF(a^1\Delta)$ densities by extrapolation of the time decay of
the emission signal measured over many ms to t = 0. Since the emissions from
excited HF and N_2 decay rapidly in time, this technique effectively avoids the
problem of spectral overlap from these species. Furthermore, the effect of
additives on the $NF(a^1\Delta)$ intensity could be observed with greater clarity.

Figure 13 shows the exponential time decay of the $NF(a^1\Delta)$ emission
observed for several experimental conditions. The lowest intensity data
(closed cicles) indicate an $NF(a^1\Delta)$ decay rate $\lambda_d = 243 \ s^{-1}$. The next higher
curve (open circles) represents data taken with ~ 223 mtorr of CO_2 added to
the system. It is clear that the addition of CO_2 significantly enhances the
$NF(a^1\Delta)$ intensity (by more than a factor of 2 at t = 0), while not appreciably
affecting the decay rate. Addition of still more CO_2 had little effect

43
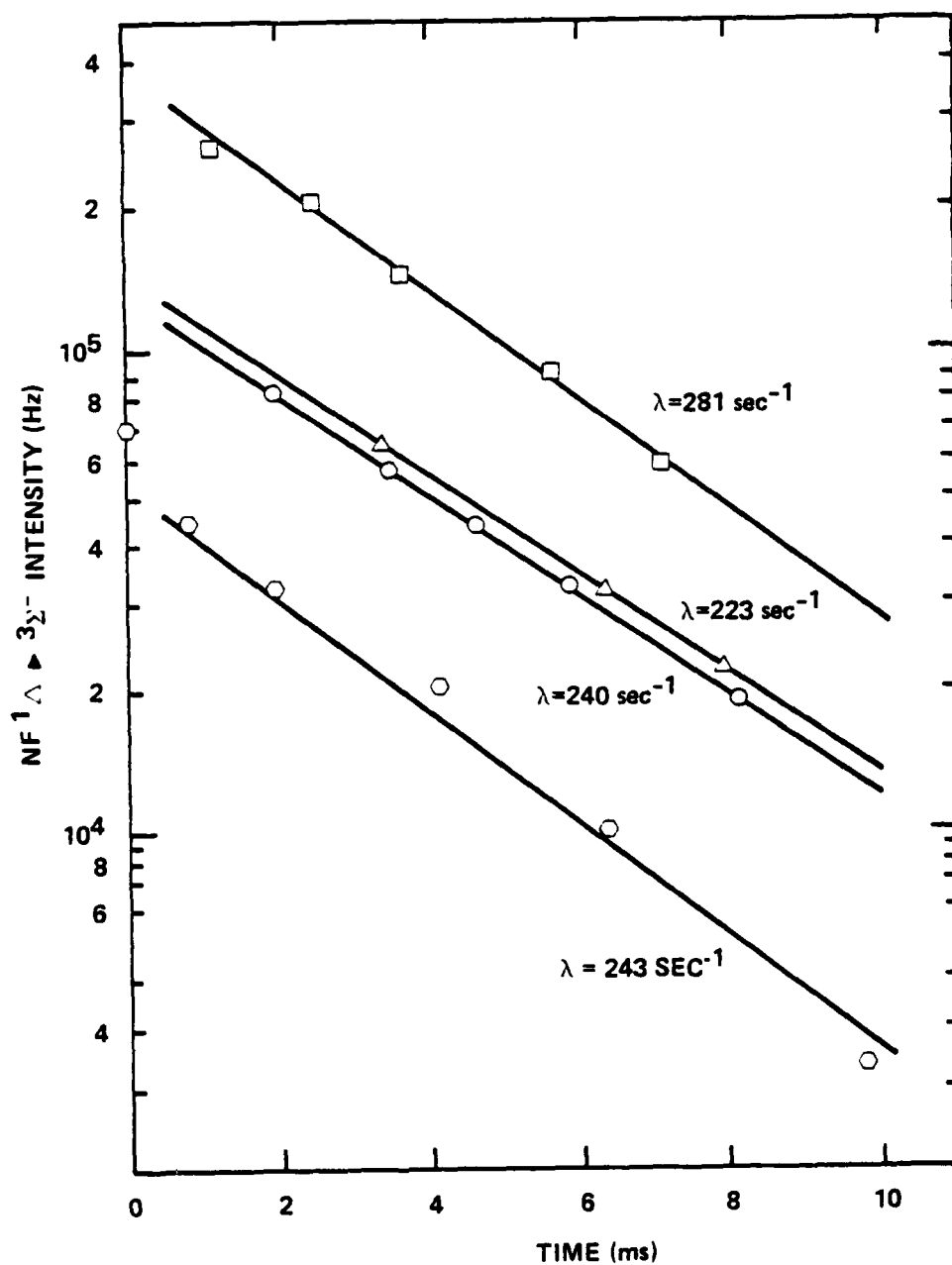
($\bullet$), $P(HN_2)=2.63$ mtorr, $p(CO_2)=0$; (o), $P(HN_3)=2.43$ mtorr, $P(CO_2)=233$ mtorr; ($\square$), $P(HN_3)=2.22$ mtorr, $P(CO_2)=297$ mtorr; ($\blacksquare$), $P(HN_3)=20.9$ mtorr, $P(CO_2)=268$ mtorr.

Figure 13. Time decay of $NF(a \cdot \Delta)$ emission produced in a low density flame.

44

(open squares). Increasing the HN_3 flow rate while maintaining a moderate CO_2 pressure increased the $NF(a^1\Delta)$ intensity, but had only a slight effect on the decay rate (closed squares). Based on data such as this, it was originally thought that CO_2 enhanced the $NF(a^1\Delta)$ intensity by quenching vibrationally hot HF, which is itself a quencher of $NF(a^1\Delta)$. Were this hypothesis correct, the dramatic effect observed would indicate that in the absence of CO_2 a significant fraction of the $NF(a^1\Delta)$ is converted to the $b^1\Sigma^+$ state, as per Eq. 5 above. A similar effect on the $NF(a^1\Delta)$ intensity was observed, however, when SF_6 was added to the mixture. Hence, it seems more likely that the role of these additives is to stabilize an intermediate (N_3) and/or vibrationally relax the excited NF.

Photon yields for the production of $NF(a^1\Delta)$ by the $F + HN_3$ reaction were measured by extrapolating intensities measured downstream to $t = 0$, as discussed above, for flows including a moderate amount of CO_2. The data were obtained with a fixed monochromator slit width of 750 mm (spectral bandpass ~ 2.5 nm). Measurements were made for several HN_3 densities at two different fluorine atom flow rates. The results of these experiments are shown in Fig. 14. The data indicate a very rapid initial decline of the yields with increasing HN_3 density, leveling off somewhat for initial HN_3 pressures over 5 mtorr. The yield at $t = 0$ would appear to be near unity. We note that this result may be somewhat fortuitous, however, owing to the uncertainties of the input parameters used for the calibration. The yield for a given HN_3 density was significantly improved by increasing the fluorine atom pressure, as shown in the figure.
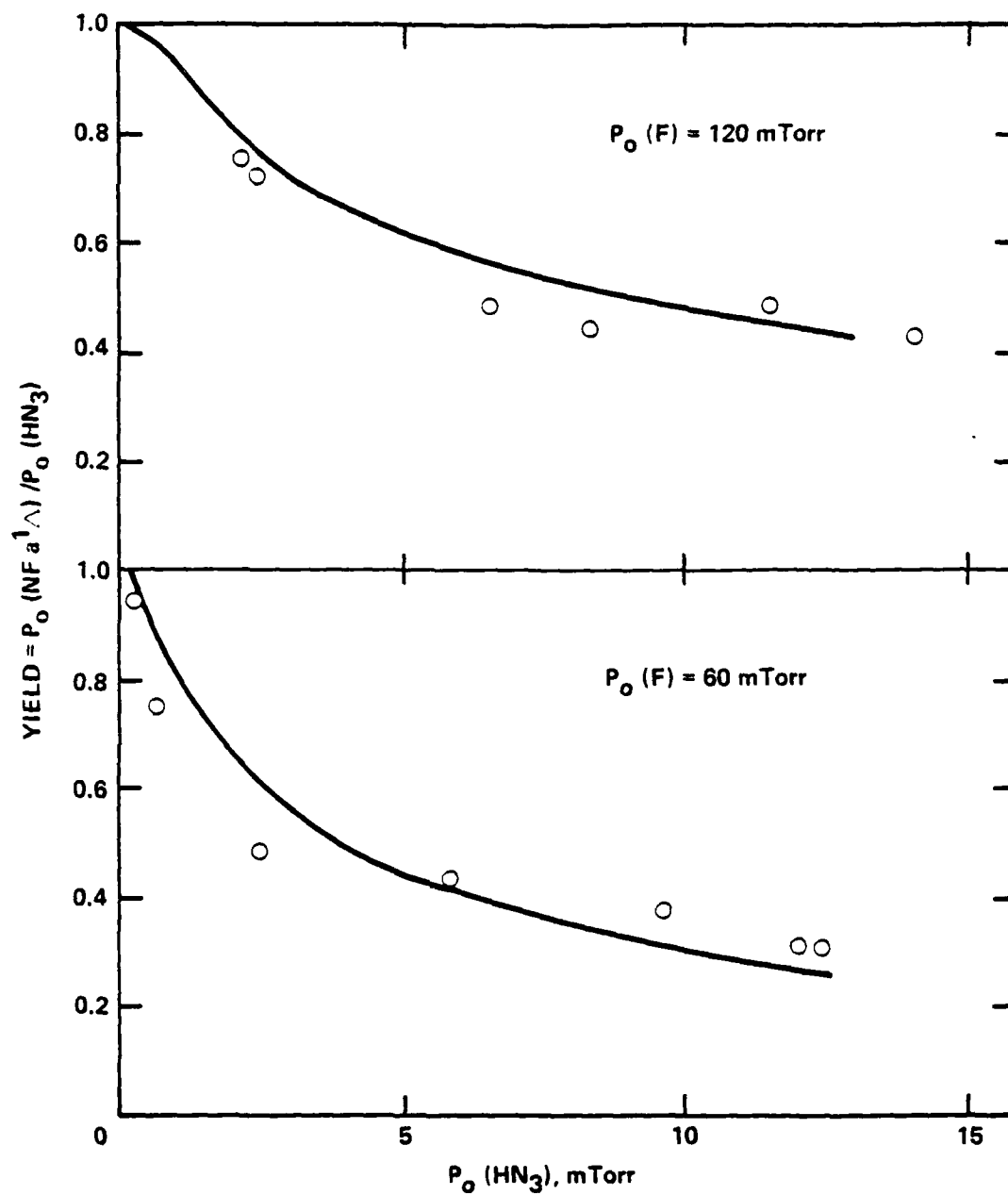
Figure 14. Photon yields for NF(a¹Λ) emission produced in a low density flame, for two initial fluorine atom pressures. (The solid lines represent results of the calculations described in the text.)

In order to investigate the chemical processes contributing to the yield data shown in Fig. 14, a very simple kinetic code describing the production of $NF(a^1\Delta)$ in the system was assembled. The model incorporated the following processes:

$$F + HN_3 \xrightarrow{k_3} HF + N_3 \tag{3}$$

$$F + N_3 \xrightarrow{k_4} NF(a^1\Delta) + N_2 \tag{4}$$

$$N_3 + HN_3 \xrightarrow{k_{11}} Products \tag{11}$$

$$N_3 + N_3 \xrightarrow{k_{12}} Products \tag{12}$$

The rate constants used in the model were $k_3 = 1.5 \times 10^{-11}$ cm^3 molecule^{-1} s^{-1},[19] $k_4 = 2 \times 10^{-12}$ cm^3 molecule^{-1} s^{-1},[10,19] $k_{11} = 2 \times 10^{-11}$ cm^3 molecule^{-1} s^{-1},[20] and $k_4 = 8 \times 10^{-11}$ cm^3 molecule^{-1} s^{-1}.[21] The coupled differential rate equations corresponding to processes (3), (4), (11) and (12) were integrated to yield time dependent values of the densities of F atoms, HN_3, N_3 and $NF(a^1\Delta)$ using a fourth order Runge-Kutta routine. The calculations were performed with a DEC 11V03 laboratory computer. Yield data obtained from the calculation (yield = peak $NF(a^1\Delta)$ concentration ÷ initial HN_3 concentration) are shown as the solid lines in Fig. 14. As is apparent from the figure, the

47

agreement between experiment and calculation is quite good, suggesting that processes (11) and (12) may account for the falloff in the yield with increasing density.

In both the small-scale experiments and the calculations, the initial density of fluorine atoms was many times greater than the density of HN_3. It is apparent that, since k_3 is much greater than k_4, a substantial concentration of N_3 builds up as the HN_3 density increases, allowing the side reactions (11) and (12) to occur. These side reactions are the probable sources of the N_2 first positive emission in the flame, which was observed to increase with increasing HN_3 density. Piper and co-workers have in fact reported the observation of N_2 $B^3\pi_g$-$A^3\Sigma_u^+$ emission from reaction (12).[22] Hence, the yield of $NF(a^1\Delta)$ falls off with increasing HN_3 density, but it seems likely that the NF population remains heavily inverted. Increasing the fluorine atom density enhances the rate of reaction (4) relative to reactions (11) and (12), and hence increases the yield, as shown in Fig. 14.

This simple model cannot predict the behavior at higher densities shown in Fig. 11. The calculations indicate that the only way for the yield to be high at this regime is for the rates of reactions (3) and (4) to become comparable, either by some dependence of the rate constants on the experimental condition (e.g., temperature), or by some artificial limit on both the rates, as in slow mixing. Under no circumstances does the model predict the strange stoichiometry apparent in Fig. 11.

The behavior of $NF(b^1\Sigma^+)$ observed in the experiments was in good agreement with previous measurements. The intensity of the $b^1\Sigma^+ \rightarrow X^3\Sigma^-$ emission increased quadratically with increasing HN_3 density (indicative of the formation of the $b^1\Sigma^+$ state by the pooling reaction, process (5)), reaching a peak at which an abrupt leveling off took place. This behavior is reflected in the photon yields measured for emission from $NF(b^1\Sigma^+)$, shown in Fig. 15. The peak yield measured was $\sim 5 \times 10^{-4}$. Two factors evident in the time decay of the emission may contribute to this low value. First, there appeared to be a mixing time of about 1 ms. Hence, extrapolation of the decay of the emission to $t = 0$ would yield an intensity substantially greater than the peak value observed. Second, the emission exhibited a very rapid decay, dropping nearly two orders of magnitude in only 4 ms. This result indicates a severe quenching problem. The most obvious potential quenchers are F atoms and F_2, which are present at much larger concentrations than other species in the mixture. For a fixed F_2 flow rate, variation of the F atom flow by changing the microwave power had little or no effect on the $b^1\Sigma^+$ intensity, indicating that quenching by fluorine atoms is negligible. The $b^1\Sigma^+$ intensity was found to be quite sensitive to the F_2 flow rate, however, indicating that molecular fluorine may be an efficient quencher of excited NF.

It is evident from the data shown in Fig. 14 that the efficient production of excited NF by the azide process should not scale to the high densities required for a high-energy chemical laser system. Although the experiments at higher densities (Fig. 11) indicated a substantial "yield" (relative to fluorine atoms), it is apparent that the chemistry responsible

49
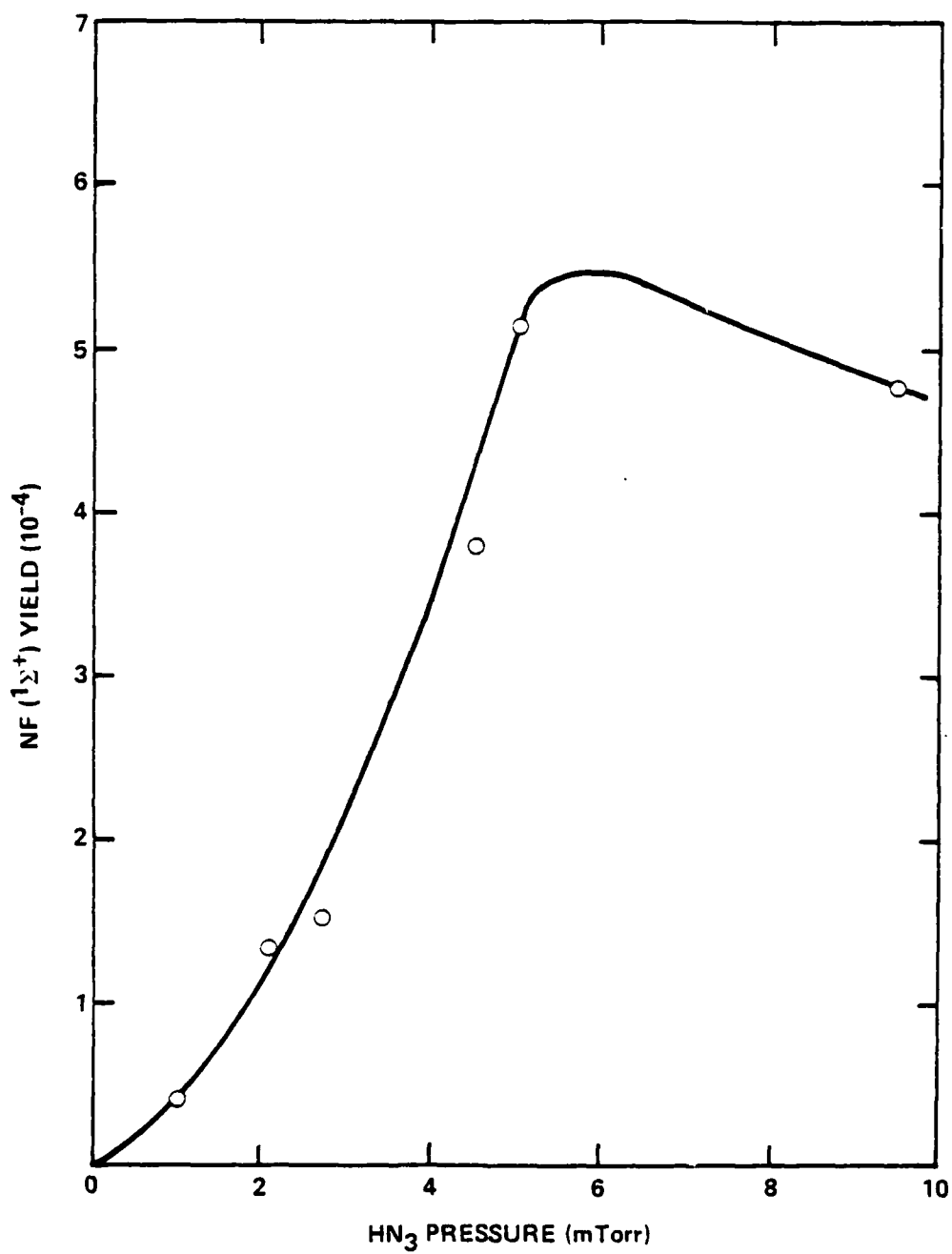
Figure 15. Photon yields for NF($b^1\Sigma^-$) emission produced in a low density flame.

for this result is quite complex. Hence, a second portion of this program was begun, directed toward assessing the utility of similar chemistry for the production of excited NCl, NBr, or NI.

III. CHEMICAL PRODUCTION OF EXCITED NCl, NBr, and NI

The results presented in Section I above indicated that, although the behavior of the F + HN_3 system at low densities is well inderstood, it does not logically extend to the high density regime. At high densities, the system appears to be more complex, and it seems likely that achieving a complete understanding of the mechanisms operative in this regime would require a considerable effort. Hence, before undertaking such a task, it is reasonable to ask if there are similar systems of greater promise which should be considered first. The most obvious such systems are azide mechanisms for the production of excited singlet NCl, NBr, or NI. These heavier nitrogen halides have potential advantages over NF in that their larger transition moments should yield higher gains for a given density of excited species. For example, comparison of the gain of an individual line in the $b^1\Sigma^+ \rightarrow X^3\Sigma^-$ transition of NCl to the analogous transition in NF, using Eq. (6) above, yields the following relationship:

$$\frac{G(NCl)}{G(NF)} = 2.15 \frac{A_{NCl}}{A_{NF}} \tag{13}$$

where rotational equilibrium at 350 K has been assumed and A_{NCl} and A_{NF} are the respective spontaneous emission rates. Since $A_{NCl}/A_{NF} \approx 35$,[2,12] the gain of the NCl transition is about 75 times the gain in NF for the same inversion density. Presumably a transition in NBr would have still higher gain, but for

such a heavy molecule, spin-forbidden production of ground state NBr $(X^3\Sigma^-)$ by the azide reaction (see Fig. 2) might be a serious consideration.

The reactions of Cl and Br atoms with N_3 hold further potential advantage over the NF case in their energetics. These reactions liberate ~ 66 kcal/mol and ~ 53 kcal/mol, respectively, sufficient for the direct population of the $b^1\Sigma^+$ states of NCl and NBr. In contrast, the exothermicity of reaction (4) is marginal for the production of NF $(b^1\Sigma^+)$, and in fact our experiments indicated that this state is generated predominantly by the resonant E-V process Eq. (5).

Azide mechanisms for the production of excited NCl and NBr were studied some years ago by Clark and Clyne.[9] These authors observed that the reactions of Cl and Br atoms with ClN_3 produced emissions from the $b^1\Sigma^+$-$X^3\Sigma^-$ transitions of NCl and NBr, respectively, with no evidence of the $a^1\Delta$ states. Strong N_2 first positive emissions were also observed, and free N_3 radicals were detected in absorption. From the presence of the N_3 radicals, the authors concluded that the Cl + N_3 reaction was much slower than Cl + ClN_3. Combourieu and co-workers[23] and Jourdain, et al,[21] obtained somewhat contradictory results in studies of the Cl + ClN_3 system using mass spectrometric techniques. No evidence of N_3 buildup was found in these experiments, and a computer fit to the data suggested a very fast rate for the Cl + N_3 reaction.

In small-scale discharge-flow experiments performed in our laboratory prior to the present program, chlorine atoms were added to the F + HN_3 system

as a logical extension of the titration of fluorine atoms with molecular chlorine. The introduction of chlorine to the system produced a brilliant red flame concentrated near the HN_3 injector. Scans of the emission spectrum revealed many bands of the $b^1\Sigma^+-X^3\Sigma^-$ transition in NCl.[24] In addition, emission bands in the vicinity of 1.1 μm were identified as the $a^1\Delta-X^3\Sigma^-$ transition of NCl.[24] In contrast to the NF experiments, the intensities of both the NCl $a(^1\Delta)$ and $b(^1\Sigma^+)$ emission varied linearily with the HN_3 flow rate, suggesting that both states may be direct products of the pumping reaction. An analysis of the time dependence of the emissions and their behavior as the reagent concentrations were varied suggested the following mechanism for the production of excited NCl:[19]

$$F + HN_3 \overset{k_3}{\rightleftharpoons} HF + N_3 \tag{3}$$

$$Cl + HN_3 \overset{k_{14}}{\rightleftharpoons} HCl + N_3 \tag{14}$$

$$F + N_3 \overset{k_4}{\rightleftharpoons} NF(a^1\Delta) + N_2 \tag{4}$$

$$Cl + N_3 \overset{k_{15}}{\rightleftharpoons} NCl(a^1\Delta, b^1\Sigma^+) + N_2 \tag{15}$$

Rate constants were deduced as follows: $k_3 > 1 \times 10^{-11}$ cm^3 molecule^{-1} s^{-1}, $k_{14} > 1 \times 10^{-11}$ cm^3 molecule^{-1} s^{-1}, $k_4 \approx 2 \times 10^{-12}$ cm^2 molecule^{-1} s^{-1},

and $k_{15} \approx 1 \times 10^{-11}$ cm^3 molecule^{-1} s^{-1} (from Jourdain, et al[21]). It is expected that the "hybrid" system reactions (3) and (15) should yield a superior performance relative to the analogous NF system (reactions (3) and (4)), since the more closely matched rates of these processes should reduce the steady-state concentration of N_3, and hence the effect of side reactions involving this species. Indeed, it was observed that addition of Cl_2 to the F+ HN$_3$ flame effectively quenched the N_2 emission while producing the red NCl flame.

In a similar manner, the addition of Br_2 to the F + HN$_3$ system was found to produce emissions from both the $b^1\Sigma^+$ and $a^1\Delta$ excited states of NBr. In this case, however, the N_2 first positive emissions were not quenched, suggesting that the Br + N_3 reaction may be slower than F + HN$_3$.

In view of these results, the objective of this portion of the program was simply to select the optimum halogen atom-azide molecule chemical system. Both the spectroscopic characteristics of the emitters and the kinetics of the pumping reactions were to be considered. Within this context, the following issues were addressed:

1. The production of N_3 radicals, and the possible utility of reagents other than HN$_3$ for this purpose.

2. The possible production of excited NI molecules by azide reactions.

3. The relative proportions of the $b^1\Sigma^+$ and $a^1\Delta$ states produced by the NCl and NBr systems.

4. The absolute yield of excited singlet molecules produced in each of the nitrogen halide systems.

With the exception of Task 1, the experiments were performed with the small-scale discharge-flow system described previously.[10]

1.   The Production of N_3 Radicals

To date, the only tested technique for observation of the N_3 radical in the gas phase involves optical absorption on the bands of the $^2\pi_g \rightarrow {}^2\Sigma_u^+$ transition near 270 nm.[25] This method was used by Clark and Clyne in their early experiments on ClN_3 systems.[9] Since the concentration of N_3 in our system is likely to be extremely small relative to the initial densities of the reagents, such an absorption experiment required a long absorption pathlength. Hence an apparatus was constructed to generate a long pathlength F + HN_3 flame, through which a beam of UV light might be passed two or more times. This apparatus, shown in Fig. 16, is essentially a transverse flow system in which HN_3 is admitted to a stream of halogen atoms via a 15.0-cm-long Teflon tube perforated with an array of holes. The flow reactor is a rectangular box with internal dimensions 15.0 cm × 2.0 cm. In the experiments, fluorine atoms were created by a passage of an F_2/Ar mixture through two parallel microwave discharge cavities as shown in the figure. Chlorine or
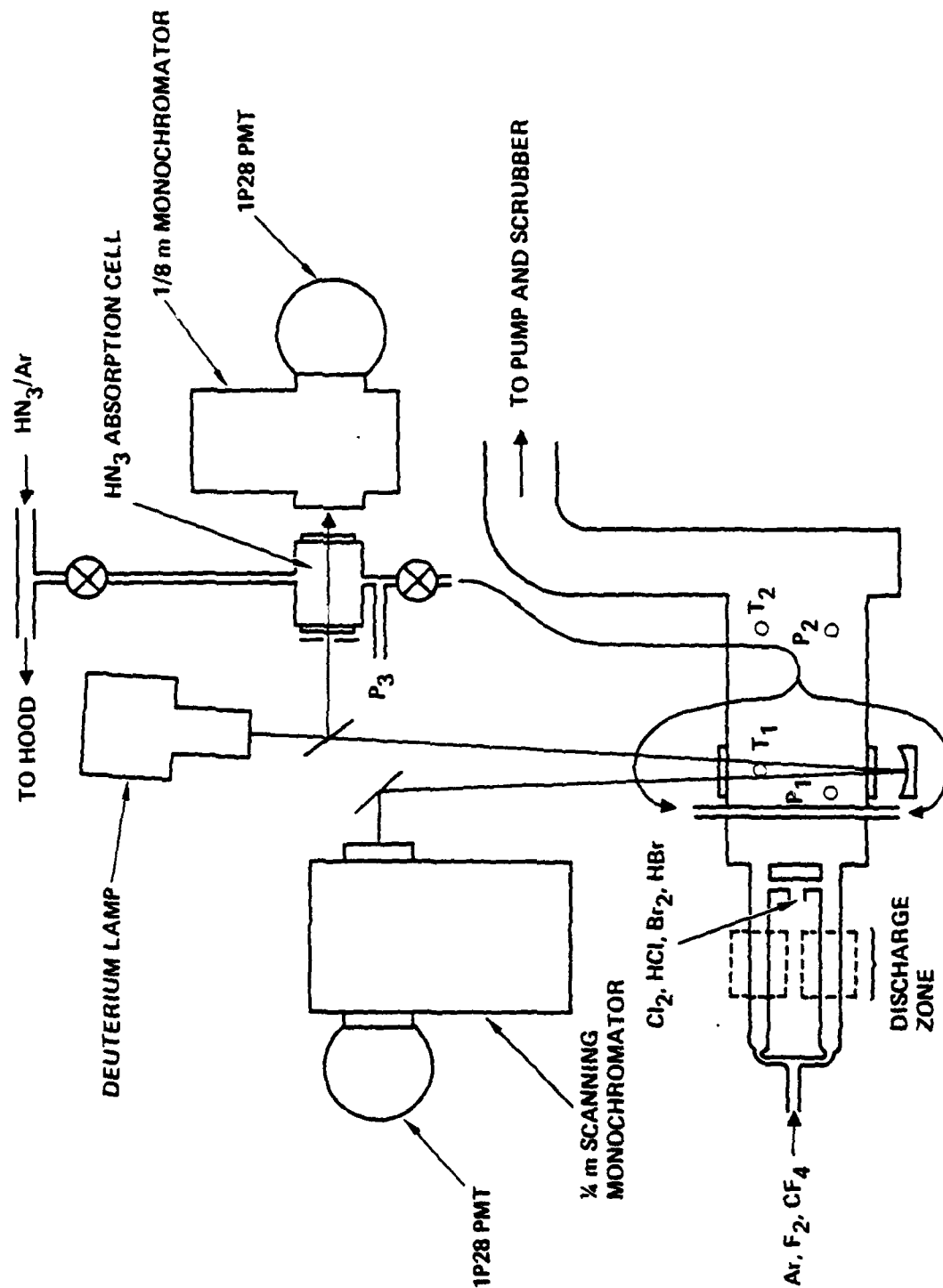
Figure 16. Schematic diagram of the 15-cm transverse flow apparatus, showing the optical arrangement used for detection of N_3 radicals. (T_1 and T_2 represent the positions of thermocouples, and P_1, P_2, and P_3 are pressure taps.)

57

bromine atoms could be produced by addition of the molecular halogens to the fluorine atom stream just downstream of each of the discharge zones. For these experiments, the position of the HN_3 injector was fixed just upstream of two 5.0-cm-long windows on each side of the flow reactor, as indicated in Fig. 16. The windows were CaF_2 rectangles cemented to the reactor wall. The temperature and pressure of the gas stream could be measured at either of two points in the reactor, as shown in the figure. Pressures were measured with an MKS Baratron capacitance manometer. The gas temperature was measured by using Pt/10% Rh:Pt thermocouples referenced to 273 K.

The light source used in the absorption experiments was an Oriel deuterium lamp. The source beam was collimated by an iris and two lenses prior to being reflected through the reactor twice by a concave reflector. The collimation of the beam was necessary so that both legs of the optical path might pass through the rather short flames generated in this apparatus (see below). The total absorption length was very nearly 30.0 cm. The light was dispersed by a Jarrell-Ash 0.25-m scanning monochromator and detected with an RCA 1P28 photomultiplier tube. In order to detect small absorptions, a null detector was incorporated into the apparatus so that its offset capabilities might be used.

For a total pressure of 500 mtorr, the linear velocity in the flow reactor was measured to be ~ 1200 cm s^{-1}. The tandem microwave discharge worked well in the sense that it was quite stable. Addition of Cl_2 to the discharged F_2/Ar stream yielded a visible Cl_2 afterflow which appeared to be uniform over the reactor volume.

58

Gaseous HN_3 was produced by using the small-scale generator discussed above and shown in Fig. 3. Nitrogen was used as a carrier gas for these experiments, and the generator was found to easily produce flows of 5%-10% HN_3 in N_2. ClN_3 was generated by passage of a dilute Cl_2/He mixture (3% Cl_2) over H_2O moistened NaN_3 suspended on glass wool in an U-tube.[9] Figure 17 shows a diagram of the apparatus constructed for this purpose. The effluent from the Cl_2-NaN_3 reactor was passed through a second U-tube containing Drierite to remove unwanted H_2O from the stream. As with the small HN_3 generator, the ClN_3 generator was operated at atmospheric pressure, a small amount being bled into the flow reactor via a metering valve. The entire apparatus was assembled in a fume hood behind a Lexan blast shield. This apparatus was found to efficiently convert Cl_2 to ClN_3, and conversion efficiencies (determined by UV absorption by the ClN_3) were measured to be 80% to 100% for some experiments.

The addition of HN_3 to the stream of fluorine atoms resulted in the familiar bright green flame dominated by NF $b^1\Sigma^+ \rightarrow X^3\Sigma^-$ transitions. The flame appeared to extend across the full width of the reactor, although its length was very sensitive to the reagent flow rates. The flame was typically shorter than the 5.0-cm length of the window. Addition of Cl_2 to the system produced the bright red NCl flame, with characteristics similar to those observed for NF.

Measurements of the absorption spectrum of the F + HN_3 flame in the 270-nm region indicated several features characteristic of N_3. These features were visible only for very low F atom flow rates with HN_3 in excess. The

59
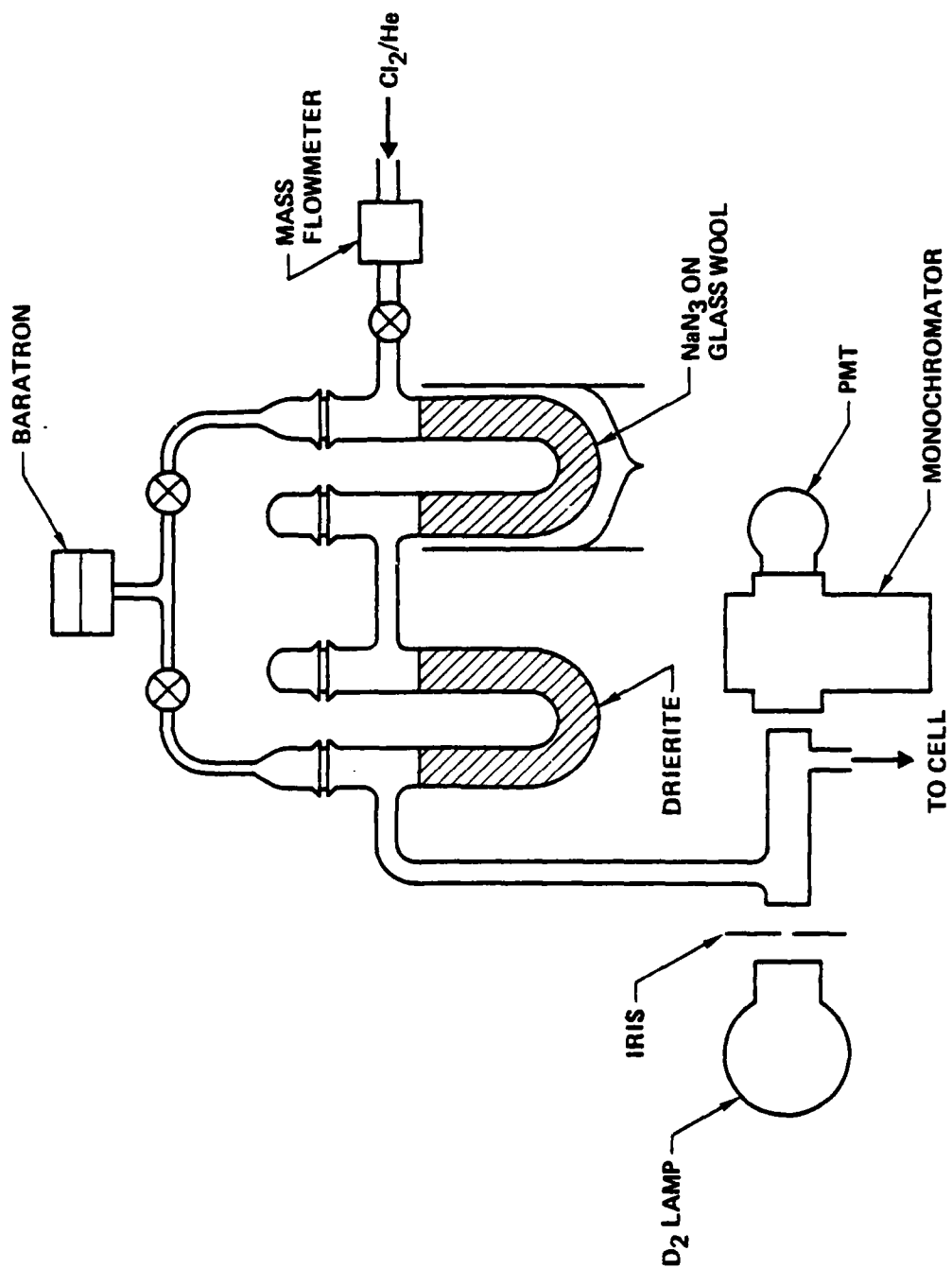
Figure 17. Small scale apparatus for the generation ClN₃.

60

spectrum is shown in Fig. 18. Definitive absorptions by four N_3 features are apparent in the figure, with the 000-000 band of the $^2\pi_g \rightarrow {}^2\Sigma_u^+$ transition having the greatest strength. The maximum absorption observed for this transition was approximately 4% over the 30 cm pathlength. Substitution of ClN_3 for HN_3 in the system resulted in a similar spectrum of comparable strength. Although a quantitative comparison between the N_3 yields in the HN_3 and ClN_3 systems could not be made, since the F atom flow rate was too low to be accurately measured (and hence reproduced), it would appear from these results that these yields are not least comparable.

As expected, the N_3 absorption diminished upon addition of Cl_2 to the F + HN_3 system (since Cl + N_3 is a faster reaction than F + N_3).[19] This phenomenon had been previously inferred from the observation that the addition of ClN_3 quenched the N_2 first positive emission present in the flame, thought to be caused by reactions involving N_3.[22] In the present experiments, the measured N_3 absorption was correlated with the N_2 emission by monitoring the latter, using an uncooled GaAs PMT and a broadband filter centered at 750 nm. For this purpose, a 6.0-mm orifice previously used to pass a thermocouple into the center of the flame was sealed with a quartz window and used as a view port. As expected, the N_2 emission increased at a faster than linear rate as the N_3 concentration was increased by the addition of HN_3 to the system. Since, however, changes in the N_3 concentration could be caused only by changing the HN_3 flow rate, these results suggest only that the production of excited N_2 is second order in HN_3 products; i.e., it may be caused by N + N_3, N_3 + N_3, or N + N + M reactions.

61
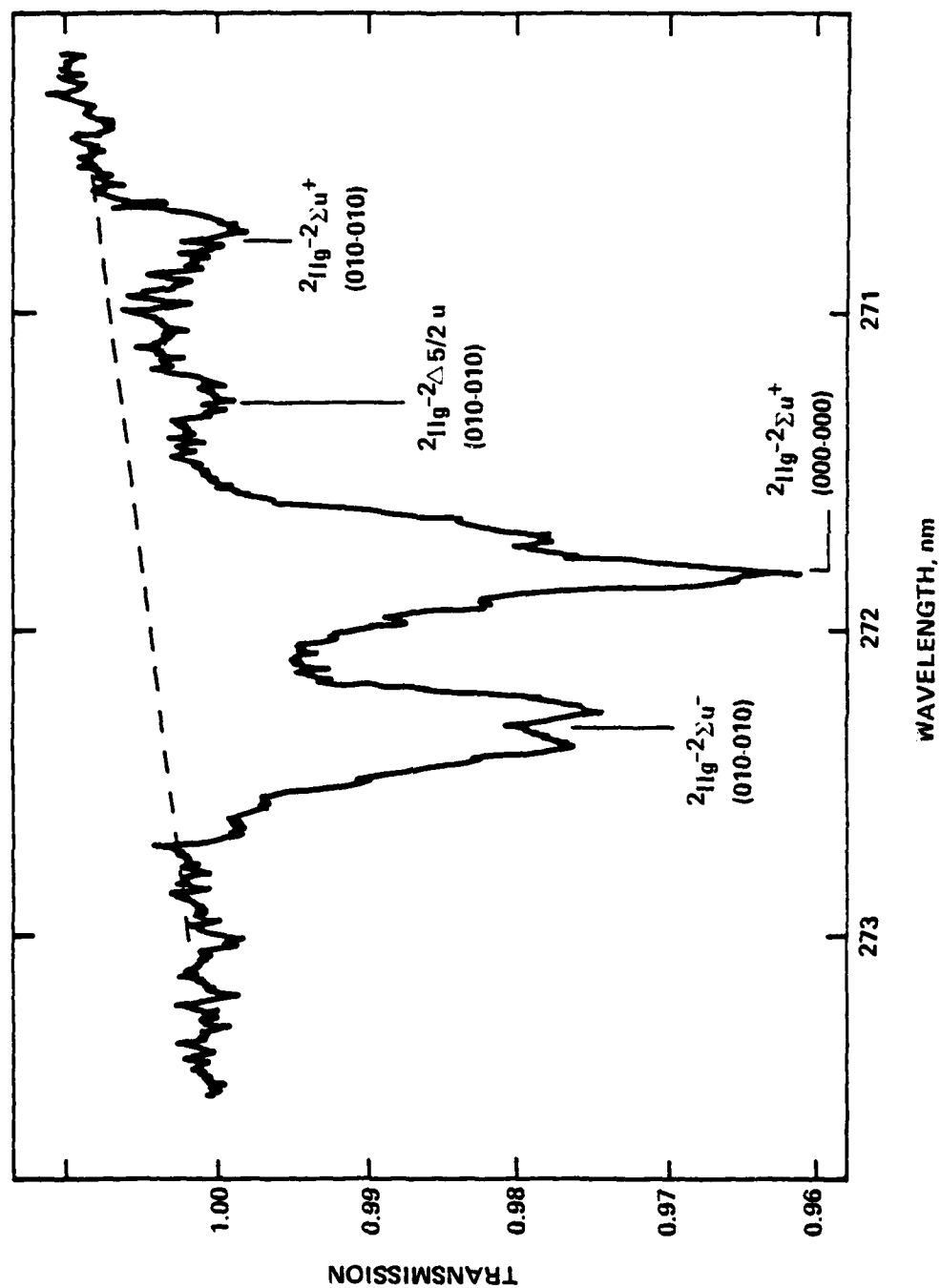
Figure 18. Absorption spectrum of N₃ radicals observed in a low density F+HN₃ flame.

In previous experiments, it was noted that addition of CO_2 or SF_6 to the F + HN_3 or F/Cl + HN_3 systems resulted in a large increase (by as much as a factor of two) in the intensity of emissions from excited NCl or NF.[10,19] Emissions from both the $a^1\Delta$ and $b^1\Sigma^+$ states exhibited this effect. One possible explanation was that CO_2 or SF_6 collisionally relaxed vibrationally excited N_3 molecules (produced by the F + HN_3 reaction) which might otherwise dissociate. Since the absorption experiments described above monitor the ground vibrational level (000) of the $N_3(^2\pi_g)$ state, this hypothesis was tested by monitoring the effect of added SF_6 on the N_3 absorption. Little or no effect on the N_3 (00 concentration was found, placing the relaxation theory in doubt. It is possible, of course, that collisional relaxation might populate levels below the predissociation zone but above the ground state; it would seem likely that some effect on the 000 population would be observed, however. Hence, no definitive explanation is at hand for the SF_6/CO_2 phenomenon at the present time.

Possible Sources of Excited NI Molecules

At this point in the program, the small discharge-flow apparatus[10] was reassembled for study of the kinetics of chemiluminescent reactions producing excited NCl, NBr, or NI. A number of experiments were performed in which NI chemiluminescence was sought from systems analogous to those producing excited NCl and NBr. Molecular iodides (HI and I_2) were added to the F + HN_3 system, such that the following sequence of reactions might occur:

$$F + RI \rightarrow RF + I \qquad\qquad (16)$$

$$F + HN_3 \rightarrow HF + N_3 \qquad\qquad (3)$$

$$I + N_3 \rightarrow NI + N_2 \qquad\qquad (17)$$

Very little information is available concerning the NI molecule. Phillips[26] deduced an NI bond strength of approximately 40 kcal/mol from $N_2^* - I_2$ chemiluminescence experiments. If this value is correct, the $I + N_3$ reaction would liberate ~ 25 kcal/mol, sufficient for exciting possible transitions only in the near IR. Miller and Andrews[27] have suggested that the $NI(^1\Sigma^+)$ state should be about 38 kcal/mol above the ground state.

Addition of HI to the flowing stream of fluorine atoms produced a very bright yellow-green flame. The spectrum of the flame exhibited many red degraded bands, which were identified as IF $B^3\pi_0^+ \rightarrow X^1\Sigma_g^+$ transitions. Addition of small quantities of HN_3 to this flame (downstream of the HI inlet) had little effect; larger quanties of HN_3 appeared to quench the flame. Similar results were obtained when HI was mixed with the HN_3 stream prior to entering the flow reactor. The UV-visible emission spectrum of the flame, recorded with the cooled GaAs PMT and photon counter, exhibited no features attributable to NI.

A stream of I_2 was produced by passing helium through a bed of solid iodine, yielding an I_2/He mixture containing about 0.3% I_2. Addition of this mixture to the stream of F atoms in the flow reactor again produced a diffuse yellow-green flame, with a banded spectrum characteristic of IF. Addition of HN_3 to this sytem downstream of the I_2 inlet appeared to quench the flame.

64

When the I_2 and HN_3 were pre-mixed prior to entering the F atom stream, the presence of the HN_3 was observed to greatly enhance the intensity of the IF flame, probably because of the heat release from the HN_3 reaction. As in the HI experiments noted above, no NI emission was evident in the UV-visible spectrum.

Assuming that the relationship between the energies of the $a^1\Delta$ and $b^1\Sigma^+$ states of NI is roughly that found for the other nitrogen halides, near IR emission from the $a^1\Delta$ state would be obscured by HF overtone transitions when HN_3 is used as an N_3 source. Hence, infrared emission from NI was sought, using DN_3 and ClN_3 as reagents, with I_2 as the source of iodine atoms. The IR spectrum of the flames produced was measured with a 0.25-m Jarrell-Ash monochromator and a liquid-N_2-cooled intrinsic germanium detector. No NI emission was found in these experiments. Two possible explanations for these negative results seem plausible. First, the $I + N_3$ reaction may be too slow relative to the N_3 production rate, such that most of the N_3 radicals are lost through side reactions. Second, the spin rules (favoring production of excited singlet states) may be very weak in the $I + N_3$ system, owing to the large spin-orbit coupling in the iodine atom.

3.   The Relative Yields of $a^1\Delta$ and $b^1\Sigma^+$ States

Given the information obtained to date, it seems likely that $X + N_3$ reactions are strongly constrained by the spin rules to produce excited singlet NX molecules, at least for the lighter NF and NCl systems. There would not seem to be any constraint on the relative amounts of the $b^1\Sigma^+$ and

65

$a^1\Delta$ states produced, however, given that sufficient energy is available to populate both states. If these reactions primarily generate the lower lying $a^1\Delta$ state, the most viable laser candidate might be the $a^1\Delta \rightarrow X^3\Sigma^-$ transition in NBr; on the other hand, if substantial proportions of the $b^1\Sigma^+$ states are produced, the best candidate might be the $b^1\Sigma^+ \rightarrow X^3\Sigma^-$ transition in NCl.

Experiments directed toward measuring the relative densities of the $a^1\Delta$ and $b^1\Sigma^+$ states were performed by recording the emission spectra of flames generated in the small discharge-flow apparatus[10] with a 0.25-m monochromator and an intrinsic germanium detector. This detector (North Coast Optics) is normally used for its sensitivity in the 1.0-µm region, but in previous experiments it was shown to also respond to the NCl $b^1\Sigma^+ \rightarrow X^3\Sigma^-$ transition near 665 nm. The relative peak intensities of the $a^1\Delta$ and $b^1\Sigma^+$ emissions were measured by recording the time decays of these emissions and extrapolating back to t = 0. Figure 19 shows a log plot of typical decay curves recorded for the NCl flame.

The ratio of the peak (t = 0) concentrations of the $b^1\Sigma^+$ and $a^1\Delta$ states is given by the following expression:

$$\left(\frac{[b^1\Sigma^+]}{[a^1\Delta]}\right)_{t=0} = \left(\frac{I(b^1\Sigma^+)}{I(a^1\Delta)}\right)_{t=0} \cdot \frac{A(a^1\Delta)}{A(b^1\Sigma^+)} \cdot \frac{R(a^1\Delta)}{R(b^1\Sigma^+)} \tag{18}$$

where the I's are measured intensities, the A's are spontaneous emission rates, and the R factors represent the spectral response of the monochromator-

66
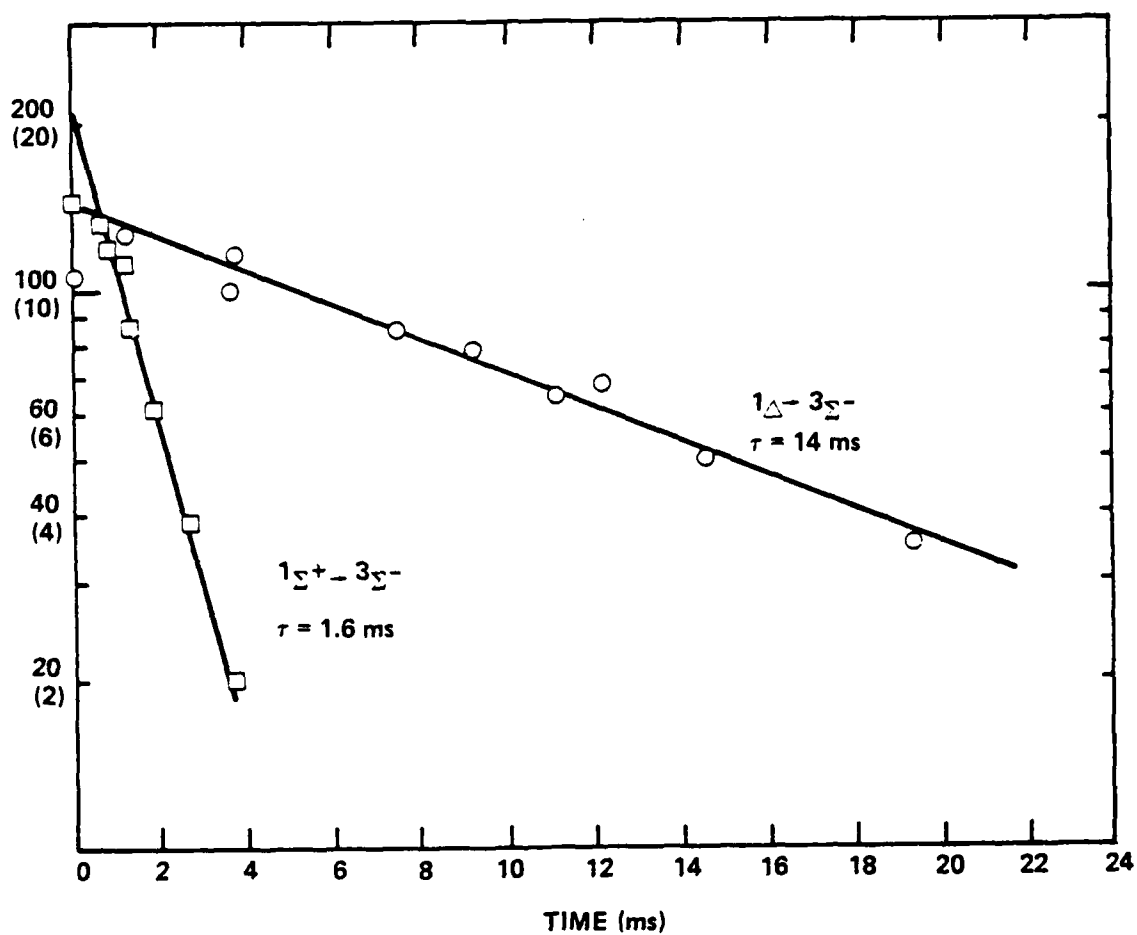
Figure 19. Relative intensities of NF(a$^1\Delta$) and NF(b$^1\Sigma^+$) emissions produced in a low density F+NH$_3$ flame. (The numbers in parenthesis refer to NF(a$^1\Delta$) intensities. The data shown were obtained with a detector which had an anomalously low sensitivity to the a$^1\Delta$ emission.)

67

detector assembly. If it is assumed that $A(a^1\Delta)/A(b^1\Sigma^+) \approx 4 \times 10^{-3}$ (from measurements of the radiative lifetimes of these states in NF[2,15]), the concentration ratio can be calculated from the data if the R factors are known. To this end, the response of the detection system was calibrated with a blackbody source at known temperatures. The value of $R(a^1\Delta)/R(b^1\Sigma^+)$ was found to be ~ 32.

Relative peak densities of the $a(^1\Delta)$ and $b(^1\Sigma^+)$ states of NCl and NBr were measured for several experiments in which either HN_3 or ClN_3 was used as the azide source. For the NBr experiments, bromine atoms were produced by the addition of a Br_2/Ar mixture to the flow reactor just upstream of the discharge zone. The mixture, containing 17% Br_2, was prepared in a passivated 35 ℓ tank prior to the experiments. Data obtained from these experiments are shown in Table I. The data for the NCl and NBr systems are quite consistent, suggesting that a similar process is responsible for the generation of excited species in each case, as expected. For the HN_3 reactions, about 14% of the excited singlets are in the $b^1\Sigma^+$ states near t = 0, such that the $b^1\Sigma^+ \rightarrow X^3\Sigma^-$ transitions have much higher "gain" than the $a^1\Delta \rightarrow X^3\Sigma^-$ transitions. Using Eq. (6) above, we find that the HN_3 data shown in Table 1 indicate that Gain $(b^1\Sigma^+ \rightarrow X^3\Sigma^-)$:Gain $(a^1\Delta \rightarrow X^3\Sigma^-) \approx 56$, if it is assumed that the relative inversion densities are given by the measured density ratios. In sharp contrast, the ClN_3 reactions produce 1% or less of the excited singlets in the $b^1\Sigma^+$ states, in agreement with inferences noted from the preliminary spectroscopic experiments described above. If in fact the $b^1\Sigma^+$ and $a^1\Delta$ states are both produced by the reactions of chlorine or bromine atoms with N_3

radicals, this difference must be caused by quenching of the $b^1\Sigma^+$ states by ClN_3 or reaction products. In subsequent experiments, in which rate constants for the collisional quenching of $NCl(b^1\Sigma^+)$ were measured, it was found that quenching by ClN_3 is in fact very rapid. The rate constant for this process was measured to be $k\ (ClN_3) = 1.5 \times 10^{-12}\ cm^3$ molecule^{-1} s^{-1}.[28]

Table 1

Peak $a^1\Delta{:}b^1\Sigma^+$ Ratios in the NCl and NBr Flames

Molecule	Azide Source	$I(b^1\Sigma^+)/Ia^1\Delta)$[a]	$[b^1\Sigma^+]/[a^1\Delta]$[b]
NCl	HN_3	43.8	0.16
NCl	HN_3	39.1	0.15
NCl	ClN_3	3.7	0.01
NCl	ClN_3	5.7	0.02
NCl	ClN_3	5.3	0.02
NBr	HN_3	41.1	0.16
NBr	$CaSO_4$	1.4	0.005

[a]Corrected for the spectral response of the detection system.
[b]Calculated assuming $A(a^1\Delta)/A(b^1\Sigma^+) = 4 \times 10^{-3}$.

It should be noted that the measured relative densities do not necessarily correspond to the intrinsic branching ratios for $b^1\Sigma^+/a^1\Delta$ production by the N_3 reactions, since the time dependences of the emissions have not been taken into account. In view of the rapid radiative rates of the $b^1\Sigma^+$ states,[12] it is likely that their measured time decay represents a formation rate, whereas the decay of the $a^1\Delta$ emissions is likely to be

dominated by collisional quenching processes. Hence, the intrinsic $b^1\Sigma^+/a^1\Delta$ branching ratios are likely to be somewhat higher than the measured density ratios. We note in this regard that a statistical distribution between the two states would yield $[b^1\Sigma^+]:[a^1\Delta] = 1:2$. In any case, it is clear from the data that the $b^1\Sigma^+ \rightarrow X^3\Sigma^-$ transitions in flames produced by the HN_3 reactions hold the greatest promise for lasing. In order to completely assess this promise, however, the actual yields of these states relative to the reagent flows must be measured. These experiments are addressed in the following section.

4.   NCl and NBr $b^1\Sigma^+ \rightarrow X^3\Sigma^-$ Photon Yields

Measurements of the photon yields of the $b^1\Sigma^+ \rightarrow X^3\Sigma^-$ transitions were complicated by two factors. First, the radiative lifetimes of the $b^1\Sigma^+$ states of NCl and NBr were unknown at the time of the experiments. Hence, a direct calculation of the peak excited state density, as had been done for measurements of the $NF(a^1\Delta)$ yield, was not possible. Second, the short time length of the flames (for the typical reagent densities used in the experiments) would make comparison to the O + NO reaction difficult, since calibration by this method assumes a uniform intensity distribution over the volume probed by the detector. In order to solve both of these problems, it was decided to stretch the flames out in time by using very low reagent concentrations. This condition yields a diffuse flame over the full reactor volume. Furthermore, since collisional quenching is not likely to be significant at such low densities, the time integrated intensity profile will

70

approach the photon yield calculated using the radiative lifetime (i.e., the local excited state density at the peak intensity for higher concentration conditions). For the low density conditions, the photon yield is given by

$$\text{Yield} = \frac{\alpha \int_t I(t)dt}{[HN_3]_0} \tag{19}$$

where α is the calibration factor obtained from the $0 + NO$ procedure and HN_3 is assumed to be the limiting reagent.

In the experiments performed, the concentrations of the atoms and HN_3 were reduced until the time decay of the $b^1\Sigma^+$ emissions stretched several cm down the length of the flow tube. Care was taken to ensure that the systems were still pseudo first-order in atoms (F, Cl, or Br atoms), i.e., that HN_3 was in fact the limiting reagent. Typically, full-time resolution of the flames required fluorine atom pressures less than 1.0 mtorr (as determined by Cl_2 titration) with roughly equivalent Br or Cl atom flows. The HN_3 flow rate was normally about 10% of the total atom flow rate. The role of HN_3 as the limiting reagent was verified by observing the sensitivity of the emission signal to the HN_3 flow rate.

Under such conditions, the NCl $b^1\Sigma^+ \rightarrow X^3\Sigma^-$ emissions generated by the F/Cl + HN_3 reaction exhibited a fully resolved rise and fall, as shown in Fig. 20. The data were taken with a 0.25-m Jarrell-Ash monochromator with

71
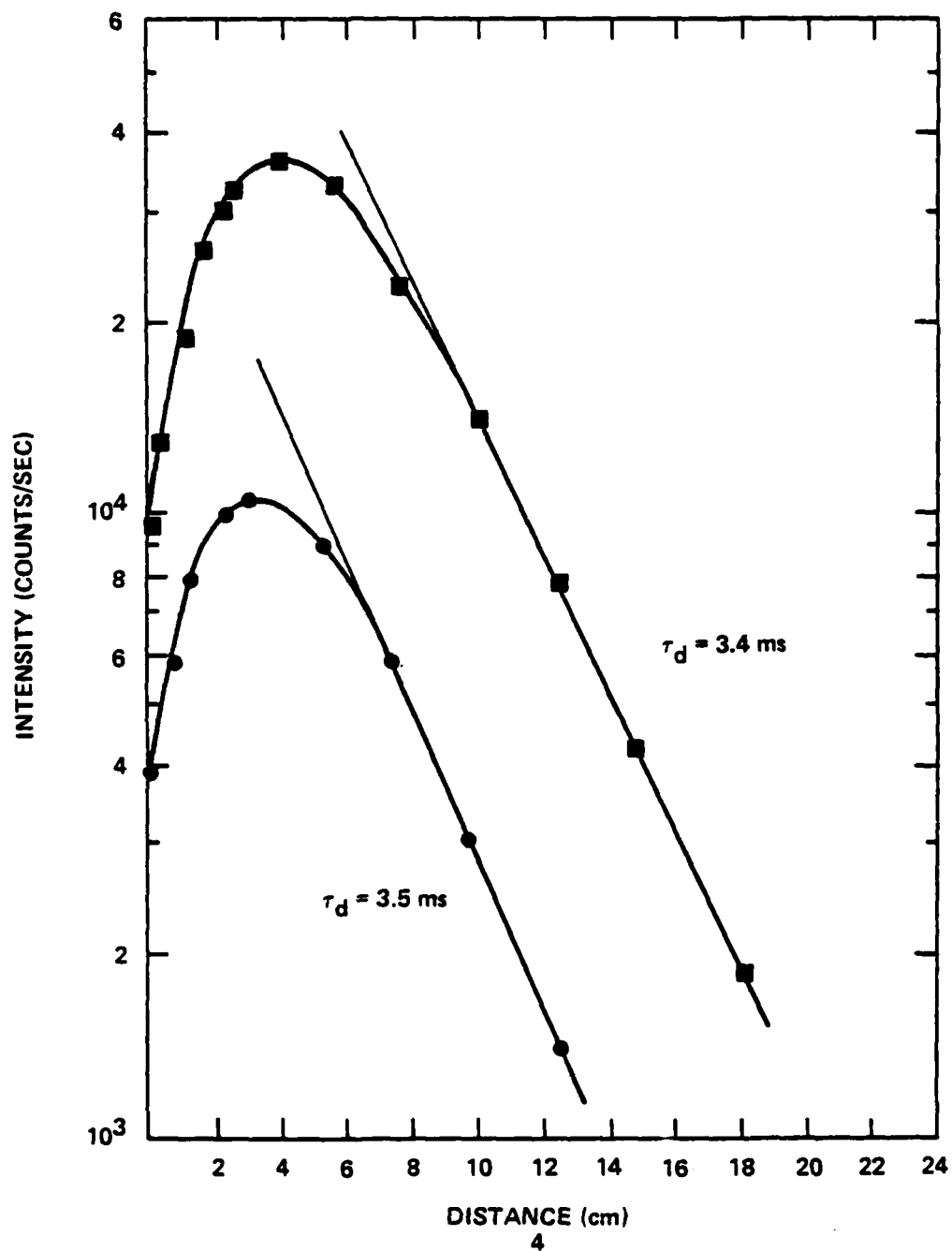
Figure 20. Time-resolved intensity of the dependence of NCl $(b^1\Sigma^+) \rightarrow X^3\Sigma^-$ emission produced in a low density flame. (■), P(HN)=0.034 mtorr; (●) P(HN₃)=0.019 mtorr.

72

1.0-mm slits, fixed at the wavelength of maximum intensity for the $\Delta v = 0$
sequence of the NCl $b^1\Sigma^+ \rightarrow X^3\Sigma^-$ transition near 665 nm. Analysis of the data
shown indicates a risetime $\tau_{rise} \approx 3$ ms and a decay time $\tau_{decay} \approx 3.5$ ms. In
view of the short radiative lifetime of NCl($b^1\Sigma^+$), $\tau_{rad} = 630$ μs,[12] it seems
likely that the measured time dependence tracks the N_3 concentration in the
system. Hence the observed rise and fall should correspond to the rates of
the F + HN_3 and Cl + N_3 processes, although which rate dominates the rise is
uncertain. Given pseudo first-order kinetics and an F or Cl atom density of
approximately 1.6×10^{13} cm^{-3}, the rate constant for the rise would be
$k_{rise} = 2 \times 10^{-11}$ cm^3 molecule^{-1} s^{-1} and the rate constant for the fall would
be $k_{fall} = 1.7 \times 10^{-11}$ cm^3 molecule^{-1} s^{-1}. These values are in good agreement
with previous measurements of rate constants for the F + HN_3 and Cl + N_3 reac-
tions,[19,21] and add credence to our hypothesis that the steady state N_3
density is minimized by the closely matched rates of these two processes.

Similar experiments performed for the NBr flame showed considerable
interference in the NBr $b^1\Sigma^+ \rightarrow X^3\Sigma^-$ spectrum by $\Delta v = 3$ bands of the N_2 first
positive transition produced at very low atom concentrations. Hence, the NBr
measurements were made at somewhat larger atom densities than those used for
the NCl experiments, and spectroscopic scans were made at several times during
the course of the experiment to make certain that the intensity being measured
was in fact due to $b^1\Sigma^+ \rightarrow X^3\Sigma^-$ transitions in NBr. The data obtained in these
experiments are shown in Fig. 21. Measurements were made for three HN_3 flow
rates, and the peak intensities scaled in a roughly linear fashion with the
HN_3. The decay rates calculated from the data are nearly equal for the three

73
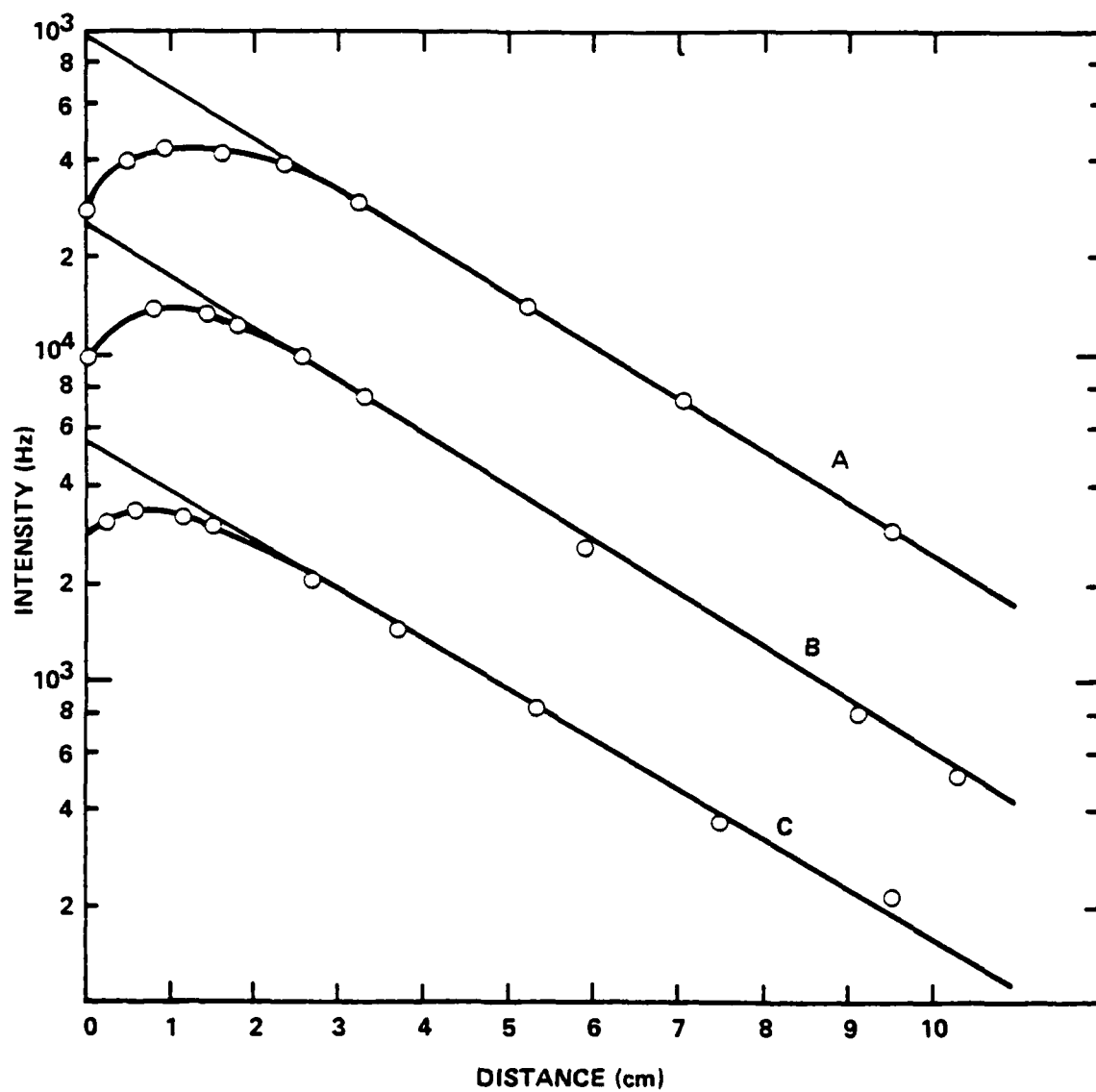
Figure 21. Time-resolved intensity of the NBr($b^1\Sigma^+$) → $X^3\Sigma^-$ emission produced in a low density flame. (A, P(HN₃)=0.030 mtorr, λ_d=634 s⁻¹; B, P(HN₃)=0.014 mtorr, λ_d=659 s⁻¹; C, P(HN₃)+0.0058 mtorr, λ_d=598 s⁻¹.)

74

experiments and are about twice the magnitude of the decay rates found for NCl (Fig. 20). This faster decay could be caused by the larger atom flow rates used in the NBr experiments. The NBr data shown in the figure exhibit an unresolved rise, clearly much faster than in the NCl case. We interpret these data to indicate that the rise of the emission is characteristic of the F + HN_3 rate and the decay characteristic of B_r + N_3. For an estimated Br atom density of 8.2×10^{13} cm^{-3}, the decay corresponds to a rate constant k = 7.2×10^{-12} cm^3 molecule^{-1} s^{-1} for the Br + N_3 process. As noted earlier, the discrepancy between the F + HN_3 and Br + N_3 rates could account for the formation of excited N_2 (from N_3 side reactions) in the system.

Conversion of these data to photon yields requires calibration of the light collection efficiency of the detection apparatus. This calibration was performed, using the O + NO reaction as a chemical actinometer, as described above. The calibration factor α was measured at the wavelength of the 0,0 bands of the $b^1\Sigma^+ \rightarrow X^3\Sigma^-$ transitions in NCl and NBr, yielding the values α(NCl) = 5.0×10^8 cm^{-3} and α(NBr) = 5.5×10^8 cm^{-3}. The uncertainties in determining these values are actually much greater than the agreement would indicate. The major source of error occurs in the N + NO titration poducing O atoms. The endpoint NO flow rates in the titration were found to vary by as much as 25%. Other errors (e.g., in the measurements of the total pressure, the gas flow rates, and the emission intensities) should have been much smaller, probably less than 10%. Hence we estimate the overall random error in the measurement of α to be about 50%. Since the published value for the absolute rate constant for photon production by the O + NO reaction has

approximately the same uncertainty,[13] the measured photon yields are uncertain within a factor of 2.

NCl and NBr $b^1\Sigma^+ \rightarrow X^3\Sigma^-$ photon yields were calculated by time integrating the measured intensity profiles, correcting by α, and dividing by the initial HN_3 density as in Eq. 19 above. The results obtained from this procedure are given in Table 2. Given the overall uncertainties in the measurements as discussed above, the yields for both the NCl and NBr transitions are about 10%. No trend with increasing HN_3 flow rate was found, suggesting that these values should be close to a low pressure limit.

Table 2

$b^1\Sigma^+ \rightarrow X^3\Sigma^-$ Photon Yields for NCl and NBr

Molecule	$P^\circ(HN_3)$, mtorr	Yield
NCl	0.019	0.07
NCl	0.034	0.15
NCl	0.049	0.16
NBr	0.030	0.07
NBr	0.014	0.04
NBr	0.006	0.07

The values for the $b^1\Sigma^+ \rightarrow X^3\Sigma^-$ yields shown in Table 2 are close to those found for the ratios of the peak densities of the $b^1\Sigma^+$ and $a^1\Delta$ states, as shown in Table 1. Hence, it is tempting to speculate that all of the HN_3

added to the system is converted to NCl or NBr in either the $a^1\Delta$ or $b^1\Sigma^+$ states. This inference is of course subject to the error bounds of both measurements, and as noted above, it is possible that the nascent $b^1\Sigma^+{:}a^1\Delta$ branching ratios are actually greater than the measured density ratios. We note as well that the density ratios were measured for much larger reagent concentrations than were the $b^1\Sigma^+$ photon yields. Nonetheless, it seems likely that, at low densities, a large fraction of the initial HN_3 is converted to excited singlet nitrenes.

5.   Kinetic Model for the Production of NCl $b^1\Sigma^+$

The experiments described above yielded information regarding the rates of processes producing excited NCl, the relative proportions of the $b^1\Sigma^+$ and $a^1\Delta$ states of NCl present in the flame, and the absolute yield of the $b^1\Sigma^+$ state at low reagent densities. In parallel experiments, the radiative lifetime of the NCl ($b^1\Sigma^+$) state and rate constants for its quenching by collisions with a variety of species were determined.[12,28] Hence, it is reasonable to consider all of these results along with additional data from the literature in order to estimate the gain levels to be expected in the NCl flame. A similar body of information is not available for the NBr system at the present time.

Table 3 shows the kinetic model assembled for the NCl system. The model assumes that the Cl + N_3 reaction produces only excited singlet NCl, with the $b^1\Sigma^+{:}a^1\Delta$ branching ratio taken from the yield data and peak density ratios presented above. Rate constants for the reactions of N_3 radicals with

77

HN_3 and N_3 were taken from the work of Jourdain and co-workers.[21] Although these authors report a range of values for these rates, we have chosen the largest rate constants for the model since these were consistent with the measured drop in the $NF(a^1\Delta)$ yield with increasing HN_3 flow (see Section 2.0 above). In some of the calculations described below, an additional reaction was added to the model, in which ground state $NCl(X^3\Sigma^-)$ was removed from the system by ClF. This process was assigned the rate constant $k = 1 \times 10^{-12}$ cm^3 $molecule^{-1}$ s^{-1}, in accord with the rate of quenching of $NCl(b^1\Sigma^+)$ by ClF.

Table 3

Kinetic Model for the NCl Flame

Process	Rate Constant	Ref.
Pumping Reactions:		
$F + HN_3 \rightarrow HF + N_3$	1.5×10^{-11} cm^3 s^{-1}	(21)[a]
$Cl + HN_3 \rightarrow HCl + N_3$	1.0×10^{-12} cm^3 s^{-1}	(21)
$Cl + N_3 \rightarrow NCl(b^1\Sigma^+) + N_2$	2.2×10^{-12} cm^3 s^{-1}	(22)[a]
$\rightarrow NCl(a^1\Delta) + N_2$	1.3×10^{-11} cm^3 s^{-1}	(22)[a]
Side Reactions:		
$F + N_3 \rightarrow NF(a^1\Delta) + N_2$	2.0×10^{-12} cm^3 s^{-1}	(10)(21)
$N_3 + HN_3 \rightarrow H + 3N_2$	2.0×10^{-11} cm^3 s^{-1}	(23)
$N_3 + N_3 \rightarrow 3N_2$	8.0×10^{-11} cm^3 s^{-1}	(22)
Quenching Processes:		
$NCl(b^1\Sigma^+) + ClF \rightarrow NCl(X^3\Sigma^-) + ClF$	1.2×10^{-12} cm^3 s^{-1}	(30)
$+ F_2 \rightarrow NCl(X^3\Sigma^-) + F_2$	2.2×10^{-13} cm^3 s^{-1}	(30)
$+ Cl_2 \rightarrow NCl(X^3\Sigma^-) + Cl_2$	1.7×10^{-14} cm^3 s^{-1}	(30)
Radiation:		
$NCl(b^1\Sigma^+) \rightarrow NCl(X^3\Sigma^-) + h\nu$	1590 s^{-1}	(12)

[a]From data presented in this report.

The time dependent behavior of the concentrations of the various species present in the flame was determined by integrating the rate equations corresponding to the processes in the model using a fourth order Runge-Kutta

routine. Finite mixing was taken into account for every bimolecular process by using the following form for the rate equations:

$$\frac{d[X]}{dt} = \pm \sum_{xy} \quad \frac{1}{M} + \left(\frac{1}{k[X][Y]}\right)^{-1} \tag{20}$$

where k is the bimolecular rate constant and M is the fixed mixing rate. Figure 22 shows the results of the calculation for the initial partial pressures $P^\circ(Cl) = P^\circ(F) = 50$ mtorr and $P^\circ(HN_3) = 10$ mtorr (densities were calculated assuming a temperature of 350 K). The mixing rate for the data shown was $M = 50$ torr s^{-1} (or 1.4×10^{18} cm^{-3} s^{-1}). This value corresponds to a mixing rate about one-fifth the value of the $F + HN_3$ reaction rate. The calculation shows that for these conditions the peak $NCl(b^1\Sigma^+)$ concentration (and hence the peak emission intensity) should occur about 270 µs after the initial contact of the reagents. The N_3 density exhibits a broad peak occurring much earlier, at about 100 µs. The ground state density rises slowly, reaching a peak at $t > 500$ µs. The calculations corresponding to Fig. 22 included the $NCl(X^3\Sigma^-) + ClF$ process noted above; exclusion of this process had only a minor effect on the results. The inversion density, ΔN, corresponding to these results was calculated as follows:

$$\Delta N = N(b^1\Sigma^+) - \frac{1}{3} N(X^3\Sigma^-) \tag{21}$$

80
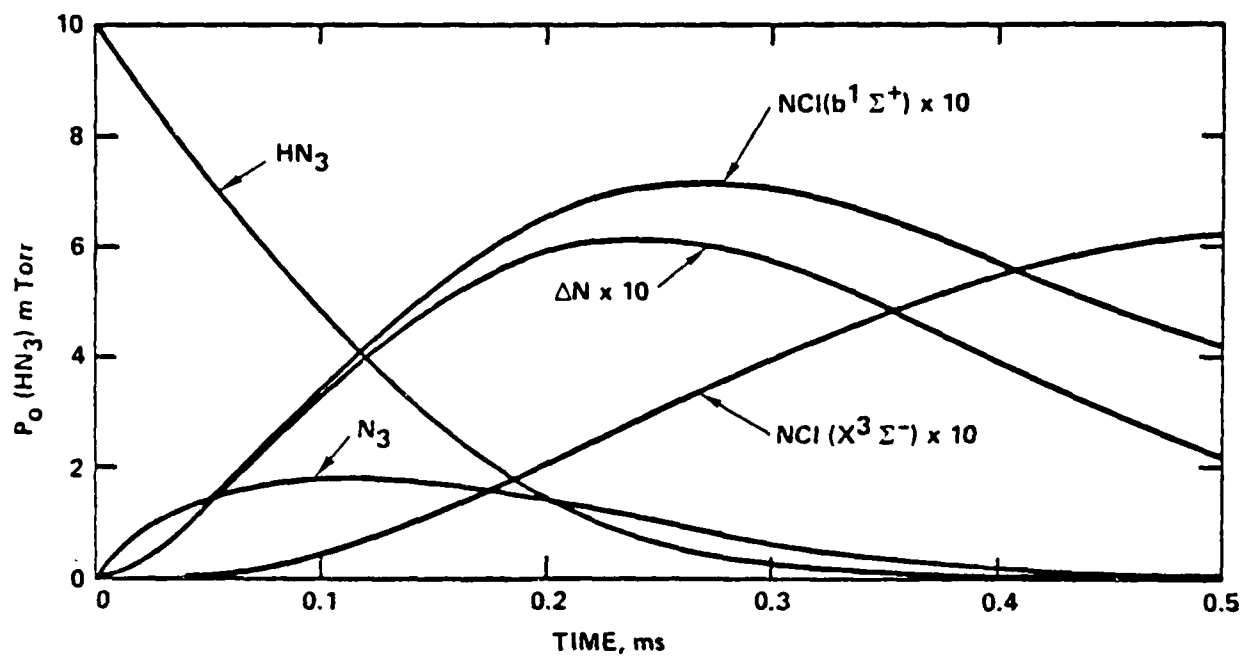
Figure 22 Calculated time evolution of selected species in the NCl flame for P(HN₃)=10 mtorr, P(Cl)=P(F)=50 mtorr.

The peak inversion for these conditions is predicted to be $\Delta N \approx 0.62$ mtorr or about 1.7×10^{13} cm^{-3} at 350 K. Assuming all of the excited $NCl(b^1\Sigma^+)$ molecules to be in the lowest vibrational level, and given rotational equilibrium at 350 K, this inversion corresponds to a gain $G = 5.8 \times 10^{-5}$ cm^{-1} for a single transition from the most populated rotational level ($J = 13$). We have assumed that the four branches of the NCl transition ($^O P$, $^Q R$, $^Q P$, and $^S R$) have roughly equal radiative rates given by one fourth the measured value.[12]

The effect of mixing on the system was investigated by performing a series of calculations in which the peak inversion density and the time elapsed from the initial contact of the reagents to the peak inversion was determined for various values of M. The results of these calculations are shown in Fig. 23. The initial pressures used were $P°(HN_3) = 10$ mtorr and $P°(Cl) = P°(F) = 50$ mtorr, again at 350 K. The peak inversion density exhibits a steep rise as the mixing rate increases from 0 to 1×10^{18} cm^{-3} s^{-1}, reaching a plateau at about $\Delta N = 1.7 \times 10^{13}$ cm^{-3} for faster mixing rates. Values of M as high as 3×10^{20} cm^{-3} s^{-1} resulted in relatively small changes from this value. The time to peak inversion exhibits a behavior nearly inverse to that found for the magnitude of the peak inversion. It drops very rapidly as M increases from 0 to 1×10^{18} cm^{-3} s^{-1}, then levels off at about 200 µs.

Calculations were also performed for somewhat higher reagent densities to probe the initial scaling of the system. For an initial HN_3 pressure of 20 mtorr and 100 mtorr each of chlorine and fluorine atoms, the results indicated an inversion density $\Delta N = 3.8 \times 10^{13}$ cm^{-3} at 350 K,
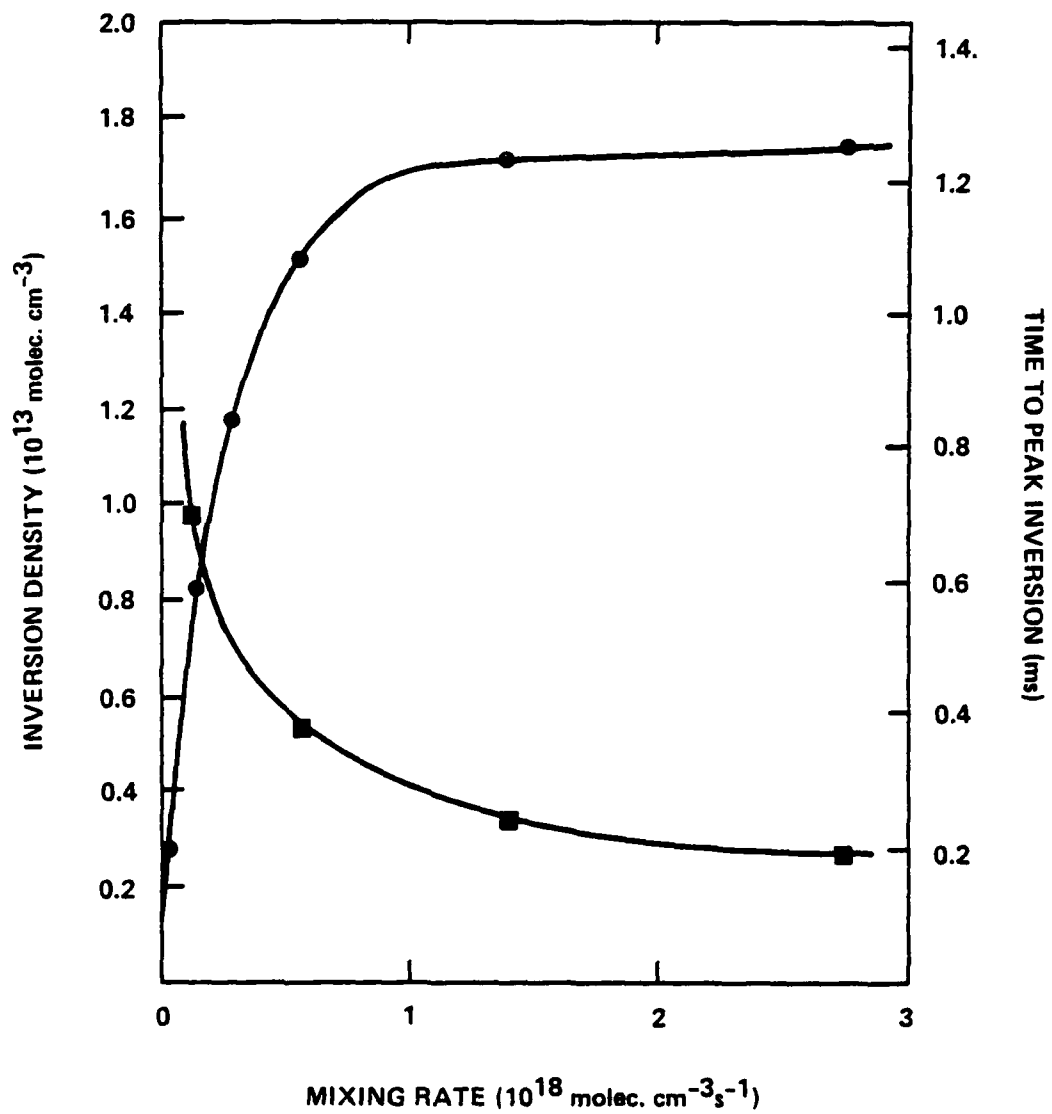
Figure 23   Dependence of the calculated inversion density (●) and time to peak
inversion (■) on the mixing rate.

83

corresponding to a gain of 1.3×10^{-4} cm^{-1} for a single line in the NCl $b^1\Sigma^+ \rightarrow X^3\Sigma^-$ transition. The mixing rate used was $M = 2.8 \times 10^{20}$ cm^{-3} s^{-1}. Clearly, if the model were to accurately reflect the kinetics of the real system, the demonstration of a laser at densities near these would seem feasible.

IV. GAIN MEASUREMENTS

As noted previously, the kinetic model for the NCl system predicts a single line gain on the order of 5×10^{-5} cm^{-1} for reagent densities typical of the experiments performed in our laboratory. For a transverse flow reactor with an active length of 10 cm, the predicted round trip gain would be 1×10^{-3}. Measurement of an optical gain of this magnitude by using standard single-pass techniques would be extremely difficult. Recently, however, Herbelin and co-workers[14] demonstrated a multiple-pass method capable of measuring absorptions or gains of 1×10^{-4} or less. Although these authors used this technique for the measurement of mirror reflectivities, it can be easily extended to measurements of attenuation or amplification in optical media. The experiment (the details of which have been thoroughly described in the literature)[14] is based on measurement of the lifetime of photons injected into a very low loss resonant optical cavity surrounding the medium to be probed. This lifetime, τ, is related to the average number of round trip cavity transits, n, by $\tau = 2nL/c$, where L is the cavity length and c is the speed of light. The round trip transmission is given by $T = \exp(-1/n)$. This factor defines the mirror reflectivites, $T = R_1 R_2$, for a cavity surrounding a vacuum or medium with negligible losses. For a medium with optical gain,

$$T_{total} = T_{mirrors} \, T_{medium} = T_{mirrors} \, (1 + G).$$

In principle, the cavity transmission might be measured directly by monitoring the attenuation of the transmitted beam. In this case, the experiment is simply a multiple-pass absorption measurement. Deconvolution of

the data would be difficult, however, since the average number of cavity transits would not be determined. A much superior method involves measurement of the optical time delay, τ, caused by the extended path length. This can be accomplished by amplitude modulation of the CW probe beam and measurement of the phase shift, δ, between the incident and transmitted light. The photon lifetime in the cavity, τ, is simply related to the tangent of the phase shift by the following expression:

$$\tau = 2nL/c = \tan \delta / 2\pi f \tag{22}$$

where f is the modulation frequency. Hence, the round trip gain of the medium is given by

$$G = \frac{4\pi fL}{c} \left(\frac{1}{\tan \delta_0} - \frac{1}{\tan \delta} \right) \tag{23}$$

where δ_0 refers to the phase shift determined by the finite mirror reflectivities.

In practice, the sensitivity of the experiment is optimized by choosing a modulation frequency such that tan δ varies around 1.0 (i.e., $\delta = 45°$), and by using a large cavity length, L, such that the time delay is large for a given number of cavity transits. For typical high reflectivity mirrors (R ≈ 0.998), the round trip transmission with no medium would be T = 0.996,

86

coresponding to n = 250. Given the relationships between τ, n, and tan δ given in Eq. (22), a modulation frequency f = 95 kHz would yield tan $\delta \approx 1.0$ for L = 100 cm and this value of n. This frequency is well within the range of acousto-optic or electro-optic modulators. An optical gain in this cavity of 1×10^{-3} would result in an increase of tan δ from 1.0 to 1.33 (or a change in the phase angle δ from 45° to 53°).

1.   The Apparatus for Gain Measurements

A schematic of the optical train and electronics of the gain apparatus is shown in Fig. 24. The light source used was a Coherent Radiation model 699-21 ring dye laser pumped by a model CR-3000K krypton ion laser. The ion laser could be operated on many different lines from the UV to the deep red portion of the spectrum. Broadband operation of this laser using optics for the yellow-green output (appropriate for pumping the Rhodamine 101 dye used in the NCl/NBr gain experiments) produced nearly 4.0 W of output. Tuning of the ring dye laser is accomplished with a birefringent filter and two etalons internal to the laser cavity, producing an output linewidth of a few MHz (limited by the frequency jitter of the device). The dye laser output is actively stabilized by continuous comparison to a temperature stabilized reference cavity. For optimum conditions, the "single frequency" output of the dye laser was $\sim$ 150 mW for $\sim$ 3.5 W of input power with Rhodamine 101 dye, with the laser tuned near the wavelength of the NCl $b^1\Sigma^+$ $X^3\Sigma^-$ transition. The output of the dye laser was analyzed with a 1.0-m monochromator (Interactive Technology) and a spectrum analyzer (Tropel model 240). The dye laser system
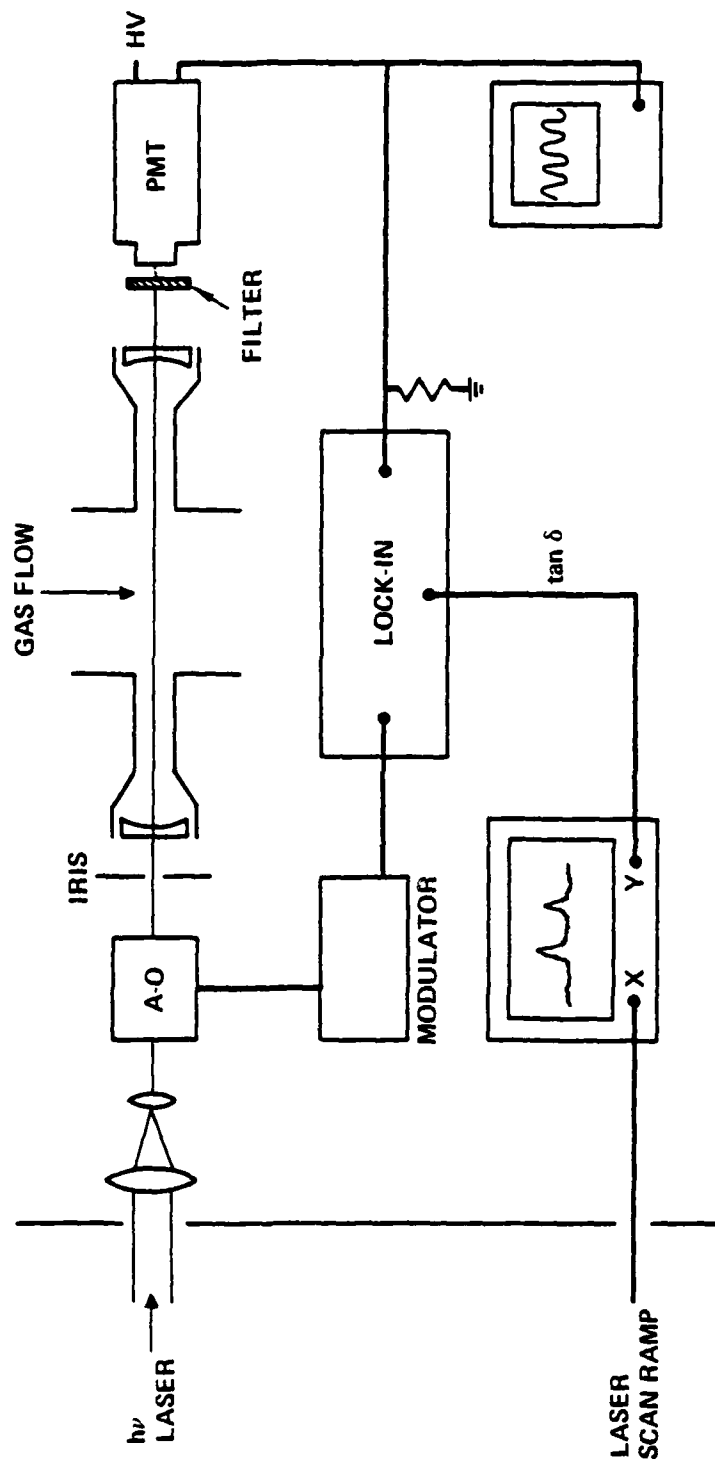
Figure 24. Schematic diagram of the optical train and electronics used for gain measurements.

88

was mounted on an air-suspended optical table; it was found that this was necessary to avoid mode-hopping during a laser scan. The laser could be automatically scanned over frequency ranges as large as 30 GHz by movement of the intracavity etalons.

The actual gain experiment was located in a separate laboratory adjacent to that in which the laser was mounted. The laser beam passed through a small hole in the wall separating the rooms. Amplitude modulation of the beam was accomplished with a Coherent Associates model 304 acousto-optic modulator. This device operates from DC to 3 MHz, with a transmission greater than 80%. The modulator was driven by a Wavetek model 148 function generator. The laser beam exhibited considerable divergence over the path from the laser to the gain experiment, and it was necessary to reduce its diameter with a small telescope prior to entering the modulator. The modulated beam was injected into the optical cavity surrounding the flow tube via the finite transmission of the mirrors. Light transmitted by the cavity was detected with a cooled GaAs photomultiplier tube (RCA C31034).

The phase shift caused by the presence of the resonant cavity in the beam was measured with a PAR 5204 lock-in analyzer. This device monitors both quadrature and in-phase components of the input signal with a phase stability of $\sim 0.2°$. The tangent of the phase shift was measured by the following procedure. First, the cavity was de-tuned and the phase of the lock-in amplifier (referenced to the modulator) adjusted such that the quadrature signal was zero. The cavity was then re-tuned to maximize the signal observed by the PMT (this corresponded to a tightly focussed spot transmitted by the

89

cavity, indicating that stable transverse cavity modes had set up). At this point, the phase shift caused by the resonator was determined by the ratio of quadrature and in-phase components of the transmitted light, as follows:

$$\tan \delta = \frac{\sin \delta}{\cos \delta} = \frac{I \; (\text{quadrature})}{I \; (\text{in-phase})} \qquad (24)$$

The value of tan δ was monitored continuously by using the ratiometer capability of the lock-in analyzer. Data were recorded, using an X-Y plotter, with the X coordinate driven by the scan control of the laser and the Y coordinate by the output of the lock-in.

The flow reactor used in the experiments was a modified version of the transverse flow device discussed above and shown in Fig. 16. Two basic modifications were made for the gain experiments. First, a new HN_3 injector was used, such that its position with respect to the optical axis of the cavity might be varied. The new injector was the full 15-cm length of the flow reactor with 45 1.0-mm-diameter holes for admission of HN_3 into the flow stream. The position of the injector could be moved over a distance of ~ 5 cm. The second change involved replacement of the windows previously cemented to the sides of the flow reactor by 1.91-cm-diameter "Ultra-Torr" fittings. These fittings were connected to the mirror mounts (Oriel) by 1.91-cm-diameter flexible stainless steel tubing, to give a total cavity

90

length on the order of 120 cm. A diagram of the modified low reactor and cavity is shown in Fig. 25.

A variety of mirrors with high reflectivities in the red visible region (appropriate to the NCl and NBr transitions) were tested in the apparatus. The mirrors ultimately used in the experiment were obtained as a loan from Dr. J.M. Herbelin of the Aerospace Corporation. Phase shift measurements at 70 kHz indicated a round trip transmission of 0.9968 for a cavity formed from these mirrors, corresponding to a reflectivity of 0.9984 for each mirror. This result was in excellent agreement with the value of 0.9989 quoted by Dr. Herbelin. This measurement also showed the phase stability of the experiment to be excellent. Measurements of tan γ made over a period of one hour indicated that tan δ varied by only $\pm$ 0.01, corresponding to a baseline sensitivity in the cavity transmission of $\pm$ 0.00003. In practice, the phase stability was found to vary considerably over many experiments, such that a typical sensitivity was on the order of $\pm$ 0.00005.

Following assembly of the apparatus, tests were performed to check the sensitivity of the measurement to the presence of absorbing species in the flow reactor. The first such test involved passage of known amounts of I_2 through the cavity. Tellinghuisen[29] has reported absorption coefficent for I_2 continuous absorption in the region 600 nm - 800 nm. For these experiments, a stream of I_2 vapor was obtained by passing N_2 through a saturator containing solid I_2 at room temperature. The $N_2 - I_2$ flow was metered into the cavity, where it was mixed with a flow of argon used to purge the cavity optics. The experiments were performed by using the broadband output of the dye laser

91
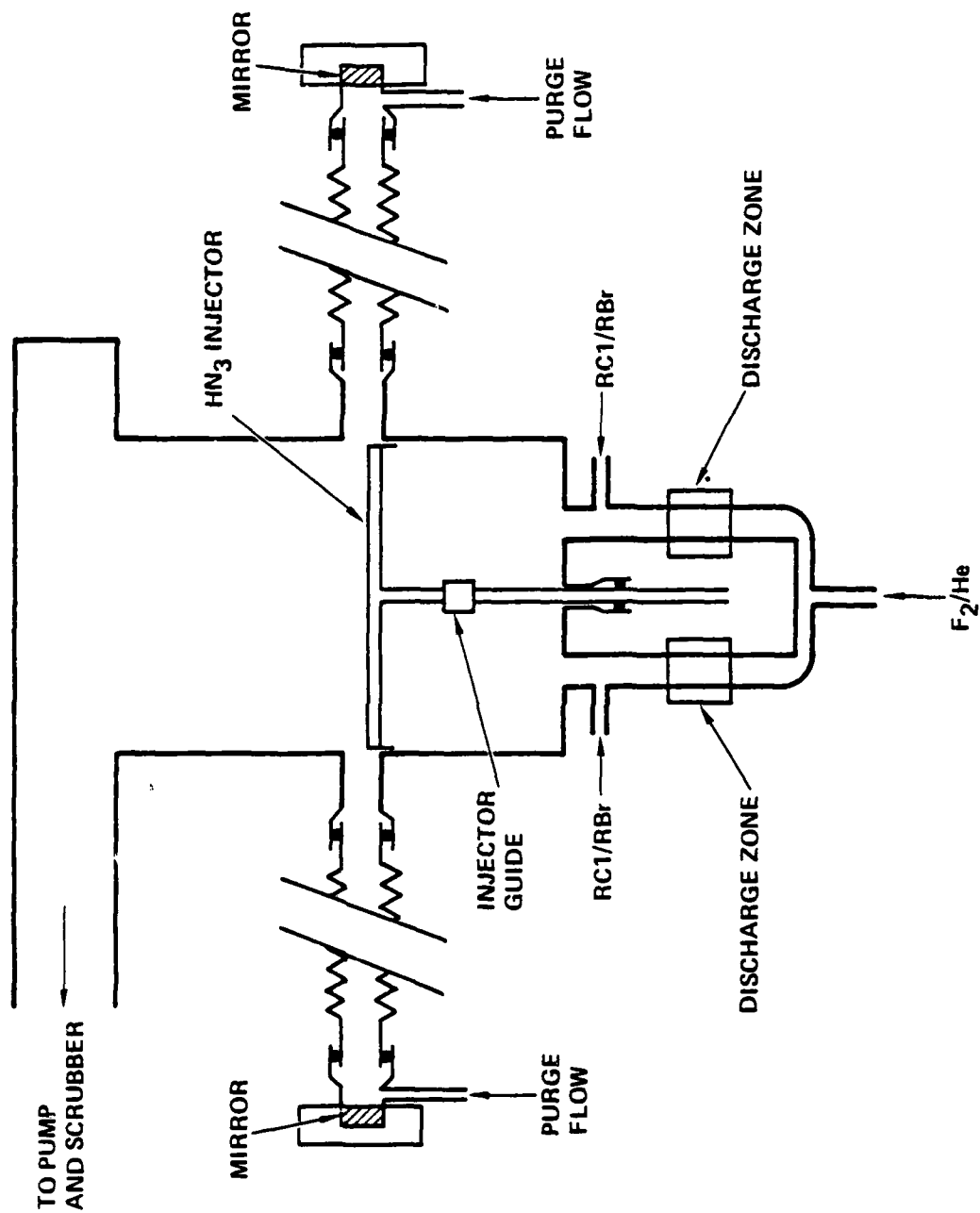
Figure 25. Diagram of the transverse flow reactor and optical cavity used for gain measurements.
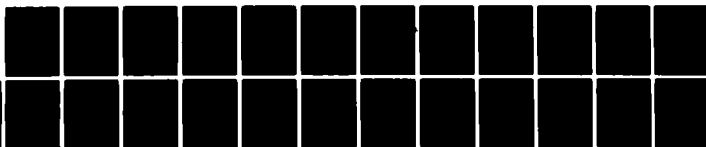
(i.e., tuned only by the birefringent filter, with the etalons out of the cavity) at 673.0 nm. No appreciable changes in tan δ were observed for flows of N_2 and Ar with no I_2 present, relative to values obtained for the cavity under vacuum. The addition of I_2 resulted in a marked change in tan δ, however. Following Eq. 23 above, the I_2 concentration in the cavity is related to the measured phase shift by the following expression:

$$[I_2] = \frac{1}{\epsilon \ell} \quad \frac{2\pi f L}{c} \quad \frac{1}{\tan \delta_0} - \frac{1}{\tan \delta} \tag{25}$$

where ϵ is the I_2 absorption coefficient at the wavelength of the probe laser and ℓ is the absorption length of the medium, 15 cm. Hence a plot of the I_2 concentration, obtained from the measured flow rate of the mixture, vs the measured values of $(1/\tan \delta_0) - (1/\tan \delta)$ should be linear with a slope characteristic of ϵ. Figure 26 shows such a plot for the data obtained in these experiments. The slope of the line drawn through the data yields an absorption coefficient $\epsilon = 24$ ℓ mole^{-1} cm^{-1}, in fair agreement with the value $\epsilon = 44$ ℓ mole^{-1} cm^{-1} reported by Tellinghiusen.[29] As is apparent in the figure, there is considerable scatter in the data, which suggests a sensitivity to a minimum of $\sim$ 500 p/m in absorption. It seems likely that the source of both the scatter and the discrepancy with Tellinghiusen's value of ϵ lies in the determination of the I_2 concentration, which was simply obtained from the measured I_2/N_2 flow rate and the I_2 vapor pressure in the

93
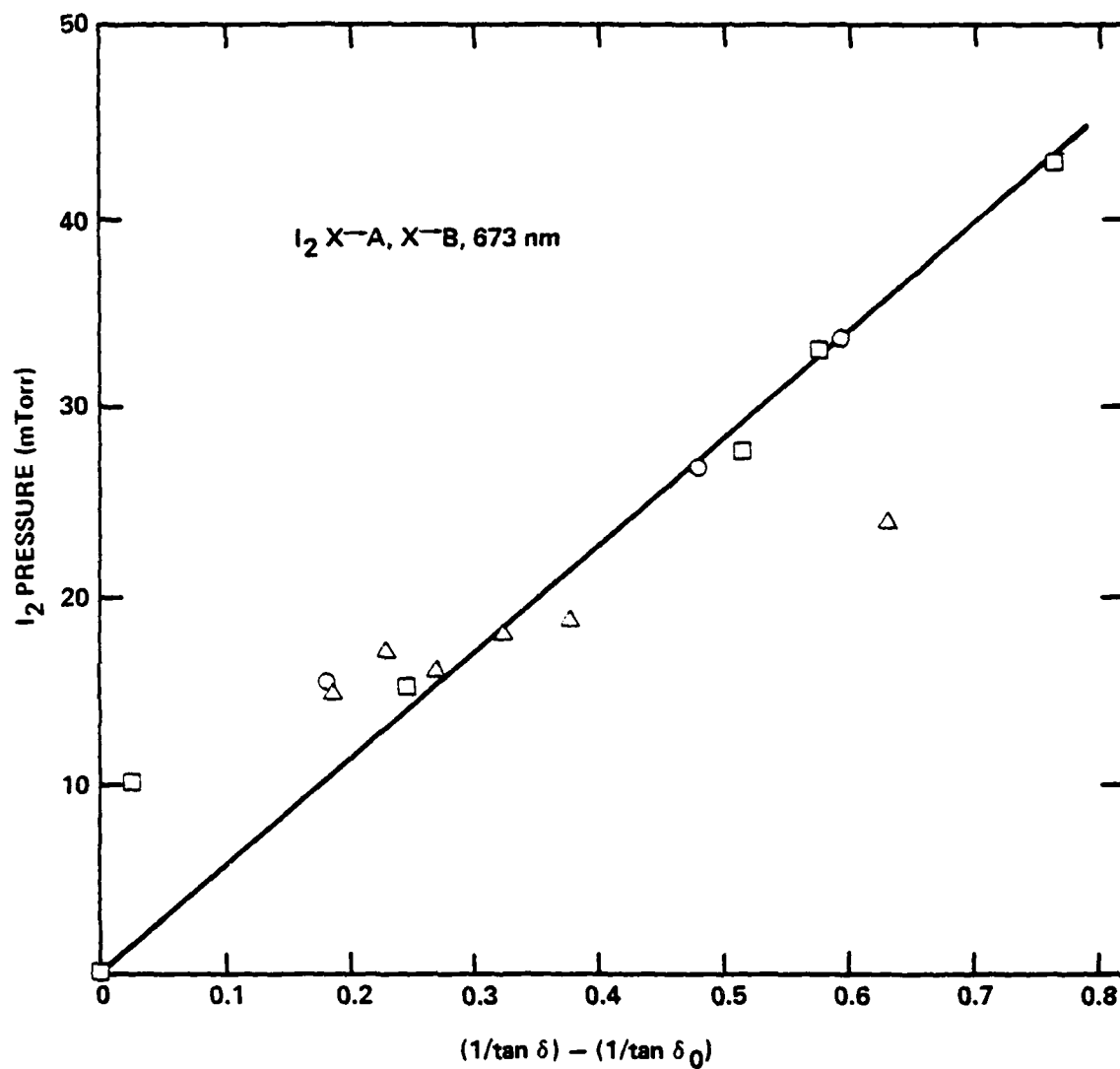
Figure 26. Plot of the I_2 partial pressure in the optical cavity vs the change in $(\tan \delta)^{-1}$ measured near 673 nm. (The slope of the line yields an absorption coefficient $\delta \approx 24$ l mole^{-1} cm^{-1}.)

94

saturator. If appreciable quantities of I_2 absorbed on the walls of the tubing or reactor vessel downstream of the saturator, the concentration of I_2 would be overestimated, and hence the value of ϵ underestimated.

A second test of the system was made by investigating the production of NH_2 by the reaction $F + NH_3 \rightarrow NH_2 + HF$. NH_2 is known to have a strong absorption on its $\tilde{X}^2B_1 \rightarrow \tilde{A}^2A_1$ transition near 630 nm.[30] For this test, fluorine atoms were generated by passage of an F_2/He mixture through the microwave discharges, and NH_3 was added to the flow via the movable injector bar. The dye laser was operated in the "single frequency" mode, scanning through 30-GHz segments. These experiments showed that single absorption features in NH_2 are very easily observed with the phase shift apparatus. A typical absorption spectrum recorded near 630.1 nm is shown in Fig. 27. Four absorption features are evident in the spectrum, labelled A, B, C, and D. The center frequency of the scan is not well known, since it lies outside the wavelength zone over which our monochromator was calibrated (calibrations were performed, with neon lines as wavelength markers). If in fact this wavelength is close to 630.1 nm, the most intense features in the spectrum (A and C) correlate well with the 414-404 and 515-505 transitions if the 080-000 band in NH_2.[32] This identification would require the center wavelength to be 630.18 nm in air. The features labelled B and D do not correlate with tabulated lines of the NH_2 spectrum. We note, however, that due to the nonlinear relationship between optical density and tan δ, these features are in fact quite weak relative to A and C, and hence may not have been seen before. The true absorption strengths of features A, B, C, and D have the relative values

95
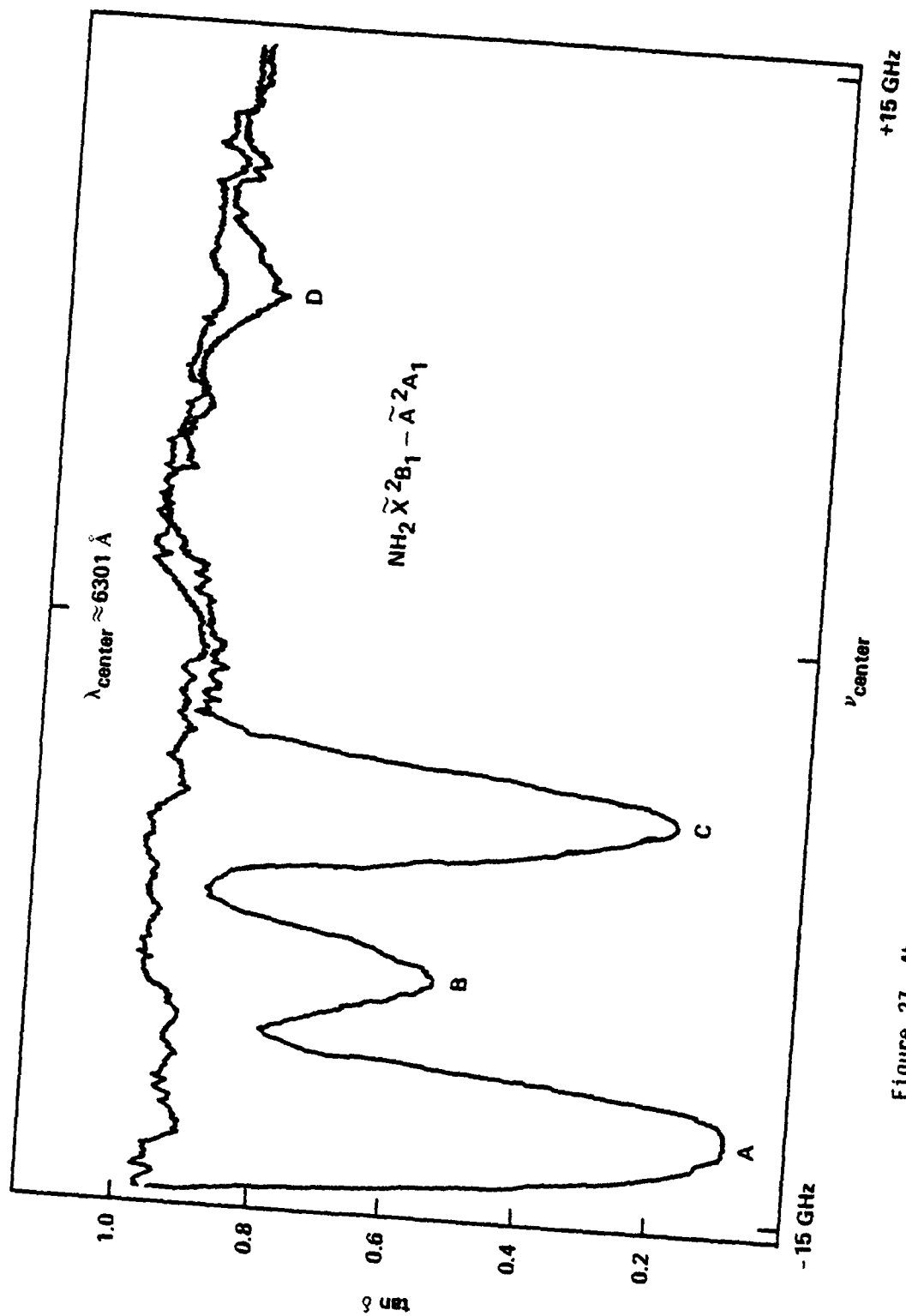
Figure 27. Absorption spectrum of the $\tilde{X}^2B_1 \leftarrow \tilde{A}^2A_1$ transition of NH_2 near 630.1 nm, measured with the phase shift apparatus.

96

11.0 : 0.7 : 4.0 : 0.1, respectively. NH_2 is apparently a long-lived species in the $F + NH_3$ flame, since movement of the NH_3 injector over a distance of a few cm had little or no effect on the spectrum. Hence, although these data suggest that the frequency selection and scanning mechanism of the system work well, they do not contain information regarding matching of the flame geometry to the region probed by the laser.

2.   Gain Experiments on the NCl and NBr Systems

The NCl flame was generated in the transverse flow reactor in the manner described above. In brief, chlorine atoms were produced by adding Cl_2 to the $F/F_2/He$ flow just downstream of the discharge zones. An HN_3/Ar mixture containing 5% to 10% HN_3 was added to the stream through the movable injector bar, generating the bright red NCl $b^1\Sigma^+ \rightarrow X^3\Sigma^-$ emission. Argon was also admitted to the stream via inlets which served to purge the flexible stainless steel tubing leading to the reflectors. For the initial tests, the total pressure in the reactor was ~ 800 mtorr, with the partial pressures of F and Cl atoms varying from 50 to 100 mtorr, and the partial pressure of HN_3 from 5 to 10 mtorr. The temperature in the reactor was measured by insertion of a chromel-alumel thermocouple in the flow. For the conditions noted above, the gas temperature was observed to rise very slowly, reaching only about 350 K after nearly an hour of operation.

NCl $b^1\Sigma^+ - X^3\Sigma^-$ chemiluminescence was monitored by replacing the temperature tap directly over the optical axis (see Fig. 16) with a small CaF_2 window. NCl emission passing through this window was detected by using a

narrow band interference filter centered near 665 nm (to pass the $\Delta v = 0$ sequence of the $b^1\Sigma^+ - X^3\Sigma^-$ (transition) and a room temperature GaAs photomultiplier tube (RCA 4832). The NCl emission was maximized for roughly equivalent flows of fluorine and chlorine atoms, in agreement with our previous observations. For the conditions yielding optimum NCl chemiluminescence intensity, the emission was quite easily visible to the eye through the cavity end reflectors. The chemiluminescence appeared as a very well defined red spot on the mirrors, indicating that the losses in the medium were sufficiently small to allow stable transverse modes to set up. The shape of the spot was quite sensitive to the mirror positions, and a symmetric circular spot could be obtained with fine tuning. It was noted that the alignment for a circular spot was somewhat different from that corresponding to minimum cavity loss for the dye laser, indicating a slight spatial mismatch between the modes generated by the flame and those produced by injection of the dye ١٠ ٠ beam into the cavity.

Laser scans in segments of 30 GHz were made in the region of the $^Q P$ head of the 0,0 band of the NCl $b^1\Sigma^+ \rightarrow X^3\Sigma^-$ transition.[24] Although a number of scans were made over the region 664 nm - 666 nm, most of the effort was concentrated in the region near 664.4 nm, corresponding to transitions from rotational levels around $N = 13$, which should have the greatest population for an equilibrium distribution near 350 K. In this region, each 30-GHz scan should include two or possibly three NCl transitions in either the $^Q P$ or $^Q R$ branches.[31] In all of the experiments, atomic species (F or Cl atoms) were in large excess over HN_3. No appreciable gain or loss was observed, although the

98

kinetic model discussed in Section III predicts a large gain ($>10^3$ p/m) for the conditions of these experiments. Moreover, absorption due to ground state NCl was not observed downstream of the flame, as predicted by the model. Although the experiment is less sensitive to absorption (because of the threefold degeneracy of the ground state), an absorption signal should have been observed with a strength approximately three to five times the intrinsic intensity of the noise (see Fig. 22).

In order to probe the effect of mixing on the system, the reagent flow rates (in particular the diluent flow) were adjusted in order to reduce the total pressure in the reactor to ~ 400 mtorr. Helium was used as a diluent in both the halogen and HN_3 streams. A simple diffusion calculation for these conditions suggests that the mixing time should be less than 50 μs. Experiments were again performed in which the partial pressures of F and Cl atoms were varied from 30 mtorr to 50 mtorr, and HN_3 partial pressures as high as 12 mtorr were achieved (for a gas temperature near 350 K). Other parameters varied included the total pressure (maintained below 500 mtorr), the identity of the diluent (He or Ar), the position of the HN_3 injector with respect to the optical axis of the cavity, and the probe laser wavelength. The laser wavelength was varied over several 30-GHz segments around the initial setting (664.4 nm), and finally over much wider zones. No evidence of gain or absorption was observed in any of the experiments. The limiting sensitivity of these tests can be determined from the magnitude and noise level of the baseline phase shift. For the conditions of the experiments, the phase shift was given by $\tan \delta = 1.08 \pm 0.03$, for a modulation frequency of

65 kHz. Using the relation $\tan \delta = 4\pi fnL/c$, the average number of cavity transits is found to be 317.4 ± 9.4, corresponding to a round trip transmission given by $T = 0.9968 \pm 0.0001$. Hence, a signal to noise ratio $S/N = 1$ would correspond to a gain or absorption of about 200 p/m.

Further experiments were performed in which SF_6 was added to the reactive flow in the hope of increasing the intensity of the 0,0 band of the NCl emission. As noted above, experiments with the cylindrical flow tube indicated that addition of either SF_6 or CO_2 increased the 0,0 intensity by as much as a factor of 2, possibly due to vibrational relaxation within the $b^1\Sigma^+$ state or to the stabilization of a reaction intermediate such as N_3. Note in this regard that the kinetic model discussed in Section III above assumes population of only the $v' = 0$ level of the $b^1\Sigma^+$ state. In the transverse flow gain experiments, addition of SF_6 again resulted in a large increase in the 0,0 intensity. For a total pressure rise of 70 mtorr caused by SF_6 addition, the NCl emission (viewed through a narrow bandpass filter) doubled in intensity. Nevertheless, no gain or absorption was observed for these conditions. We note, however, that the mixing rate in the system may have been significantly reduced by the presence of large amounts of SF_6 in the flow.

One final series of these tests was performed on the NCl system in which an effort was made to reduce the intrinsic signal to noise level to the minimum possible value. This was accomplished by incorporating a signal averager (Tracor-Northern NS-570) into the data collection apparatus. This change resulted in an ultimate sensitivity to less than 50 p/m in gain or

100

absorption for 20 scans over the 30-GHz zone probed. As before, no variation in the baseline phase shift attributable to gain or loss was observed. Tests were made for several 30-GHz regions in both the 0,0 and 1,0 bands of the $b^1\Sigma^+$ - $X^3\Sigma^-$ transition. This result sets a limit on the maximum value of the inversion density present in the system, $\Delta N = [b^1\Sigma^+] - 1/3\ [X^3\Sigma^-] < 1.6 \times 10^{12}$ cm^{-3}, for an initial HN_3 density of ~ $2.7 \times 10^{14}\ cm^{-3}$. The temperature in the system was measured to be 350 K just downstream of the optical axis, in agreement with previous results. Since no absorption was observed at any position downstream of the HN_3 injector (i.e., in time zones where most of the excited NCl had radiated), the maximum density of ground state NCl downstream was $[NCl\ (X^3\Sigma^-)] < 4.8 \times 10^{12}$ for similar conditions. Since precautions were taken to avoid any optical saturation effects, it would seem that the discrepancy must be due to reactive removal of excited NCl by a process not included in the model. This process cannot involve F_2, Cl_2, or ClF, in view of the known rate constants for NCl $(b^1\Sigma^+)$ quenching by these species.[28] The most likely reagent would appear to be chlorine or fluorine atoms. We note that the photon yield experiments for NCl and NBr (see Section III above) were performed with very low densities of these atoms, in an effort to maximize the time resolution of the flame. To test this hypothesis, the reaction F + NCl $(b^1\Sigma^+)$ → products was added to the kinetic model, with a rate constant $k = 1.5 \times 10^{-11}\ cm^3\ mole^{-1}\ s^{-1}$ (about one-tenth the gas kinetic rate). The calculation predicted a maximum inversion density of ~ $4.8 \times 10^{12}\ cm^{-3}$ for the same initial conditions tested previously, which should be observable with a signal-to-noise ratio S/N ≈ 3 for the optimum sensitivity. Hence, if such a

101

process is the source of the transparency of the NCl system, its rate must approach the gas kinetic value.

The NBr $b^1\Sigma^+$ - $X^3\Sigma^-$ transition should be significantly more allowed than the analogous process in NCl, since the larger mass of the molecule should correlate to a much weaker spin constraint on the transition. In view of the measured radiative lifetime[12] for NCl ($b^1\Sigma^+$, $v' = 0$), $\tau = 630$ μs, it is expected that the lifetime for NBr ($b^1\Sigma^+$) will be 100 μs or less. Hence, it was expected that gain experiments on the NBr system would yield strong absorption signals, since radiation from excited NBr should be much faster than its production by chemical reactions for the reagent densities typically used in the experiments. Moreover, NBr ($b^1\Sigma^+$) radiation to the ground state should compete favorably with reactive processes removing the excited species, such as those inferred above. Because of the degeneracies of the $b^1\Sigma^+$ and $X^3\Sigma^-$ states (1 and 3, respectively), the experiment is intrinsically less sensitive to absorption by a factor of 3. We note also that the 1:1 abundance ratio of the $N^{79}Br$ and $N^{81}Br$ isotopes will reduce the sensitivity still further. It was expected that the increased transition moment and the relatively fast buildup of NBr ground state molecules would compensate for these factors, however.

The NBr experiments began with assembly of a stable source of Br_2 vapor. A simple bubbler was set up for this purpose, with helium passed into liquid Br_2 via a coarse fritted disc. Since the helium pressure was regulated to about 900 torr in the bubbler, and the liquid Br_2 was held at ambient temperature, Br_2 vapor comprised about 20% of the total Br_2/He flow. The NBr

102

flame was generated in the transverse flow apparatus by simply substituting the Br_2/He stream for Cl_2. The bright red flame was easily generated, and the flow of Br_2 was found to be quite stable and controllable. The flame intensity (observed with the uncooled GaAs PMT as described above) exhibited a sharp maximum with respect to the relative flow rates of Br_2 and F_2.

Gain/absorption measurements on the NBr system were perform in the manner noted above. The wavelength of the probe laser was set near ..5 nm, in the 0,0 band of the NBr $b^1\Sigma^+ - X^3\Sigma^-$ transition. Since a high re: on study of this band has not, however, been reported, the distribution .. individual features present within a given 30-GHz segment was unknown. In fact, NBr absorption features were easily found, with fourteen lines with strengths up to 2500 p/m being apparent within an 80 GHz-zone around 673.6 nm. This absorption spectrum is shown in Fig. 28. These data were obtained for an initial HN_3 pressure of 10 mtorr. It was observed that the absorption features were maximized by reducing the F_2 flow rate to a value well below that typically employed. This change resulted in Br atom densities well in excess over F atoms, and suggests that either the Br + N_3 rate is much slower than F + N_3, or that NBr ($b^1\Sigma^+$) is quenched by F_2 or fluorine atoms. Since, as noted above, results obtained using the cylindrical flow tube suggest that the Br + N_3 rate is actually faster than F + N_3, the quenching argument seems much more likely. Clearly, quenching by F atoms would agree with our inferences from the NCl gain experiments. Variation of the position of the HN_3 injector with respect to the optical axis indicated that the NBr absorption strength passed through a relatively flat peak about 1 ms
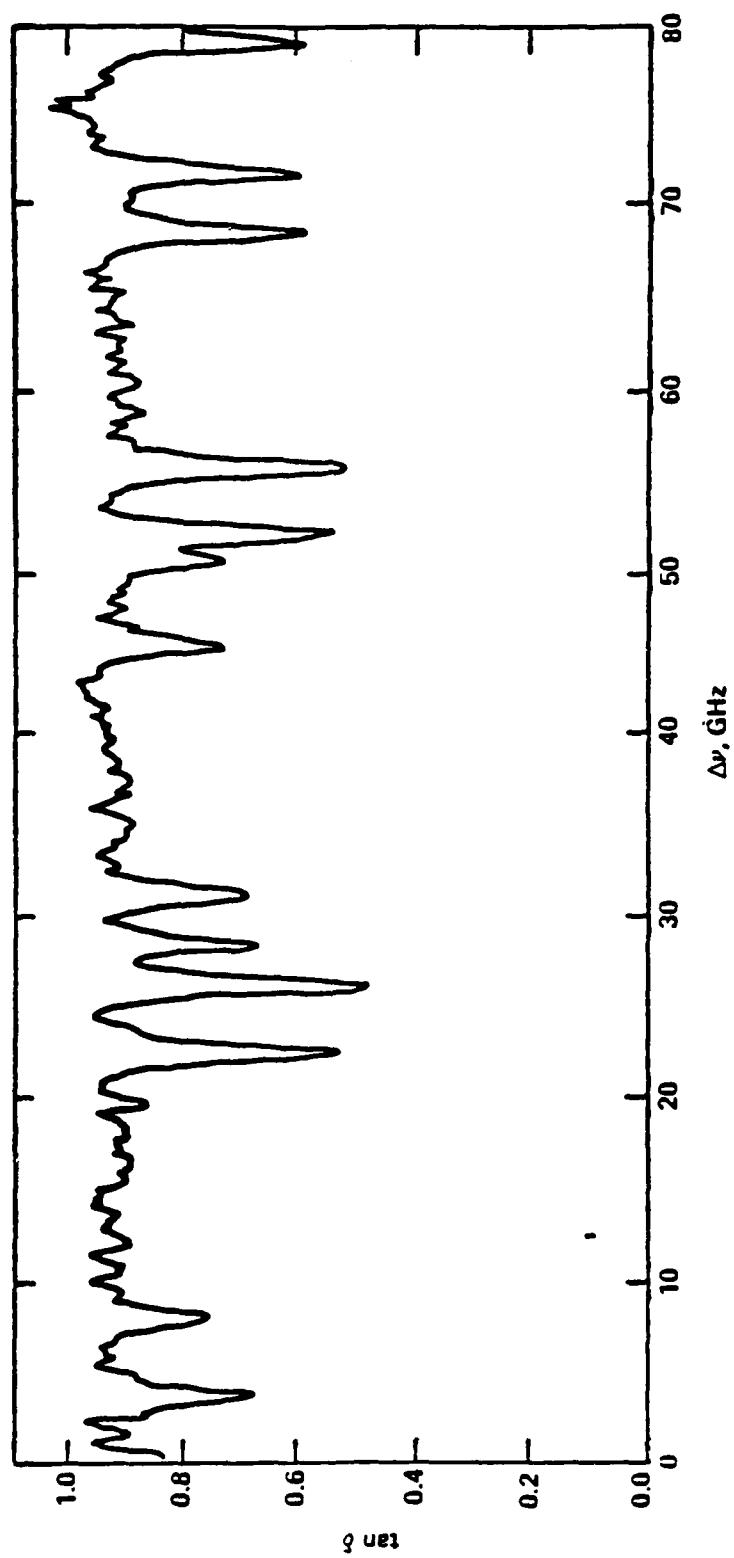
103

Figure 28. Absorption spectrum of the $X^3\Sigma^-$ – $b^1\Sigma^+$ transition of NBr produced by the F/Br + HN$_3$ reaction.

downstream of the injector. Some evidence of saturation of the $b^1\Sigma^+$ - $X^3\Sigma^-$ transition (i.e., an inverse dependence of the absorption strength on the incident laser energy) was found. This effect was completely eliminated by attenuating the probe beam ($\sim$ 100 mW) by a factor of 10^3.

If it is assumed that the transitions observed correspond to rotational states near the peak of the equilibrium distribution for T = 350 K, and that the radiative lifetime of NBr ($b^1\Sigma^+$) is 100 μs, then the maximum absorption strengths observed in our experiments indicate a density of ground state NBr molecules of about 3×10^{13} cm^{-3}. In view of its radiative lifetime, the concentration of excited NBr should be much less than that of the ground state. The calculated density corresponds to about 10% of the initial HN_3 density, in rough agreement with the measured photon yield for this system. Hence, it is feasible that the ground state NBr molecules are produced solely by radiation from the excited state.

3.   The NF-Bi Energy Transfer System

Although the $a^1\Delta$ state of NF can be generated in high yield by the azide system discussed in Section I, or by reactions of NF_2 radicals,[5] the very long radiative lifetime of this state, 5.6 seconds,[2] precludes lasing on the $a^1\Delta$ - $X^3\Sigma^-$ transition. Hence it is reasonable to consider systems in which the energy stored in the excited NF is transferred to species more amenable to lasing, in a manner analogous to the O_2^* - I^* system.[32] Capelle and co-workers[33] have shown that NF $a(^1\Delta)$ can participate in a very rapid energy transfer process with atomic bismuth, producing the $6^2D_{3/2}$ excited

105

state of the atom:

$$NF\ (a^1\Delta) + Bi\ (6^4S_{3/2}) \rightarrow NF\ (X^3\Sigma^-) + Bi\ (6^2D_{3/2}) \qquad (26)$$
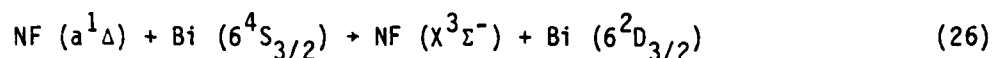
Since the energy defect for this process is only 16 cm^{-1} (the forward reaction being exothermic), it seems likely that under appropriate conditions an equilibrium would set up, much as in the O_2^* - I^* system. If it is assumed that the electronic, vibrational, and rotational partition functions of NF ($a^1\Delta$) are eqivalent to those in NF ($X^3\Sigma^-$), the equilibrium constant for Eq. 26 would be 1.62 at 300 K. Hence, addition of a small concentration of Bi to a stream of chemically generated NF ($a^1\Delta$) could result in efficient excitation of the bismuth atoms. If the concentration of NF ($a^1\Delta$) is much greater than that of bismuth, the nearly total inversion in NF would be reflected in the Bi atoms. For example, if 0.1 mtorr of Bi were added to a stream of gases containing 4 mtorr of NF ($a^1\Delta$) and no NF ($X^3\Sigma^-$), establishment of the equilibrium would result in partial pressures as follows: 3.902 mtorr NF ($a^1\Delta$), 0.098 mtorr Bi ($^2D_{3/2}$), 0.002 mtorr Bi ($^4S_{3/2}$) and 0.098 mtorr NF ($X^3\Sigma^-$). Energy might be drained out of the equilibrium pool by collisional quenching processes, spontaneous emission, or stimulated emission.

Clearly, one of the principal advantages of the NF-Bi system relative to O_2-I lies in the fact that nearly total population inversions can be produced chemically in NF, permitting maximum power extraction. Another advantage lies in the intrinsically higher gain of the Bi $6^2D_{3/2}$ - $6^4S_{3/2}$ transition, for which the spontaneous emission rate has been calculated to be

31 s^{-1},[34] about four times greater than that for the I $5^2P_{1/2} - 5^2P_{3/2}$ transition. In addition, potential systems advantages may be gained from the shorter wavelength of the bismuth transition, which occurs near 875.2 nm. A clear disadvantage lies with the difficulties in generating a flow of Bi atoms well mixed with a stream of excited NF. Moreover, a key question is the degree to which excited bismuth undergoes reactions with the fluorides present in the mixture (including NF) to produce BiF. The objective of this last portion of the program was to investigate these issues and, if possible, to demonstrate gain in the NF-Bi system by using the resonant cavity phase shift method.

The experiments began by testing sources of gas phase bismuth atoms. The diagnostic employed was absorption of the 306.8-nm resonance line emitted by a hollow cathode bismuth lamp. This line corresponds to the $7^4P_{1/2} - 6^2D_{3/2}$ transition in atomic bismuth. In view of the large oscillator strength of this transition (A = 1.9×10^8 s^{-1}),[35] a density of Bi atoms on the order of 10^{12} cm^{-3} would almost totally attenuate this emission over a pathlength of only 2.0 cm, assuming the linewidth of the lamp radiation to be approximately equal to the absorption linewidth of the Bi atoms in the flow. Curves of growth measured for the 306.8 nm line using known vapor pressures of bismuth generated in an oven suggested, however, that the lamp output was significantly broader than the absorption linewidth. Hence, this technique appeared to be an adequate diagnostic in the low density regime.

Two sources of bismuth atoms were tested. The first of these was thermal decompostion of trimethylbismuth (TMB), a technique used by Herbelin

107

and co-workers at the Aerospasce Corporation. In our experiments, a stream of
gaseous TMB was obtained by either premixing the vapor with argon in a storage
vessel (TMB:Ar = 1 : 24) or by bubbling a rare gas directly through the
liquid. The second method tested involved reactions of $BiCl_3$, a solid with a
room temperature vapor pressure of ~ 2 torr. In this case, a stream
containing $BiCl_3$ vapor was generated by passing argon through a fritted disc
which supported a sample of $BiCl_3$ powder.

Several tests of bismuth atom generation from decomposition of TMB
were performed with the small cylindrical flow tube. In the first experi-
ments, the TMB/Ar mixture was admitted to a stream of atomic and molecular
fluorine (prepared by microwave discharge) diluted in argon. A blue-white
flame appeared at the point where the TMB entered the flow, but the intensity
of the 306.8-nm resonance line was not attenuated. Similarly, no absorption
was found at any point downstream of the TMB injector. In a second group of
experiments, molecular hydrogen was added to the flow in excess of the total
fluorine flow (atoms and molecules) about 20 cm upstream of the TMB injector,
producing a highly diffuse blue-white flame. Addition of TMB to this mixture
produced an absorption of nearly 30%. It was noted in these experiments that
the flow tube became very hot. In subsequent experiments, TMB absorptions
were found only when the flow tube was hot, suggesting that Bi atoms are
produced by thermal decomposition of the TMB.

Further experiments on the generation of gas phase Bi atoms were
performed by using the 15-cm transverse flow reactor, since this all-metal
system was more amenable to the high temperatures apparently required for TMB

108

dissociation. For this purpose, the mirror and purge line assemblies used for gain experiments were replaced by quartz end windows, and the output of the bismuth hollow cathode lamp was directed down the axis of the reactor. Fluorine atoms were produced by passage of an F_2/He mixture through the two parallel microwave discharges, and H_2 was admitted just upstream of the main chamber of the reactor (i.e., through the ports used for Cl_2 or Br_2 in the NCl and NBr experiments described above). In the initial experiments performed with this apparatus, TMB or $BiCl_3$ was admitted via the movable injector normally used for HN_3. Dilute mixtures of these reagents in rare gases were obtained as described above. Strong absorptions (as high as 80%) were obtained when TMB was added to the F_2-H_2 flame, and transmission of the 306.8-nm resonance line was restored when the flow of either TMB, H_2, or F_2 was turned off. The H_2 was always in excess over F_2, such that all of the fluorine atoms were reacted away prior to contact with the TMB. Absorptions were also found in experiments in which $BiCl_3$ was used as a reagent. In this case, bismuth atoms are probably formed by sequential stripping of chlorine atoms from the molecule by hydrogen atoms present in the flow. The absorption signals produced by $BiCl_3$ were quite erratic, however, and could not be reliably generated for given flow conditions.

Further experiments were performed for the TMB system in an effort to quantify the yield of bismuth atoms. For these experiments, the configuration of the apparatus was slightly modified, such that the TMB was premixed with the H_2 stream prior to entry of the gases into the reactor. In this case, the optical axis (the point in the flow where Bi atoms were detected) was about

109

12 cm downstream of the TMB/H_2 inlet. The temperature of the flowing gases was measured 12 cm downstream of the optical axis with a chromel-alumel thermocouple referenced to room temperature. For partial pressures of TMB in the flow varying from 1.4×10^{-2} mtorr to 1.0×10^{-1} mtorr, the density of Bi atoms present downstream was determined from the transmission of the 306.8-nm resonance line and the known oscillator strength of this ^4P - ^4S transition.[35] Since the lineshape of the emission from the lamp was unknown, it was assumed that $\alpha = \Delta\nu_{lamp}/\Delta\nu_{gas} = 1.5$, and that the lamp output was not self-reversed. Although these arbitrary assumptions result in a very large uncertainty in the calculation of the Bi densities, it seems unlikely that α would be less than 1.5, and hence the values obtained may be considered to be lower limits. The data obtained in these experiments are shown in Table 4. Bismuth densities as high as 10^{10} to 10^{11} atoms cm^{-3} were produced, and there is a clear correlation between increasing temperature and increasing density. Comparison of the calculated densities with the TMB flow rates indicates that a significant proportion of the parent molecules were dissociated at the higher temperatures.

A series of similar experiments were performed in which D_2 was substituted for H_2 as a fuel in the reactive flow. The results of these tests are also shown in Table 4. The data indicate Bi densities and yields quite similar to those found for the H_2 experiments under comparable conditions. This result supports the hypothesis that the TMB is dissociated by thermal excitation, rather than by an energy transfer process involving vibrationally excited HF or DF.

110

Table 4
Generation of Bismuth Atoms by Dissociation of Trimethylbismuth

Fuel	Temp (K)	ϕ_{Bi} (atoms cm^{-3})	Yield*
H_2	366	1.1×10^{10}	0.02
H_2	355	1.3×10^{10}	0.03
H_2	355	2.9×10^{10}	0.01
H_2	373	1.5×10^{10}	0.02
H_2	423	1.2×10^{11}	0.17
D_2	366	8.3×10^{9}	0.01
D_2	452	1.3×10^{11}	0.17
D_2	482	9.4×10^{10}	0.13

*Yield = $\phi_{Bi} \div \rho_{TMB}$

No evidence indicating a falloff in the Bi yield with increasing TMB flow rate was found, within the range of densities which could be probed by the resonance absorption method. In order to monitor the generation of greater densities of atoms at higher TMB flow rates, absorption on the $^4S_{3/2} - \,^2D_{3/2}$ transition was directly measured by the resonant cavity phase shift method. These experiments required that the CW dye laser be operated at the wavelength of this transition, 875.2 nm. Lasing at this wavelength was obtained by pumping HITC dye dissolved in a mixture of propylene carbonate and ethylene glycol with the red lines of the krypton ion laser.[36] For an input power of ~ 5 W, a stable, single frequency output of ~ 150 mW was readily

obtained near 875 nm. Steady performance at this level over a period of hours was achieved by passing the dye solution through a cooler which chilled it to ∽ 9°C.

By using the output of the dye laser as a probe, a search was made for absorption by the $^4S_{3/2}$ - $^2D_{3/2}$ transition in bismuth vapor generated by heating solid bismuth. Two bismuth sources were used for these tests. The first was a quartz heat pipe, with a wick ∽ 10 cm in length. The bismuth transition was observed with this apparatus, but the poor signal to noise ratio of the spectrum obtained and the large density gradient undoubtedly present in the tube precluded any quantitative analysis. Much better results were obtained by using an apparatus in which a sealed quartz cell containing solid bismuth was suspended inside a commercial tube furnace (Marshall Product Co.). The cell, which was 14.7 cm in length, was positioned in the center of the 32-cm-long oven, the ends of which were sealed with insulating material save for a 5-mm-diameter aperture for transmission of the laser beam. The cell temperature was measured with a shielded chromel-alumel thermocouple, data from which indicated no measurable temperature gradient along the length of the cell. Temperature measurements made with an optical pyrometer agreed with the thermocouple readings to within ± 10 K. The incident laser intensity (I_0) was monitored with a photodiode integral to the dye laser system. The transmitted intensity (I) was detected by a room temperature GaAs PMT (RCA 4832), whose response was monitored by a Kiethley 610C electrometer. The optical density of the bismuth vapor (OD = log $[I_0/I]$) was measured directly by using the ratiometer capability of a PAR 5204 lock-in analyzer. Spectra

112

were recorded by an X-Y plotter, with the X channel driven by the ring laser scan control and the Y channel by the output of the ratiometer. Typical scans were 30 GHz wide, as calibrated by an etalon with a 7.5-GHz free spectral range.

A typical spectrum of the Bi $6^4S_{3/2} - 6^2D_{3/2}$ transition recorded in this manner is shown in Fig. 29. The spectrum exhibits nine of the ten hyperfine lines expected for a magnetic dipole transition between these two states ($\Delta F = 0, \pm 1$), and the relative intensities of the lines are in excellent agreement with calculated values for such a transition.[37] Only the 4,4 transition is missing, since its intensity is calculated to be only 0.3% of that of the most intense feature, the 6,6 line. The hyperfine splittings evident in the spectrum are in good agreement with previously reported values obtained from the spectra of allowed transitions terminating on the $6^4S_{3/2}$ and $6^2D_{3/2}$ states.[38,39] No evidence of electric quadrapole transitions ($\Delta F = 0, \pm 1, \pm 2$) is apparent in the spectrum.

Since the optical pathlength was fixed for the closed cell experiment, measurements of the total integrated absorption coefficient of the transition were possible. For small laser powers, the integrated absorption coefficient is related to the spontaneous emission rate, A, by the following expression:

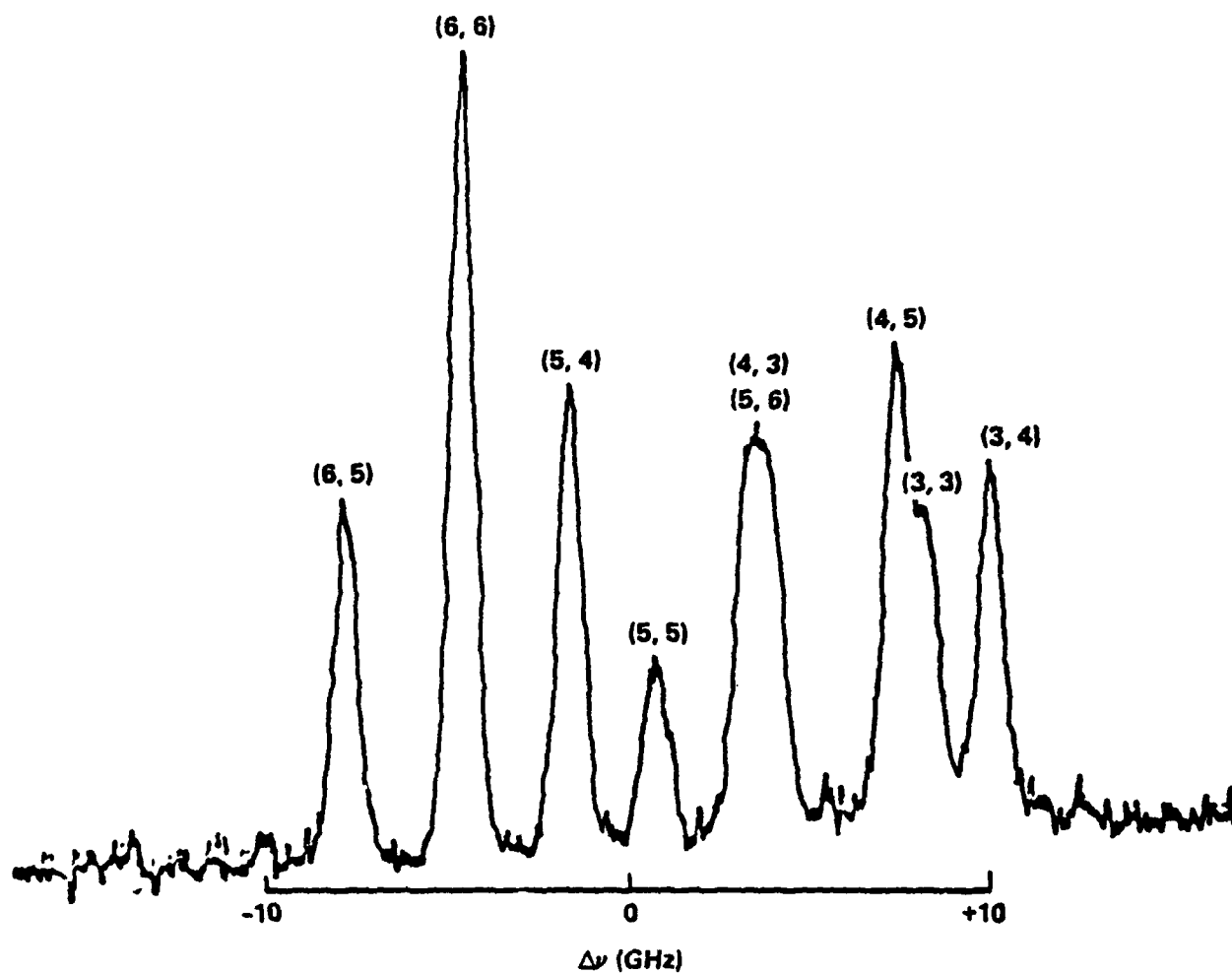$$\int k_\nu \ell d\nu = \frac{\lambda_0^2}{8\pi} \frac{g_2}{g_1} AN\ell \tag{27}$$

113

Figure 29. High resolution spectrum of the $6\ ^4S_{3/2} - 6^2D_{3/2}$ transition in atomic bismuth, showing nine F',F" hyperfine lines.

114

where g_2 and g_1 are the degeneracies of the $6^2D_{3/2}$ and $6^4S_{3/2}$ states, respectively, N is the number densities of bismuth atoms, and $k_\nu\ell$ = 2.303 OD (ν) . A plot of 2.303 $(8\pi/\lambda_0^2\ell)$ $\int$ OD(ν)dν vs N is therefore linear with a slope equal to A. Such a plot for the data obtained in several experiments is shown in Fig. 30. The total intensities of the nine lines were integrated with a planimeter, and data recorded for various oven temperatures. The densities indicated in Fig. 30 were obtained from the vapor pressure data tabulated by Hultgren and co-workers.[40] The slope of the plot yields a spontaneous emission rate A = 22.5 ± 1.4 s^{-1}. This value is in reasonable agreement with that calculated by Garstang,[34] 31 s^{-1}, given possible systematic errors in the vapor pressure data.

This information was used in experiments directed toward detecting free bismuth atoms produced by thermal dissociation of TMB in the transverse flow reactor. A portion of the CW probe laser beam was passed through the bismuth so that the laser might be locked on to the frequency of the 6,6 hyperfine line. The beam was amplitude modulated with an acousto-optic device and injected into a resonant cavity surrounding the flow reactor, as in previous experiments. The cavity reflectors were loaned to us by Dr. J.M. Herbelin of the Aerospace Corporation. A value of tan δ near 1.0 was obtained for a modulation frequency of 21 kHz with no reagent flow, implying an average photon lifetime corresponding to 1015 round trip passes, or individual mirror reflectivities of 0.9995. This result is in good agreement with data from Dr. Herbelin's laboratory. As in the experiments described above, TMB diluted in helium was added to a flow in which fluorine atoms reacted with excess H_2,

115
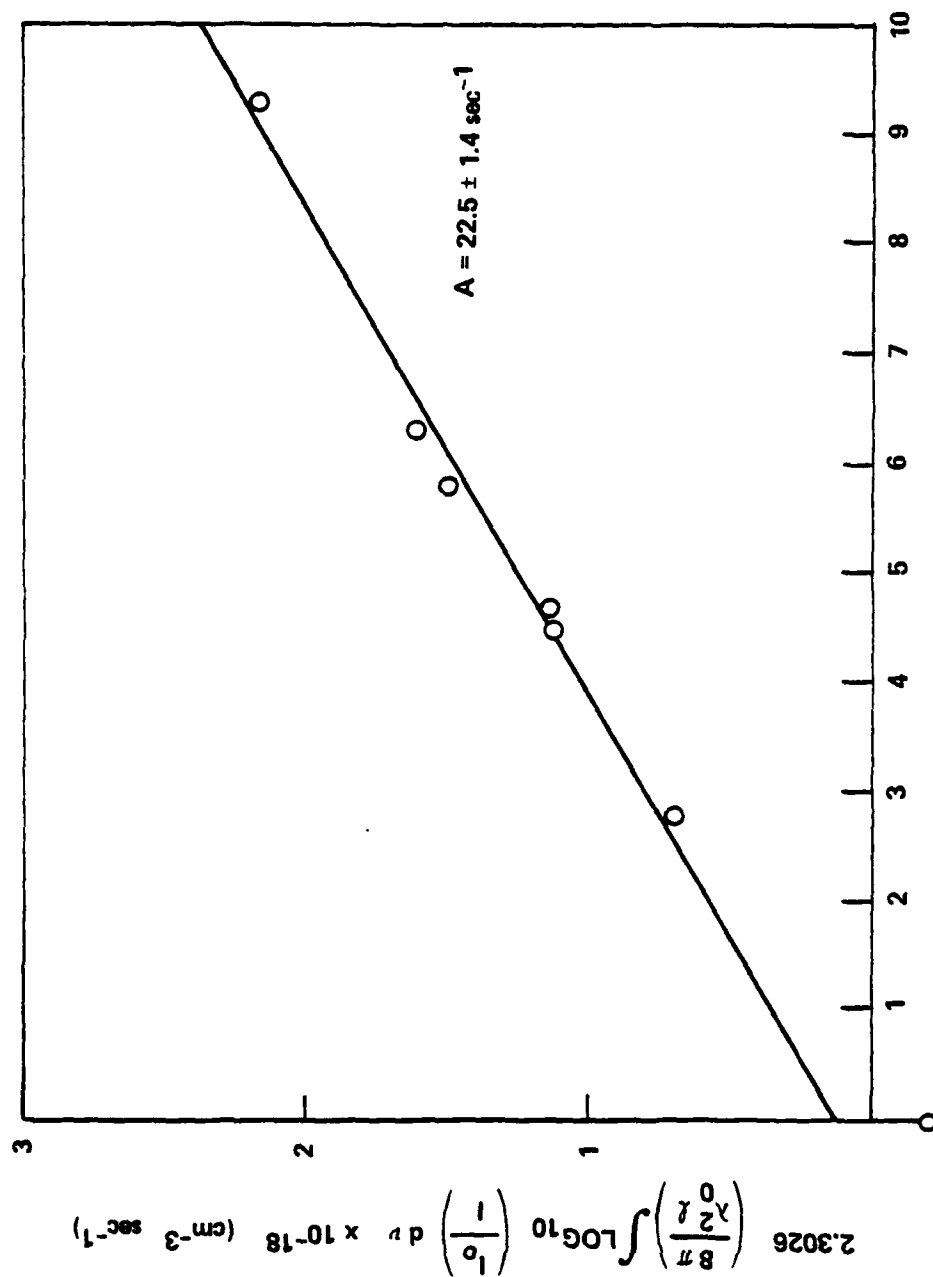
Figure 30. Plot of the integrated absorption coefficient of the Bi $6^4S_{3/2}$ - $6^2D_{3/2}$ transition vs the bismuth density. (The slope of the plot yields a spontaneous emission rate A=22.5±1.4 s^{-1} for the $6^2D_{3/2}$ state.)

116

generating a temperature in excess of 100°C. The TMB entered the system
through the movable injector bar. Addition of large flows of TMB to the
system resulted in a drop in tan δ from 1.0 to 0.7, corresponding to a round
trip absorption of about 400 p/m. The absorption signal disappeared when the
laser frequency was moved off the 6,6 line and reappeared when the laser was
tuned to the nearby 5,4 line. The magnitude of the absorption was very
unsteady, however. In a subsequent experiment, a steady absorption was
obtained by using large flows of undiluted TMB. The flow rate used
corresponded to a TMB density in the reactor of ~ 6.5×10^{14} cm^{-3}, to be
compared to a bismuth atom density of ~ 10^{12} cm^{-3} calculated from the
magnitude of the absorption signal. Clearly, the yield of Bi atoms relative
to the TMB flow is only on the order of 0.1%.

These data clearly indicate that a density of bismuth atoms suf-
ficient for the observation of absorption, and hence gain, can be produced in
the flow reactor using TMB. The dissociation yield is very low, however.
Since undissociated TMB quenches Bi $(6^2D_{3/2})$ at a near gas kinetic rate,[41] it
is unlikely that optical gain on the $6^4S_{3/2} - 6^2D_{3/2}$ transition could be
demonstrated under these conditions.

V. CONCLUSIONS

The data presented above support the hypothesis that a similar mechanism is operative in all of the halogen atom-azide molecule reactions investigated. This mechanism involves the generation of N_3 free radicals by the F + HN_3 reaction, followed by reaction of the N_3 with F, Cl, or Br atoms. Spin constraints on the N_3 reactions lead to the preferential population of accessible singlet states of the products, in particular the $a^1\Delta$ and $b^1\Sigma^+$ states of the nitrenes (NX). In none of the experiments was any evidence suggesting direct population of ground state nitrenes ($X^3\Sigma^-$) obtained.

The scalability of these systems, i.e., the rate at which the density of excited products increases with increasing reagent flow, is a sensitive function of the relative rates of formation and decay of N_3 radicals in each system. In the NF case, the yield of excited singlets falls off rapidly because the rate of the F + HN_3 reaction is nearly an order of magnitude greater than the rate of F + N_3. This situation causes a buildup of the steady-state concentration of N_3 radicals, which can undergo very rapid second-order side reactions producing molecular nitrogen. Hence, the F + HN_3 system will not scale to the densities required for an efficient NF or NF-Bi chemical laser.

Effective scaling would appear to be much more probable for the NCl system, since the rate constants of reactions producing and removing N_3 are nearly equivalent in this case. The sum of all the information currently

available concerning the kinetics of processes producing excited NCl, side reactions of N_3, collisional decay processes, and NCl radiative decay, leads to the prediction of easily measurable gain on the $b^1\Sigma^+ \rightarrow X^3\Sigma^-$ transition of NCl. It seems very likely that the optical transparency indicated by the gain experiments described above results from removal of excited NCl ($b^1\Sigma^+$) prior to radiation, probably by reaction with halogen atoms present in excess in the flow. The rates of these reactions are unknown. Even if their rate constants approached the gas kinetic value, however, it is possible that gain on the NCl $b^1\Sigma^+ \rightarrow X^3\Sigma^-$ transition might be demonstrated by employing stoichiometric flows of HN_3 and halogen atoms, i.e., to remove the excess atoms. The flow rates of HN_3 required for stoichiometric reaction, while maintaining the absolute rates necessary to produce excited NCl on a time frame competitive with its radiative relaxation, cannot be produced with the apparatus used in these experiments, however.

The absorption spectrum obtained for the NBr system demonstrates the viability of the resonant cavity phase shift technique for the measurement of small gains or absorptions. Although very little is known concerning the decay kinetics of NBr ($b^1\Sigma^+$), the appearance of the absorption spectrum is in accord with the expected short radiative lifetime of this species. This shorter lifetime would make NBr a higher gain system than NCl (and perhaps more easily demonstrated at low densities), but kinetics information from the flow tube experiments suggests that NBr may not scale as well as NCl. The rate constant for $Br + N_3$ appears to be intermediate between $Cl + N_3$ and $F + N_3$, and about one-half as large as that for $F + HN_3$. This inference is

119

supported by the appearance of N_2 first positive emission in the NBr flame. More detailed information concerning the kinetics of NBr production and decay is necessary to fully assess the potential of this system.

The data presented above on the bismuth system represent the first high resolution measurement of the spectrum of the $6^4S_{3/2} - 6^2D_{3/2}$ transition, and the first direct measurement of the radiative lifetime of the $6^2D_{3/2}$ state. Although an NF-Bi gain experiment was not performed, the issues to be addressed by such an experiment were defined and an appropriate diagnostic system was demonstrated. The major hurdle to be overcome before a gain measurement can be performed is the demonstration of an adequate source of Bi atoms. Thermal dissociation of trimethylbismuth or reactions of $BiCl_3$ would not appear to be viable sources. For a small-scale gain measurement, simple evaporation of elemental bismuth may be the most appropriate method. An efficient thermal or chemical source must be developed for a large-scale laser device, however.

REFERENCES

1. M.A.A. Clyne and I.F. White, Chem Phys Let. 6, 465 (1970).

2. R.J. Malins and D.W. Setser, J. Phys. Chem, 85, 1342 (1981).

3. A.E. Douglas and W.E. Jones, Can. J. Phys. 44, 2251 (1966).

4. W.E. Jones, Can. J. Phys. 45, 21 (1967).

5. J.M. Herbelin and N. Cohen, Chem. Phys. Lett. 20, 605 (1973).

6. C.T. Cheah and M.A.A. Clyne, J. Chem. Soc. Faraday II, 76, 1543 (1980).

7. M.A. Kwok and J.M. Herbelin, Electronic Transition Lasers II (MIT Press, Cambridge, Mass., L.E. Wilson, Ed. 1977) p. 100.

8. R.G. MacDonald and J.J. Sloan, Chem. Phys. Lett. 61, 137 (1979).

9. T.C. Clark and M.A.A. Clyne, Trans. Faraday Soc. 66, 877 (1970).

10. R.D. Coombe and A.T. Pritt, Jr., Chem. Phys. Lett, 58, 606 (1978).

11. T.C. Clark and M.A.A. Clyne, Trans. Faraday Soc. 65, 2994 (1969).

12. R.D. Coombe, D. Patel, A.T. Pritt, Jr., and F.J. Wodarczyk, J. Chem. Phys. 75, 2177 (1981).

13. G.A. Woolsey, P.A. Lee, and W.D. Slafer, J. Chem. Phys. 67, 1220 (1977).

14. J.M. Herbelin, J.A. McKay, M.A. Kwok, R.H. Uenten, D.S. Uregig, D.J. Spencer, and D.J. Benard, Appl. Optics, 19, 144 (1980).

15. P.H. Tennyson, A. Fontijn, and M.A.A. Clyne, Chem. Phys. to be published.

16. J.R. McDonald, J.W. Rabalais, and S.P. McGlynn, J. Chem. Phys. 52, 1332 (1970).

17. J.J. Hinchen, J. Appl. Phys. 45, 1818 (1974).

18. P.S. Ganguli and M. Kaufman, Chem. Phys. Lett. 25, 221 (1974).

19. A.T. Pritt, Jr., and R.D. Coombe, Int. J. Chem. Kinetics, 12, 741 (1980).

20. R.J. Paur and E.J. Bair, Int. J. Chem. Kinetics, 8, 139 (1976).

21. J.L. Jourdain, G. LeBras, G. Poulet and J. Combourieu, Comb. and Flame, 34, 13 (1979).

22. L.G. Piper, R.H. Krech, and R.L. Taylor, J. Chem. Phys. 71, 2099 (1979).

23. J. Combourieu, G. LeBras, G. Poulet and J.L. Jourdain, Proc. Int. Symp. Comb. XVI, (The Combustion Institute, 1977), p. 863.

24. A.T. Pritt, Jr., D. Patel and R.D. Coombe, J. Mol. Spectrosc. 87, 401 (1981).

25. A.E. Douglas and W.E. Jones, Can. J. Phys. 43, 2216 (1965).

26. L.F. Philips, Can. J. Chem. 46, 1429 (1968).

27. J.C. Miller and L. Andrews, J. Chem. Phys. 71, 5276 (1979).

28. A.T. Pritt, Jr., D. Patel, and R.D. Coombe, J. Chem. Phys. in press.

29. J. Tellinghuisen, J. Chem. Phys. 58, 2821 (1973).

30. J.W.C. Johns, D.A. Ramsay and S.C. Ross, Can. J. Phys. 54, 1804 (1976).

31. R. Colin and W.E. Jones, Can. J. Phys. 45, 301 (1967).

32. W.E. McDermott, N.R. Pchelkin, D.J. Benard, and R.R. Bousek, Appl, Phys. Lett. 32, 469 (1978).

33. G.A. Capelle, D.G. Sutton, and J.I. Steinfeld, J. Chem. Phys. 69, 5140 (1978).

34. J. Garstang, J. Res. Natl. Cur. Std. (US), A68, 61 (1964).

35. P.T. Cunningham and J.K. Link, J. Opt. Soc. Amer. 57, 1000 (1967).

36. J.M. Herbelin and J.A. McKay, Optics. Comm. 36, 63 (1981).

37. S. Mrozowski, Phys. Rev. 57, 207 (1940).

38. S. Mrozowski, Phys. Rev. 62, 526 (1942).

39. J. Heldt, J. Opt. Soc. Amer. 58, 1516 (1968).

40. R. Hultgren, R.C. Orr, and K.K. Kelley, Selected Values of Thermodynamic Properties of Metals and Alloys, I, University of California, Lawrence Berkeley Laboratory, Berkeley, California, 1970.

41. M.J. Bevan and D. Husain, J. Phys. Chem. 80, 217 (1976).

DATE FILME 8